USGS
science for a changing world

Prepared in cooperation with the U.S. Environmental Protection Agency,
National Exposure Research Laboratory

Simulation of Streamflow in the McTier Creek Watershed, South Carolina

National Water-Quality Assessment Program

Scientific Investigations Report 2010–5202

U.S. Department of the Interior
U.S. Geological Survey

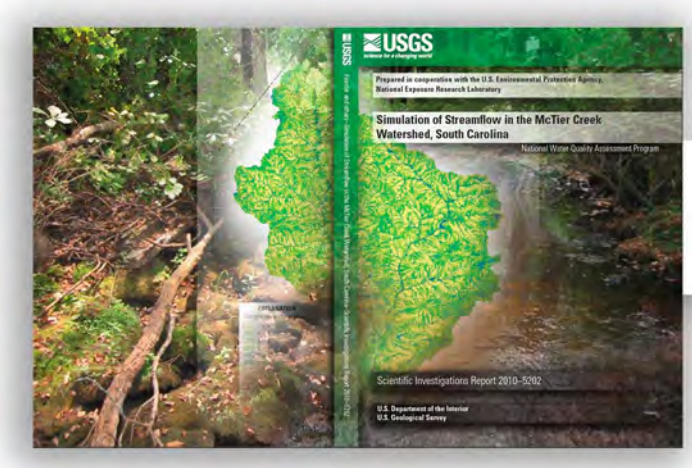

Cover art: Photographs of McTier Creek upstream from the streamgage near Monetta at the Secondary Road 25 crossing, Aiken County, South Carolina, August 17, 2007 (*Toby D. Feaster*). Map image from report appendix figure 1–1.

Simulation of Streamflow in the McTier Creek Watershed, South Carolina

By Toby D. Feaster, Heather E. Golden, Kenneth R. Odom, Mark A. Lowery, Paul A. Conrads, and Paul M. Bradley

National Water-Quality Assessment Program

Prepared in cooperation with the U.S. Environmental Protection Agency, National Exposure Research Laboratory

Scientific Investigations Report 2010–5202

U.S. Department of the Interior
U.S. Geological Survey

U.S. Department of the Interior
KEN SALAZAR, Secretary

U.S. Geological Survey
Marcia K. McNutt, Director

U.S. Geological Survey, Reston, Virginia: 2010

For more information on the USGS—the Federal source for science about the Earth, its natural and living resources, natural hazards, and the environment, visit http://www.usgs.gov or call 1-888-ASK-USGS

For an overview of USGS information products, including maps, imagery, and publications, visit http://www.usgs.gov/pubprod

To order this and other USGS information products, visit http://store.usgs.gov

Any use of trade, product, or firm names is for descriptive purposes only and does not imply endorsement by the U.S. Government.

Although this report is in the public domain, permission must be secured from the individual copyright owners to reproduce any copyrighted materials contained within this report.

Suggested citation:
Feaster, T.D., Golden, H.E., Odom, K.R., Lowery, M.A., Conrads, P.A., and Bradley, P.M., 2010, Simulation of streamflow in the McTier Creek watershed, South Carolina: U.S. Geological Survey Scientific Investigations Report 2010–5202, 61 p.

Foreword

The U.S. Geological Survey (USGS) is committed to providing the Nation with reliable scientific information that helps to enhance and protect the overall quality of life and that facilitates effective management of water, biological, energy, and mineral resources (*http://www.usgs.gov/*). Information on the Nation's water resources is critical to ensuring long-term availability of water that is safe for drinking and recreation and is suitable for industry, irrigation, and fish and wildlife. Population growth and increasing demands for water make the availability of that water, measured in terms of quantity and quality, even more essential to the long-term sustainability of our communities and ecosystems.

The USGS implemented the National Water-Quality Assessment (NAWQA) Program in 1991 to support national, regional, State, and local information needs and decisions related to water-quality management and policy (*http://water.usgs.gov/nawqa*). The NAWQA Program is designed to answer: What is the quality of our Nation's streams and groundwater? How are conditions changing over time? How do natural features and human activities affect the quality of streams and groundwater, and where are those effects most pronounced? By combining information on water chemistry, physical characteristics, stream habitat, and aquatic life, the NAWQA Program aims to provide science-based insights for current and emerging water issues and priorities. From 1991 to 2001, the NAWQA Program completed interdisciplinary assessments and established a baseline understanding of water-quality conditions in 51 of the Nation's river basins and aquifers, referred to as Study Units (*http://water.usgs.gov/nawqa/studies/study_units.html*).

National and regional assessments are ongoing in the second decade (2001–2012) of the NAWQA Program as 42 of the 51 Study Units are selectively reassessed. These assessments extend the findings in the Study Units by determining water-quality status and trends at sites that have been consistently monitored for more than a decade, and filling critical gaps in characterizing the quality of surface water and groundwater. For example, increased emphasis has been placed on assessing the quality of source water and finished water associated with many of the Nation's largest community water systems. During the second decade, NAWQA is addressing five national priority topics that build an understanding of how natural features and human activities affect water quality, and establish links between *sources* of contaminants, the *transport* of those contaminants through the hydrologic system, and the potential *effects* of contaminants on humans and aquatic ecosystems. Included are studies on the fate of agricultural chemicals, effects of urbanization on stream ecosystems, bioaccumulation of mercury in stream ecosystems, effects of nutrient enrichment on aquatic ecosystems, and transport of contaminants to public-supply wells. In addition, national syntheses of information on pesticides, volatile organic compounds (VOCs), nutrients, trace elements, and aquatic ecology are continuing.

The USGS aims to disseminate credible, timely, and relevant science information to address practical and effective water-resource management and strategies that protect and restore water quality. We hope this NAWQA publication will provide you with insights and information to meet your needs, and will foster increased citizen awareness and involvement in the protection and restoration of our Nation's waters.

The USGS recognizes that a national assessment by a single program cannot address all water-resource issues of interest. External coordination at all levels is critical for cost-effective management, regulation, and conservation of our Nation's water resources. The NAWQA Program, therefore, depends on advice and information from other agencies—Federal, State, regional, interstate, Tribal, and local—as well as nongovernmental organizations, industry, academia, and other stakeholder groups. Your assistance and suggestions are greatly appreciated.

William H. Werkheiser
USGS Associate Director for Water

Acknowledgments

The authors gratefully acknowledge the support and guidance provided by Leon Kauffman and Dave Wolock of the U.S. Geological Survey. The version of the TOPMODEL used in this study was based on a version originally documented by Dave Wolock (1993) and later modified by Leon Kauffman (Kennen and others, 2008). Both scientists graciously took time to answer questions by e-mail and telephone concerning the application of TOPMODEL and proper interpretations of results. Their previous work and guidance for the current application of TOPMODEL added significantly to this investigation.

The U.S. Environmental Protection Agency, through its Office of Research and Development, partially funded the research described in this report through Interagency Agreement DW14922794.

Contents

Figures

Tables

Conversion Factors

SI to Inch/Pound

Multiply	By	To obtain
	Length	
centimeter (cm)	0.3937	inch (in.)
meter (m)	3.281	foot (ft)
kilometer (km)	0.6214	mile (mi)
	Area	
hectare (ha)	2.471	acre
square kilometer (km^2)	247.1	acre
square kilometer (km^2)	0.3861	square mile (mi^2)
	Volume	
cubic meter (m^3)	35.31	cubic foot (ft^3)
	Flow rate	
meter per second (m/s)	3.281	foot per second (ft/s)
cubic meter per day (m^3/d)	35.31	cubic foot per day (ft^3/d)
	Hydraulic conductivity	
meter per day (m/d)	3.281	foot per day (ft/d)
	Hydraulic gradient	
meter per kilometer (m/km)	5.27983	foot per mile (ft/mi)

Inch/Pound to SI

Multiply	By	To obtain
	Length	
inch (in.)	2.54	centimeter (cm)
inch (in.)	25.4	millimeter (mm)
foot (ft)	0.3048	meter (m)
mile (mi)	1.609	kilometer (km)
	Area	
acre	0.004047	square kilometer (km^2)
square mile (mi^2)	2.590	square kilometer (km^2)
	Volume	
cubic foot (ft^3)	0.02832	cubic meter (m^3)
	Flow rate	
cubic foot per second (ft^3/s)	0.02832	cubic meter per second (m^3/s)
cubic foot per second per square mile [$(ft^3/s)/mi^2$]	0.01093	cubic meter per second per square kilometer [$(m^3/s)/km^2$]
inch per hour (in/h)	0.0254	meter per hour (m/h)
	Hydraulic conductivity	
foot per day (ft/d)	0.3048	meter per day (m/d)
	Hydraulic gradient	
foot per mile (ft/mi)	0.1786	meter per kilometer (m/km)

Temperature in degrees Celsius (°C) may be converted to degrees Fahrenheit (°F) as follows:

$$°F = (1.8 \times °C) + 32$$

Temperature in degrees Fahrenheit (°F) may be converted to degrees Celsius (°C) as follows:

$$°C = (°F - 32) / 1.8$$

Horizontal coordinate information is referenced to the North American Datum of 1927 or 1983 (NAD 27 or NAD 83, respectively).

Vertical coordinate information is referenced to the North American Datum of 1988 (NAVD 88) or National Geodetic Vertical Datum of 1929 (NGVD 29).

Elevation, as used in this report, refers to distance above the vertical datum.

Acronyms and Abbreviations Used in the Report

BASINS	Better Assessment Science Integrating Point and Non-Point Sources
Calibration period	model simulations at Monetta for February 7, 2001, to September 30, 2009
Concurrent period	model simulations at Monetta for June 13, 2007, to September 30, 2009
Confirmation period	model simulations at New Holland for June 13, 2007, to September 30, 2009
DDS	dynamically dimensioned search
DEM	digital elevation model
DOC	dissolved organic carbon
E	Nash-Sutcliffe coefficient of model-fit efficiency index
ET	evapotranspiration
GBMM	grid-based mercury model
GIS	geographic information system
Hg	mercury
HSPF	Hydrologic Simulation Program–Fortran
ISC	total impervious surface cover
MA01–MA12	model assessment points
MAE	mean absolute error
MeHg	methylmercury
Monetta	Station 02172300, McTier Creek near Monetta, SC
New Holland	Station 02172305, McTier Creek near New Holland, SC
NHD	National Hydrography Dataset
NLCD	National Land-Cover Dataset
NRCS	Natural Resources Conservation Service
NWS	National Weather Service
PEST	parameter estimation program
PET	potential evapotranspiration
ppt	precipitation
qb	subsurface flow
qimp	impervious flow
qinf	infiltration-excess overland flow
qof	overland saturation flow
qpred	total in-stream flow
qret	return flow
qsrip	flow from open-water bodies (lakes, ponds, precipitation directly into the channel)
r	Pearson's correlation coefficient
RMSE	root mean square error
SC	South Carolina
SCS	Soil Conservation Service
SCS-CN	Soil Conservation Service curve number
South Fork Edisto	Station 02172300, South Fork Edisto River near Denmark, SC
SSURGO	Soil Survey Geographic Database
SWAT	Soil and Water Assessment Tool
TOPMODEL	topography-based hydrological model
TR-55	Technical Release 55
TWI	topographic wetness index
USDA	U.S. Department of Agriculture
USEPA	U.S. Environmental Protection Agency
USGS	U.S. Geological Survey
WASP	Water-Quality Analysis Simulation Program
WATER	Water Availability Tool for Environmental Resources

Simulation of Streamflow in the McTier Creek Watershed, South Carolina

By Toby D. Feaster, Heather E. Golden, Kenneth R. Odom, Mark A. Lowery, Paul A. Conrads, and Paul M. Bradley

Abstract

The McTier Creek watershed is located in the Sand Hills ecoregion of South Carolina and is a small catchment within the Edisto River Basin. Two watershed hydrology models were applied to the McTier Creek watershed as part of a larger scientific investigation to expand the understanding of relations among hydrologic, geochemical, and ecological processes that affect fish-tissue mercury concentrations within the Edisto River Basin. The two models are the topography-based hydrological model (TOPMODEL) and the grid-based mercury model (GBMM). TOPMODEL uses the variable-source area concept for simulating streamflow, and GBMM uses a spatially explicit modified curve-number approach for simulating streamflow. The hydrologic output from TOPMODEL can be used explicitly to simulate the transport of mercury in separate applications, whereas the hydrology output from GBMM is used implicitly in the simulation of mercury fate and transport in GBMM. The modeling efforts were a collaboration between the U.S. Geological Survey and the U.S. Environmental Protection Agency, National Exposure Research Laboratory.

Calibrations of TOPMODEL and GBMM were done independently while using the same meteorological data and the same period of record of observed data. Two U.S. Geological Survey streamflow-gaging stations were available for comparison of observed daily mean flow with simulated daily mean flow—station 02172300, McTier Creek near Monetta, South Carolina, and station 02172305, McTier Creek near New Holland, South Carolina. The period of record at the Monetta gage covers a broad range of hydrologic conditions, including a drought and a significant wet period. Calibrating the models under these extreme conditions along with the normal flow conditions included in the record enhances the robustness of the two models.

Several quantitative assessments of the goodness of fit between model simulations and the observed daily mean flows were done. These included the Nash-Sutcliffe coefficient of model-fit efficiency index, Pearson's correlation coefficient, the root mean square error, the bias, and the mean absolute error. In addition, a number of graphical tools were used to assess how well the models captured the characteristics of the observed data at the Monetta and New Holland streamflow-gaging stations. The graphical tools included temporal plots of simulated and observed daily mean flows, flow-duration curves, single-mass curves, and various residual plots. The results indicated that TOPMODEL and GBMM generally produced simulations that reasonably capture the quantity, variability, and timing of the observed streamflow. For the periods modeled, the total volume of simulated daily mean flows as compared to the total volume of the observed daily mean flow from TOPMODEL was within 1 to 5 percent, and the total volume from GBMM was within 1 to 10 percent. A noticeable characteristic of the simulated hydrographs from both models is the complexity of balancing groundwater recession and flow at the streamgage when flows peak and recede rapidly. However, GBMM results indicate that groundwater recession, which affects the receding limb of the hydrograph, was more difficult to estimate with the spatially explicit curve number approach. Although the purpose of this report is not to directly compare both models, given the characteristics of the McTier Creek watershed and the fact that GBMM uses the spatially explicit curve number approach as compared to the variable-source-area concept in TOPMODEL, GBMM was able to capture the flow characteristics reasonably well.

Introduction

An important part of the USGS mission is to provide scientific information for the effective water-resources management of the Nation. To assess the quantity and quality of the Nation's surface water, the USGS collects hydrologic and water-quality data from rivers, lakes, and estuaries by using standardized methods and maintains the data from these stations in a national database. In 2007, the USGS developed a science strategy (U.S. Geological Survey, 2007a) outlining the major natural science issues facing the Nation in the next decade. The hydrologic study of McTier Creek, along with a concurrent mercury (Hg) study in the watershed, directly addresses the strategic goals of understanding ecosystems and predicting ecosystem change as well as providing the Nation with information needed to meet the challenges of the 21st century.

In South Carolina, levels of mercury concentrations in fish tissue that may be harmful have resulted in consumption advisories for several river basins within the Coastal Plain Physiographic Province, including the Edisto River Basin (South Carolina Department of Health and Environmental Control, 2006). Understanding the fundamental hydrologic, geochemical, and ecologic processes that affect the levels of fish-tissue mercury concentrations within the Edisto River Basin is an environmental priority.

The risk of mercury in the Edisto River Basin aquatic environment, including the risk to human health, is inextricably linked to hydrology. Water provides habitat for aquatic biota, limits oxygen supply in saturated soil/sediment, and contributes to the onset of iron- and sulfate-reducing conditions, which support microbial production of toxic alkyl-mercury species (Compeau and Bartha, 1985; Benoit and others, 2003; Fleming and others, 2006). Methylmercury (MeHg), in particular, is neurotoxic (Clarkson and others, 2003) and readily accumulated in aquatic food webs (Bloom, 1992; Hall and others, 1997; Brumbaugh and others, 2001). Methylmercury is the primary form of mercury in fish (Bloom, 1992). Wetlands are recognized source areas for environmental methylmercury (St. Louis and others, 1994; Grigal, 2002; Hall and others, 2008; Rypel and others, 2008; Brigham and others, 2009).

Thus, a fundamental control on mercury bioaccumulation in the Edisto River Basin is the transport of methylmercury from the site and matrix of production in the wetlands to the base of the stream aquatic food web (Bradley and others, 2009; Chasar and others, 2009). A recent study (P.M. Bradley, U.S. Geological Survey, unpub. data, 2010) demonstrated that the characteristically coarse-grained sediments of the Coastal Plain in South Carolina favor efficient exchange of water between streams and shallow groundwater systems in this physiographic province. This efficient exchange of water promotes transport of methylmercury from riparian wetland source areas to the stream aquatic habitat and, consequently, creates an inherent vulnerability to mercury bioaccumulation in Coastal Plain streams. Stream systems, such as the Edisto River, are particularly vulnerable to mercury bioaccumulation because they are entirely or largely within this Coastal Plain region and, consequently, are primarily subject to a groundwater flood mechanism that transports methylmercury to the stream channel aquatic habitat.

In light of the critical role of hydrology as a driver of methylmercury concentrations within the stream aquatic habitats of the Edisto River Basin, numerical tools that reliably simulate the direction, timing, and quantity of water transport can contribute substantially to an understanding of the temporal and spatial variability of methylmercury bioavailability in the stream aquatic habitat. This report documents the application of two distinct approaches to modeling the hydrology of the surface and shallow subsurface flow system in McTier Creek, which is a small headwater watershed within the Edisto River Basin of South Carolina.

Purpose and Scope

The purpose of this report is to present analyses and simulations of the hydrology of the McTier Creek watershed. The study area is from the headwater of McTier Creek to the New Holland gage and the surficial aquifer above the confining bedrock. As part of the analysis, two watershed hydrology models—the topography-based hydrological model (TOPMODEL) and the grid-based mercury model (GBMM)—were applied to the McTier Creek watershed. TOPMODEL uses the variable-source-area concept for simulating streamflow, and GBMM uses a spatially explicit modified curve-number approach for simulating streamflow. Hydrologic output from both models is used to better understand the spatial and temporal variability relation of mercury and hydrology. The hydrologic output from TOPMODEL can be used explicitly to simulate the transport of mercury in separate applications, whereas the hydrologic output from GBMM is used implicitly in the simulation of mercury fate and transport in GBMM. The applications of the models were a collaborative effort between the U.S. Geological Survey (USGS) and the U.S. Environmental Protection Agency, National Exposure Research Laboratory.

This report does not compare the two hydrologic models but rather provides documentation of the application of the two models. Although the two models use the same datasets for calibration, no attempt was made to use the same calibration techniques as would be required for a hydrologic model comparison.

USGS streamflow data are measured and reported in English units; consequently, most of the data presented in this report are provided using English units. However, because the TOPMODEL used in this investigation includes both English and International System of Units (SI) and GBMM uses SI units, the report includes both systems of measurement.

Previous Studies

TOPMODEL is a physically based watershed model that simulates the variable-source-area concept of streamflow generation (Wolock, 1993). The model was first described by Beven and Kirkby (1979) and has continually evolved along with the understanding of how precipitation moves over and through watersheds and ultimately contributes to streamflow. By design, the modeling concepts in TOPMODEL have been kept simple to preserve a flexible model structure that can be tailored based on the researcher's perceptions of the behavior of a particular watershed (Singh, 1995). As a result, numerous versions of TOPMODEL exist. Beven (1997) documents a variety of versions and applications of TOPMODEL.

The version of TOPMODEL used in this investigation was documented by Kennen and others (2008) and has most recently been incorporated into the Water Availability Tool for Environmental Resources (WATER) as part of an investigation to model ungaged streams in Kentucky (Williamson and others, 2009). In the investigation by Kennen and others (2008), TOPMODEL was part of an integrated hydroecological model that provided a comprehensive set of hydrologic variables representing major components of the flow regimes at 856 aquatic-invertebrate monitoring sites in New Jersey. Kennen and others (2008) noted that the TOPMODEL code used in their study had been modified from an earlier version used in an investigation by Wolock (1993). The purpose of the Wolock (1993) report was to describe the theoretical background of TOPMODEL, the model equations, the methods used to determine parameter values, and the FORTRAN computer code. The introduction to the Wolock (1993) report also provides an extensive list of papers and reports for which TOPMODEL has been used to study a variety of research areas.

Wolock (1993) stated that the version of TOPMODEL described in his report was derived from the version documented by Hornberger and others (1985), with extensive modifications. Hornberger and others (1985) modified the version of TOPMODEL documented by Beven and Wood (1983) and applied it to a small forested catchment in Shenandoah National Park, VA.

With respect to assessing water chemistry in a catchment, Hornberger and others (1994) applied TOPMODEL (Beven and Kirkby, 1979) to the Snake River catchment near Montezuma, CO. The model was used to examine hydrological mechanisms for the purpose of explaining the observed variability of dissolved organic carbon (DOC) in the Snake River. Conceptually, the DOC model represented a soil reservoir in which DOC accumulated during low-flow periods and was flushed out by infiltrating snowmelt water. The work of Hornberger and others (1994) represented one of the first attempts to quantitatively describe the hydrological controls on DOC dynamics in a headwater stream.

GBMM is a recently developed, spatially explicit, watershed-scale model that computes daily mass balances for hydrology, sediment, and mercury within each geographic information system (GIS) raster grid cell (Dai and others, 2005; Tetra Tech, 2006). The model has been validated in several catchments in the southeastern United States with strong reproduction of daily and monthly hydrographs and is currently being added to the Better Assessment Science Integrating Point and Non-Point Sources (BASINS) modeling framework (U.S. Environmental Protection Agency, 2009: Tim Wool, U.S. Environmental Protection Agency, Region IV, oral commun., 2009). A recent application of GBMM focuses on the hydrological component of watershed mercury fate and transport in the Haw River and Deep River watersheds, located in the upper Cape Fear River Basin in North Carolina (Golden and others, 2010). The authors assessed whether precipitation implemented within a regional air-quality model links efficiently with the standard precipitation sources used to calibrate watershed models (for example, rain-gage data) so that GBMM-simulated runoff and, subsequently, biogeochemical flux estimates are not substantially offset. Based on this study, GBMM currently is being implemented to evaluate the response of mercury fluxes, as well as nitrate fluxes, to diverse land-cover change in the Haw River watershed. Nitrate fluxes are estimated using a simple nitrate flux model linked to GBMM (H.E. Golden, U.S. Environmental Protection Agency, oral commun., 2010).

Description of the McTier Creek Watershed

Headwaters typically are defined as the upper reaches of a basin or watershed and, thus, contain smaller streams and tributaries to larger water bodies. McTier Creek is a small headwater stream located in the Edisto River Basin and is a tributary to the South Fork Edisto River (fig. 1). The entire McTier Creek watershed encompasses about 38 square miles (mi^2), is designated by the 12-digit hydrologic unit code 030502040102, and lies completely in the county of Aiken, SC (Eidson and others, 2005). The study area encompasses about 31 mi^2 of the watershed, and land-cover categories are as follows: 50 percent forest, 20 percent grassland/herbaceous, 16 percent agriculture, 8 percent wetland, 5 percent developed, and about 1 percent open water (Homer and others, 2004; fig. 2).

McTier Creek lies within the inland part of the Coastal Plain Physiographic Province known as the Sand Hills (Griffith and others, 2002; fig. 1). Some studies integrate the Sand Hills within a broader area referred to as the inner or upper Coastal Plain (Bloxham, 1976; Marshall, 1993; Bennett and Patton, 2008). The McTier Creek watershed begins near the Fall Line (fig. 1), which is the name given to the boundary between the Piedmont and Coastal Plain Physiographic Provinces. In general, this boundary is characterized by a series of rapids or falls where the streams cascade off the more resistant rocks of the Piedmont into the deeper valleys worn in the softer sandy sediments of the Coastal Plain (Cooke, 1936). Commonly, the headwaters of watersheds located just below the Fall Line transition from characteristics similar to Piedmont streams in the headwaters to Coastal Plain characteristics

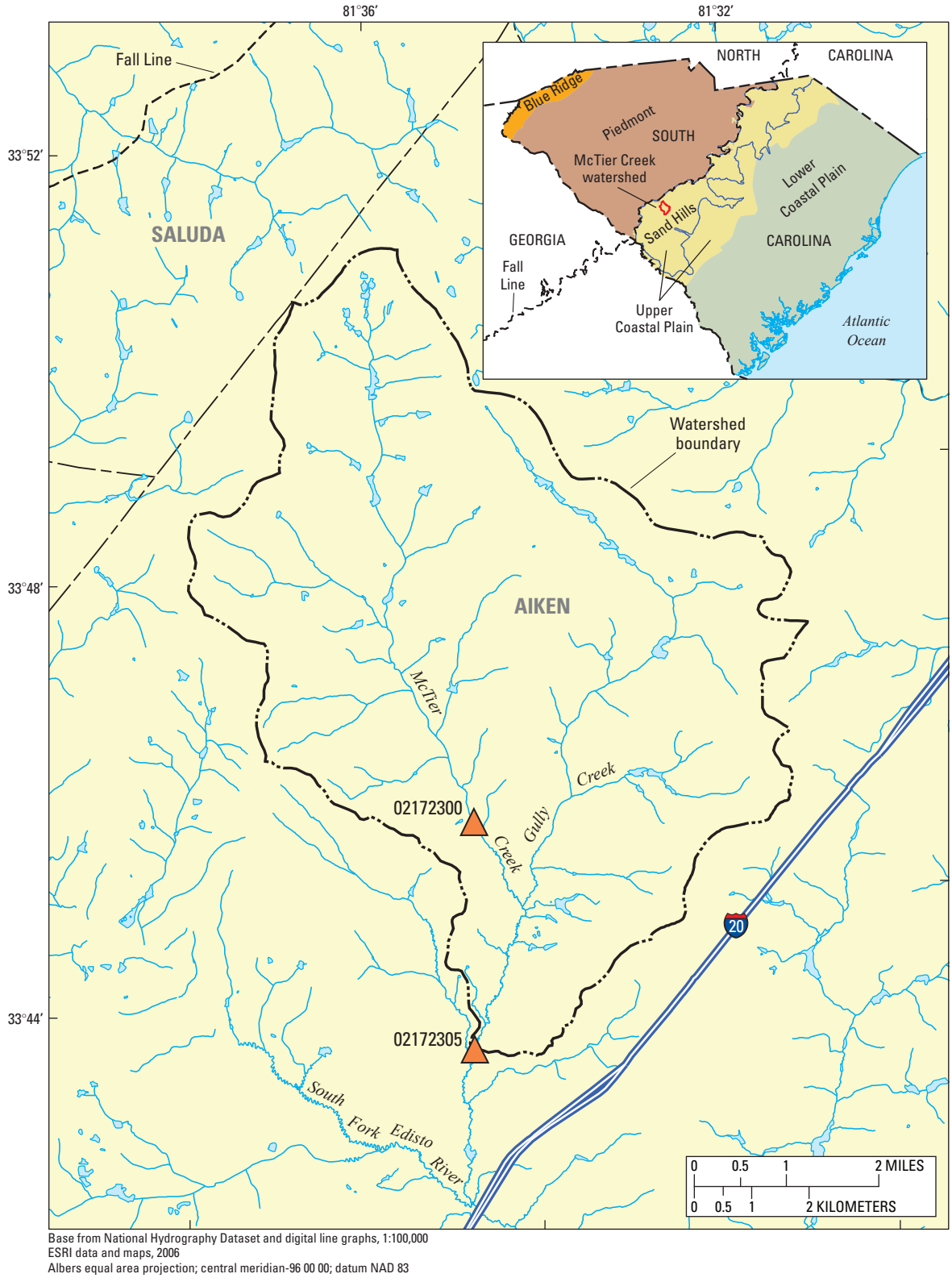

Figure 1. Location of the McTier Creek study area, Aiken County, South Carolina.

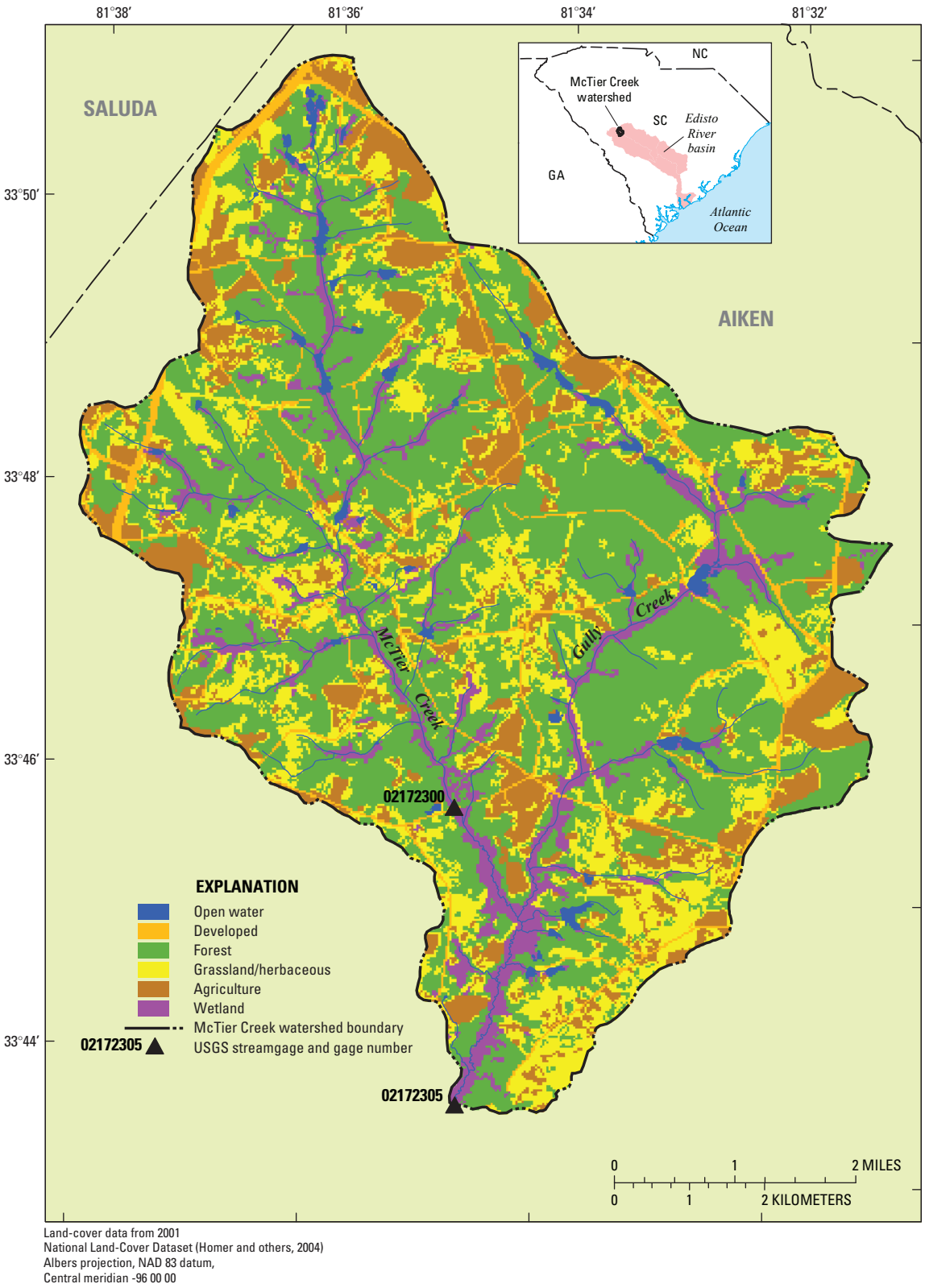

Land-cover data from 2001
National Land-Cover Dataset (Homer and others, 2004)
Albers projection, NAD 83 datum,
Central meridian -96 00 00

Figure 2. McTier Creek watershed land cover, Aiken County, South Carolina.

downstream. In the upper part of the McTier Creek watershed, the channel is characterized by rock outcrops, a characteristic of many Piedmont streams (fig. 3). The hillside cross section in figure 4 illustrates the transition to Coastal Plain characteristics. The survey rod shown in figure 4 is extended approximately 20 feet to illustrate the depth of the sand deposits in the area of the Sand Hills, which is only located about 0.2 mile (mi) from the location shown in figure 3.

Figure 3. McTier Creek near the upper part of the watershed displaying characteristics similar to streams in the Piedmont Physiographic Province in South Carolina.

Figure 4. Cross section of hillside displaying soil characteristics similar to those of the Coastal Plain Physiographic Province in South Carolina. Note that this location is only about 0.2 mile from the location shown in figure 3.

Surficial Geology

The surficial geology of the McTier Creek watershed is described by Horton and Dicken (2001) and Nystrom and others (1986). The oldest rocks that underlie the study area are Cambrian-age migmatitic paragneiss and schist of the Kiokee belt (Horton and Dicken, 2001). Unconsolidated sands and clays of Cretaceous age nonconformably overlie the Kiokee belt rocks (Nystrom and others, 1986). Unconformably overlying the Cretaeous-age sediments are sand and clays of the Eocene-age Huber Formation and Barnwell Group (Nystrom and others, 1986). The informally named Upland unit, consisting of clayey sand and gravel, occurs in the highest elevations of the study area.

Climate

The climate of the McTier Creek watershed is characterized by typical subtropical humid conditions. Based on climate data for Aiken, SC, for the period from 1945 to 2008, the average annual mean air temperature was 64 degrees Fahrenheit (°F) (South Carolina Department of Natural Resources, 2009). The average annual temperatures ranged from a minimum of 53 °F to a maximum of 80 °F. The highest maximum temperature of 109 °F occurred on August 22, 1983. The lowest minimum temperature of 4 °F was recorded on January 9 and 10, 1970, and again on December 26, 1985.

Annual average rainfall in Aiken County is 47 inches. Based on the precipitation summary from 1893 to 2008, the driest year occurred in 1933 when 21 inches of rainfall was recorded (South Carolina Department of Natural Resources, 2009). The wettest year occurred in 1964 when 71 inches of rainfall was recorded. The highest daily rainfall occurred on April 16, 1969, when 9.68 inches of rainfall was recorded. Although a rare occurrence in the Sand Hills, the highest daily snowfall of 15 inches was recorded in Aiken County on February 10, 1973.

Total monthly precipitation data obtained from the National Weather Service Aiken 5SE station for the period from 1948 to 2008 indicate that typically March, June, July, and August have the highest total precipitation and October and November have the lowest (fig. 5). Additionally, the cumulative annual rainfall data as depicted in the single-mass curve (fig. 6) show no significant change in the slope of the cumulative curve, indicating no long-term change in the rainfall patterns at this station.

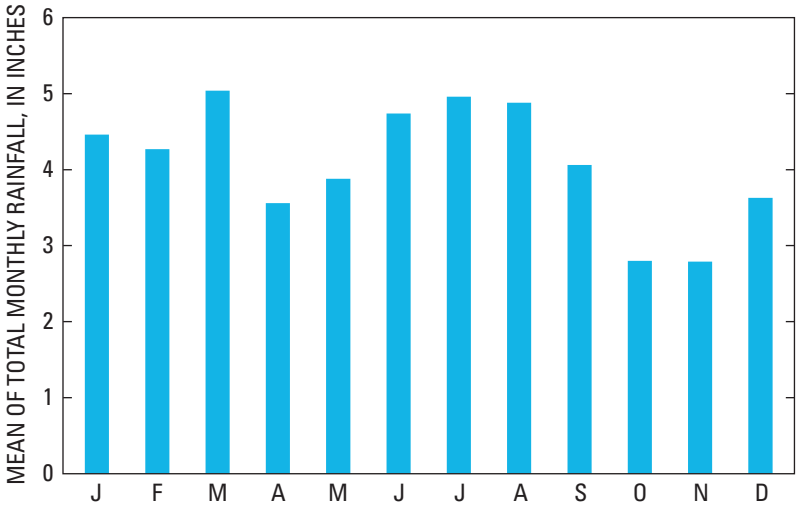

Figure 5. Mean of total monthly rainfall for Aiken, South Carolina, 1948–2008.

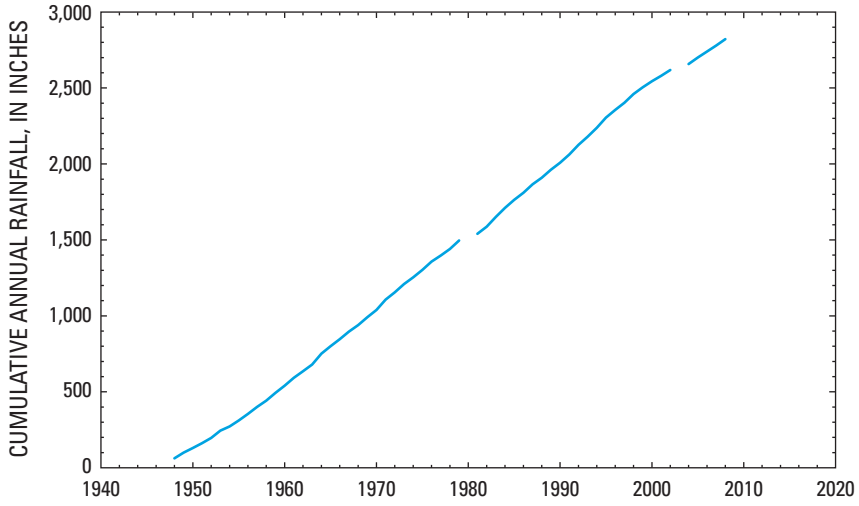

Figure 6. Cumulative annual rainfall for Aiken, South Carolina, 1948–2008. (Line breaks indicate missing data.)

Streamflow

The average of the monthly mean streamflow data in McTier Creek, as recorded at USGS streamflow-gaging station 02172300, McTier Creek near Monetta, SC, for the period October 1995 to September 1997 and March 2001 to September 2008, shows a seasonal variation that is common for natural streams in South Carolina (fig. 7). (Hereafter, streamflow-gaging stations discussed in this report will be referred to by the reference name listed in table 1.) The 1argest average monthly mean streamflow occurs in winter or early spring, and the lowest average monthly mean streamflow occurs in late summer or early fall. The observation that summer months have the highest monthly rainfall totals while the streamflow records show a continuous recession of monthly streamflow throughout the summer is explained by the fact that the highest evapotranspiration rates for a given year occur during the growing season.

To assess the streamflow record at Monetta in the context of a longer flow period, a comparison was made with the South Fork Edisto station. Streamflow data from South Fork Edisto, which has record available from September 1931 to August 1971 and from October 1980 to September 2008, were analyzed in a similar manner as data from the Monetta station. The average monthly mean flow data (fig. 8) show a pattern similar to that for Monetta (fig. 7).

To more directly compare streamflow data from the two stations, the data were normalized by drainage area, which allows for comparison of streamflow in units of cubic feet per second per square mile. For the concurrent periods of record, the average monthly mean flow per square mile is higher at Monetta than at South Fork Edisto (fig. 9).

It is interesting to note that the flow per unit area is smaller for South Fork Edisto than for Monetta. Exploration of the reason for this is beyond the scope of this investigation. Possibilities include differences in watershed sizes or differences in amounts of precipitation for the two watersheds. Also, average evapotranspiration may be higher in the South Fork Edisto Basin because of variations in the land cover (Homer and others, 2004). Additionally, the South Fork Edisto could be losing water to an aquifer that discharges outside of the basin.

In order to put the monthly mean streamflow per unit area at McTier Creek into a longer historical context, additional comparisons of the minimum, average, and maximum monthly mean flow per square mile for the concurrent period of record at Monetta and South Fork Edisto were made along with the same characteristics for the complete period of record at South Fork Edisto (fig. 10*A*, *B*, *C*). The minimum monthly mean flow per square mile at the two stations are quite similar, indicating similarity in the groundwater sources feeding these systems during periods of low flow. The minimum monthly

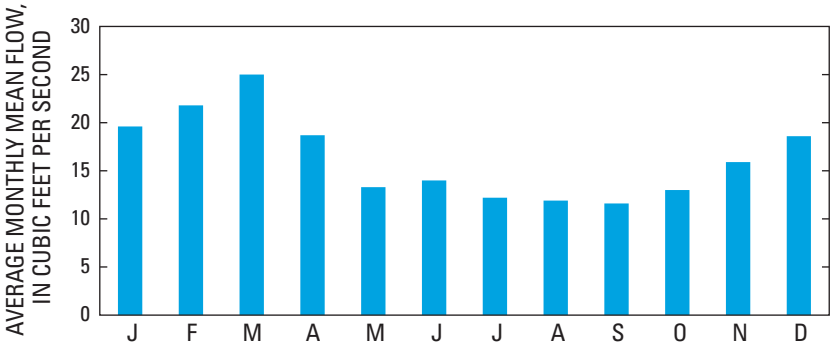

Figure 7. Average monthly mean streamflow at USGS streamflow-gaging station 02172300, McTier Creek near Monetta, South Carolina, 1995–1997 and 2001–2008.

Table 1. U.S. Geological Survey streamflow-gaging stations, reference names, and periods of record.

Station number	Station name	Reference name used in this report	Period of record
02172300	McTier Creek near Monetta, SC	Monetta	October 1995–September 1997; February 2001–September 2009
02172305	McTier Creek near New Holland, SC	New Holland	June 2007–September 2009
02173000	South Fork Edisto River near Denmark, SC	South Fork Edisto	September 1931–August 1971; October 1980–September 2008

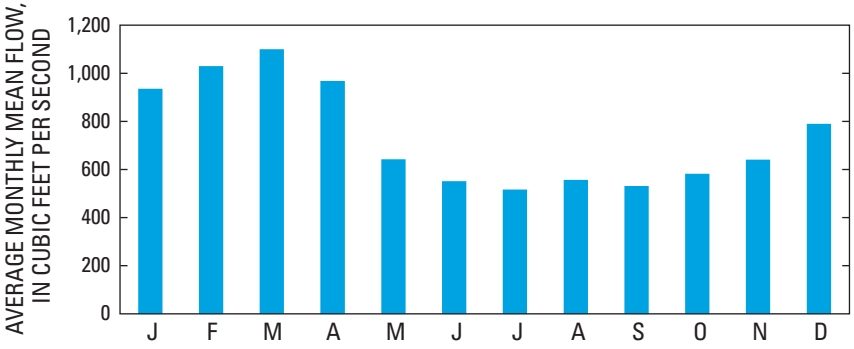

Figure 8. Average monthly mean streamflow at South Fork Edisto River near Denmark, South Carolina, 1931–1971 and 1980–2008.

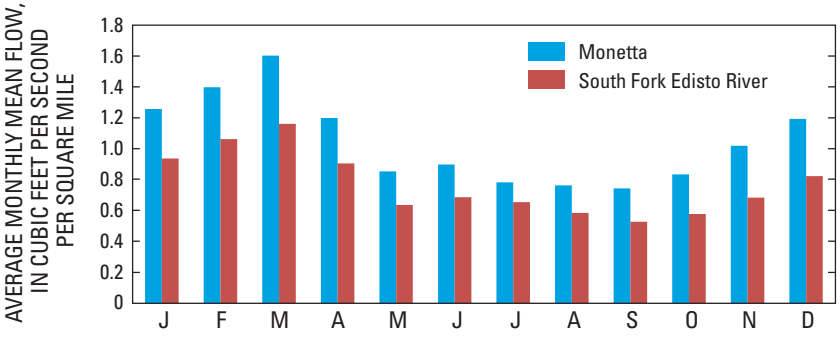

Figure 9. Average monthly mean streamflow at McTier Creek near Monetta and South Fork Edisto River near Denmark, South Carolina, for the concurrent period of record (October 1995–September 1997 and March 2001–September 2008) at both stations.

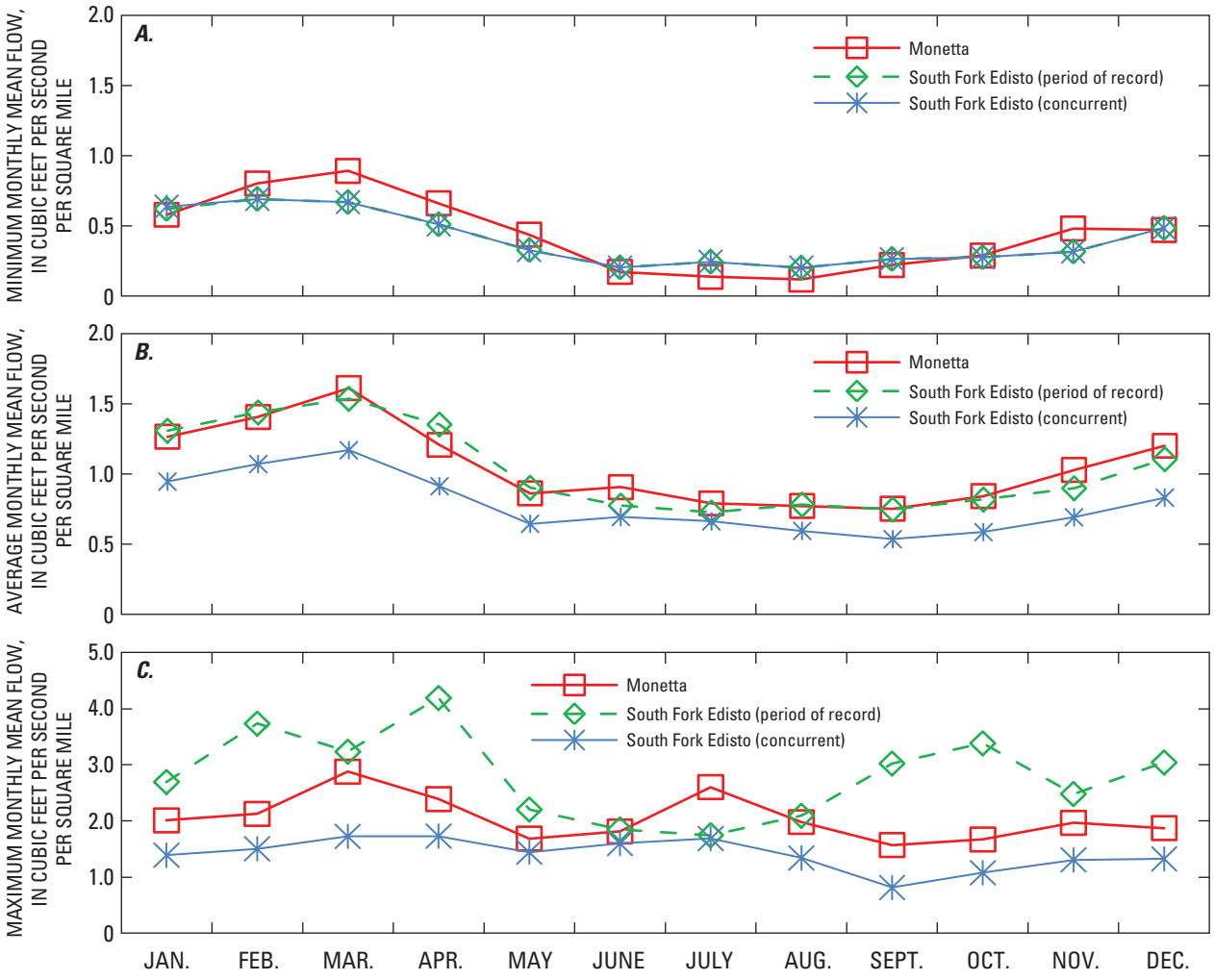

Figure 10. (*A*) minimum, (*B*) average, and (*C*) maximum monthly mean flow per square mile at McTier Creek near Monetta (October 1995–-September 1997 and March 2001–September 2008) and South Fork Edisto River near Denmark (September 1931–August 1971 and October 1980–September 2008), South Carolina.

mean flows per square mile at South Fork Edisto for the complete period of record (about 70 years) and for the period of record that is concurrent with Monetta (about 11 years) are the same (fig. 10*A*). Consequently, this indicates that the period of record at Monetta captures the lowest flow periods that have occurred in at least 70 years. Figure 10*C* shows a significant difference in the maximum monthly mean flow per square mile between the complete record at South Fork Edisto and the period that is concurrent with Monetta for nearly all months except July, implying that the short record at Monetta is biased toward lower flow conditions. Hypotheses concerning the differences in average monthly mean flow were discussed earlier; however, as figure 10*B* indicates for South Fork Edisto, it is reasonable to assume that the longer term average monthly mean flows at Monetta will increase over time.

TOPMODEL Streamflow Concepts

TOPMODEL (a topography-based hydrological model) is a physically based watershed model that simulates streamflow based on the variable-source-area concept of streamflow generation. It is a semi-distributed model that groups hydrologically similar portions of a watershed based on a topographic index. In the variable-source-area concept, saturation land-surface areas are sources of streamflow during precipitation events in several ways. Saturation overland flow (also called Dunne overland flow) is generated if the subsurface hydraulic characteristics are not transmissive and if slopes are gentle and convergent (Dunne and Black, 1970; Wolock, 1993). Saturation overland flow can arise from direct precipitation on the saturated land-surface areas or from return flow of subsurface water to the surface in the saturated areas. Subsurface stormflow is generated if the near-surface soil zone is very transmissive (large saturated hydraulic conductivity) and if gravitational gradients (slopes) are steep. Whipkey (1965) defined subsurface stormflow as underground stormflow that reaches the stream channel without entering the groundwater storage zone.

Topographic Wetness Index

The original conceptualization of TOPMODEL was based on three basic assumptions (Singh, 1995; Beven, 1997).

1. The dynamics of the saturated zone can be approximated by successive steady-state representations.

2. The hydraulic gradient of the saturated zone can be approximated by the local surface topographic slope, tan β.

3. The distribution of downslope transmissivity, *T*, with depth is an exponential function of storage deficit or depth to the water table:

$$T = T_o e^{-S/m}, \tag{1}$$

where

T_o is the lateral (horizontal) transmissivity when the soil is just saturated (dimensions of length squared per time),

e is the exponential function approximately equal to 2.718281828,

S is a local storage deficit below saturation (dimensions of length), and

m is a model parameter controlling the rate of decline of transmissivity in the soil profile (dimensions of length).

These assumptions lead to relations between watershed storage (or storage deficit) and local levels of the water table (or storage deficit due to drainage) in which the main factor is the topographic wetness index (TWI), defined as

$$\mathrm{TWI} = \ln(a / \tan\beta), \tag{2}$$

where a is the upslope contributing area per unit contour length, and tan β is the local slope. High values of the TWI indicate areas with large contributing areas and relatively flat slopes, which typically occur at the base of hillslopes and near the stream (large a value and small tan β value). These areas tend to correspond with locations where groundwater discharge would be expected to occur. Low TWI values tend to be found at the tops of hills where there is relatively little upslope contributing area, and slopes are steep (small a value and large tan β value). These areas generally correspond with groundwater recharge areas (Hornberger and others, 1998). Inamdar (2009) defined high TWI values as those being in the range of 9 to 16 and low TWI values as those being in the range of 2 to 5.

The TWI is used to derive the areas of saturation or variable-source areas. The variable-source-area concept states that streamflow during precipitation events is generated on saturated surface areas called "source areas," which occur in places where the water table rises to the land surface (Wolock, 1993). The rise in the water table occurs because of infiltration of precipitation into the soil and down to the saturated subsurface zone and the subsequent downslope movement of water in the saturated subsurface zone. Saturated land-surface areas commonly develop near existing stream channels and expand as more water enters the subsurface through infiltration and moves downslope as saturated subsurface flow.

TOPMODEL Water Balance

TOPMODEL is a process-oriented watershed hydrology model that systematically accounts for water as it enters the watershed as precipitation until it leaves the watershed through evapotranspiration, by direct withdrawal, or as streamflow. TOPMODEL can simulate snow accumulation and melt, and routing of flow from delivery to the stream to the watershed outlet; however, the snow-related and routing algorithms were not used in this study because of the characteristics of the McTier Creek watershed.

In the water balance, rain on a given day is used first to satisfy the potential evapotranspiration for the day. The remainder moves overland to a stream if the rain falls on impervious surface that is connected to a stream (*qimp*), soil that is already saturated (*qof*), or soil through which the water cannot infiltrate rapidly enough (*qinf*) (fig. 11). Precipitation that falls on a surface-water body is added to the streamflow (*qsrip*). The remaining water infiltrates into the upper soil zone. Any water stored in the saturated subsurface zone is assumed to move downslope toward the stream channel and enters the stream as return flow (*qret*) in saturated areas and (or) subsurface flow (*qb*) at the streambanks. The portion of the subsurface water that drains into the stream depends on the volume in storage and the values of the TOPMODEL input parameters.

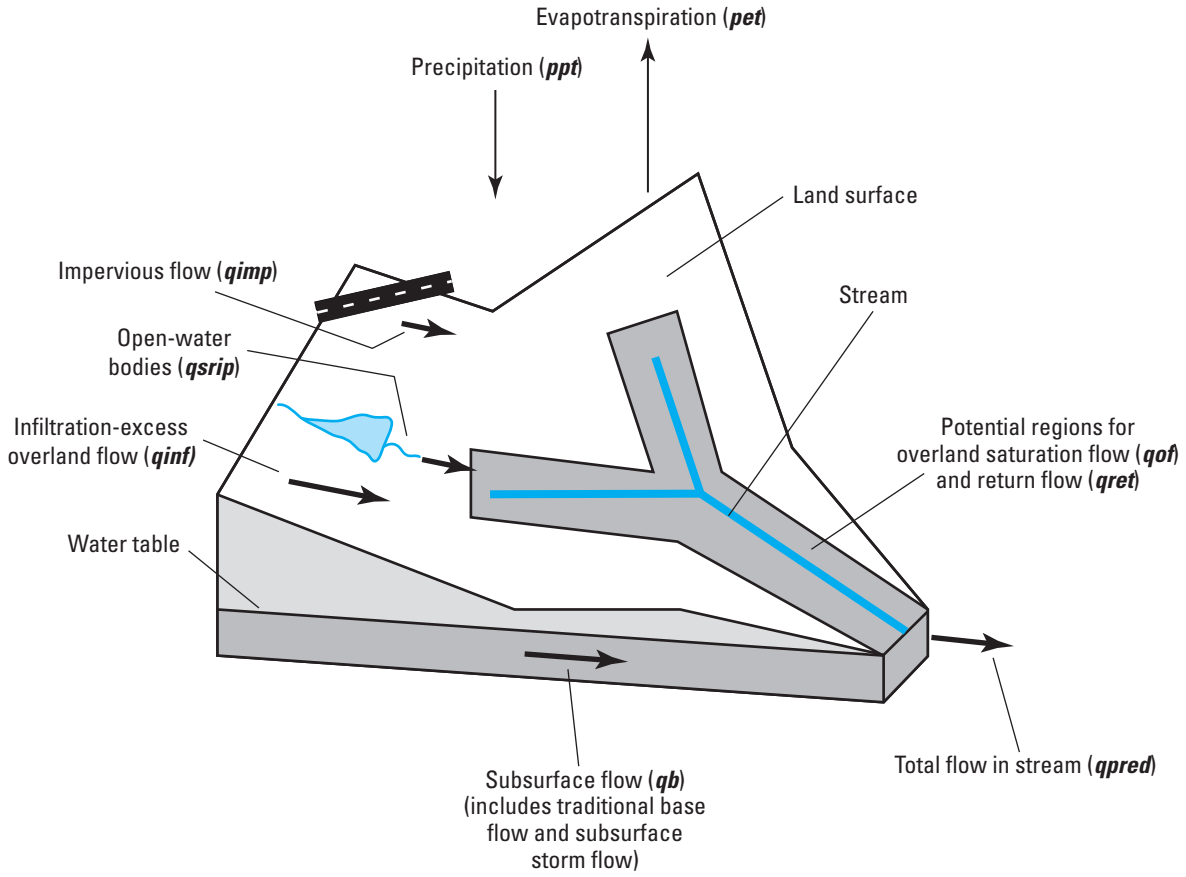

Figure 11. Definition of selected water-source variables from TOPMODEL (modified from Wolock, 1993).

GBMM Streamflow Concepts

The GBMM computes daily mass balances for hydrology, sediment, and mercury within each GIS raster grid cell (Dai and others, 2005; Tetra Tech, 2006). In the hydrology module, GBMM has three hydrological layers: the unsaturated zone, shallow groundwater, and deep groundwater. Runoff generation occurs by overland flow and base flow (groundwater flow). In this study, GBMM implements a simple daily water balance per 10-meter (m) grid cell on pervious surfaces to compute available soil water in the unsaturated zone (S_w, in centimeters) when levels are greater than or equal to wilting point using the equation

$$S_w = S_{wo} + P_{tot} - R_o - ET - P_c, \quad (3)$$

where

S_{wo} is the initial water in the unsaturated zone (in centimeters),
P_{tot} is the total available water inputs at the soil surface (rainfall + snowmelt, in centimeters),
R_o is the surface runoff (in centimeters),
ET is actual evapotranspiration (in centimeters), and
P_c is soil percolation from the unsaturated to saturated groundwater zones (in centimeters).

Runoff is computed using a modified Soil Conservation Service (SCS) curve-number approach (SCS-CN) for each grid cell, now called the Natural Resources Conservation Service (NRCS) curve-number method, which is similar to the Soil and Water Assessment Tool (SWAT), a widely used model for estimating runoff and nutrient loading from watersheds (Neitsch and others, 2005). The SCS-CN also is sometimes referred to as the TR-55 curve number, where TR is an abbreviation for a NRCS Technical Release document (U.S. Department of Agriculture, 1986). The modified SCS-CN method varies the curve-number calculations daily based on 5-day antecedent moisture conditions. Kim and Lee (2008) provide a detailed explanation of the modified SCS-CN methods, and further details can be found in appendix 2.

GBMM computes a simple daily shallow groundwater balance for inclusion in the total streamflow output as

$$G_w = G_{wo} + P_c - G_o - S_p, \quad (4)$$

where

G_w is the shallow groundwater at the end of each time step (in centimeters),
G_{wo} is the shallow groundwater at the beginning of each time step (in centimeters),
G_o is shallow groundwater outflow (in centimeters per day), and
S_p is seepage to a deep aquifer (in centimeters per day).

Shallow groundwater outflow is computed as

$$G_o = g_r * G_w, \quad (5)$$

where g_r is the groundwater recession coefficient (per day), and G_w is shallow groundwater storage (in centimeters). The groundwater recession coefficient can be derived from observed streamflow during the recession of the hydrograph using the formula

$$g_r = \frac{\ln(F_2) - \ln(F_1)}{t_2 - t_1}, \quad (6)$$

where

F_2 is streamflow at t_2 (in cubic meters per day),
F_1 is streamflow at t_1 (in cubic meters per day),
t_2 is the time for streamflow F_2 (per day), and
t_1 is the time for streamflow at F_1 (per day).

Groundwater seepage to a deep aquifer (S_p, in centimeters per day) is computed using the following simple equation:

$$S_p = s_r * G_w, \quad (7)$$

where s_r is the groundwater seepage coefficient (per day).

Flow travel time, both overland and in-stream, is computed from each grid cell to the designated watershed outlet using calculations derived from the NRCS (U.S. Department of Agriculture, 1986). Total flow travel time from each grid cell to the watershed outlet (T_{tot}, in hours) is

$$T_{tot} = T_{ov} + T_{ch}, \quad (8)$$

where T_{ov} is the overland flow travel time (in hours), and T_{ch} is the within-channel flow travel time (in hours). Overland flow travel time (T_{ov}) is calculated using the formula

$$T_{ov} = \frac{0.0289 * (n * L)^{0.8}}{P_2^{0.5} * S^{0.4}}, \quad (9)$$

where

n is Manning's roughness coefficient,
L is flow length (in meters),
P_2 is the 2-year, 24-hour rainfall (in centimeters) computed regionally across the United States, and
S is the slope of the land surface (in meters per meter).

The within-channel flow travel time (T_{ch}) is computed as

$$T_{ch} = \frac{L}{3600 * V}, \quad (10)$$

where V is the flow velocity (in meters per second). Velocity in the stream channel is calculated using Manning's equation:

$$V = \frac{1}{n} R^{\frac{2}{3}} * S^{\frac{1}{2}}, \quad (11)$$

where R is the hydraulic radius of the channel (in meters).

Stream dimensions (for example, hydraulic radius and channel cross-sectional area, depth, and width) are computed using regional regression equations (Dai and others, 2005). Flow routing for both overland and within the stream channel flow is dependent on a base digital elevation map, which is used for computing flow direction and length, in addition to creating daily overland travel time zones (water that is routed through travel time zones from which water is accumulated and transferred). A grid for Manning's roughness coefficient is computed for each 2001 Multi-Resolution Land Chacterization, National Land-Cover Database (NLCD; Homer and others, 2004) land-cover type within the study watershed, and the average of the coefficients for each grid cell along a flow path is used for calculating surface and in-stream flow travel times.

Methods of Study

The following sections of the report document the data needed to develop the TOPMODEL and GBMM, the compilation and review of the data, and the calibration procedures for the models. In addition, the goodness-of-fit statistics used to assess the simulated and measured data are described.

Data Collection

Watershed simulations and calibration of TOPMODEL and GBMM require the following types of data: (1) meteorological parameters (precipitation and air temperature) and (2) watershed characteristics. Streamflow data are not required for the model calibration but are used to assess how well the simulations capture the characteristics of the measured data. In addition to these, TOPMODEL uses the topographic wetness indices to estimate runoff, and GBMM implements a curve number (see Pervious-Area Runoff and Impervious-Area Runoff sections in appendix 2) based on soil type and land cover for each 10-m grid cell. For both models, measured streamflow also is needed to assess the model performance. The following sections of the report document the collection, assembly, and analyses of these various model inputs.

Meteorological Parameters

The meteorological parameters required for the watershed modeling are daily precipitation and average daily temperature. An assessment of National Weather Service (NWS) meteorological stations near the McTier Creek watershed was made to determine data available for use in the model simulations. Stations chosen for inclusion in the study were based on period of available record and location from the centroid of the McTier Creek watershed. Based on those criteria, five NWS stations were chosen (table 2; fig. 12). In addition, two USGS rainfall gages in or near the watershed were available for assessment; however, due to the limited amount of record at the USGS rainfall gages and differences in collection and reporting methods, only the NWS rainfall data were used in the model calibration.

The meteorological data were reviewed and compared using single-mass curves, which present a cumulative plot of data over time and represent the volume of the parameter being reviewed (fig. 13). For precipitation data, a significant change in the slope of the single-mass curve would indicate a change in the hydrologic regime or a systematic problem with the recording device. For the NWS precipitation data, the single-mass curves seemed reasonable because all stations had similar slopes and shapes. It should be noted that if a station had missing record, the cumulative value computed up to the point when the data became missing was used as the starting point once the data began to be collected again. Thus, for significant periods of missing record, this approach causes

Table 2. Meteorological stations in the vicinity of the McTier Creek watershed, South Carolina, considered for use in this investigation.

[°, degrees; ′, minutes; NWS, National Weather Service; USGS, U.S. Geological Survey]

Meteorological station		Latitude (north)	Longitude (west)	Parameters available	Agency
Number	Name				
380074	Aiken 5SE	33°30′	81°42′	rainfall, temperature	NWS
380506	Batesburg	33°54′	81°32′	rainfall	NWS
382712	Edgefield 3 NNE	33°50′	81°55′	rainfall	NWS
384607	Johnston 4 SW	33°47′	81°51′	rainfall, temperature	NWS
386775	Pelion 4 NW	33°43′	81°16′	rainfall, temperature	NWS
387631	Saluda	34°00′	81°46′	rainfall, temperature	NWS
02172300[a]	McTier Creek near Monetta, SC	34°45′	81°66′	rainfall	USGS
335358081331900[a]	USGS Raingage at Batesburg Fire Department at Batesburg, SC	33°54′	81°33′	rainfall	USGS

[a] USGS raingages were not used in the model calibration because of limited data and differences in collection and reporting methods compared to the NWS stations.

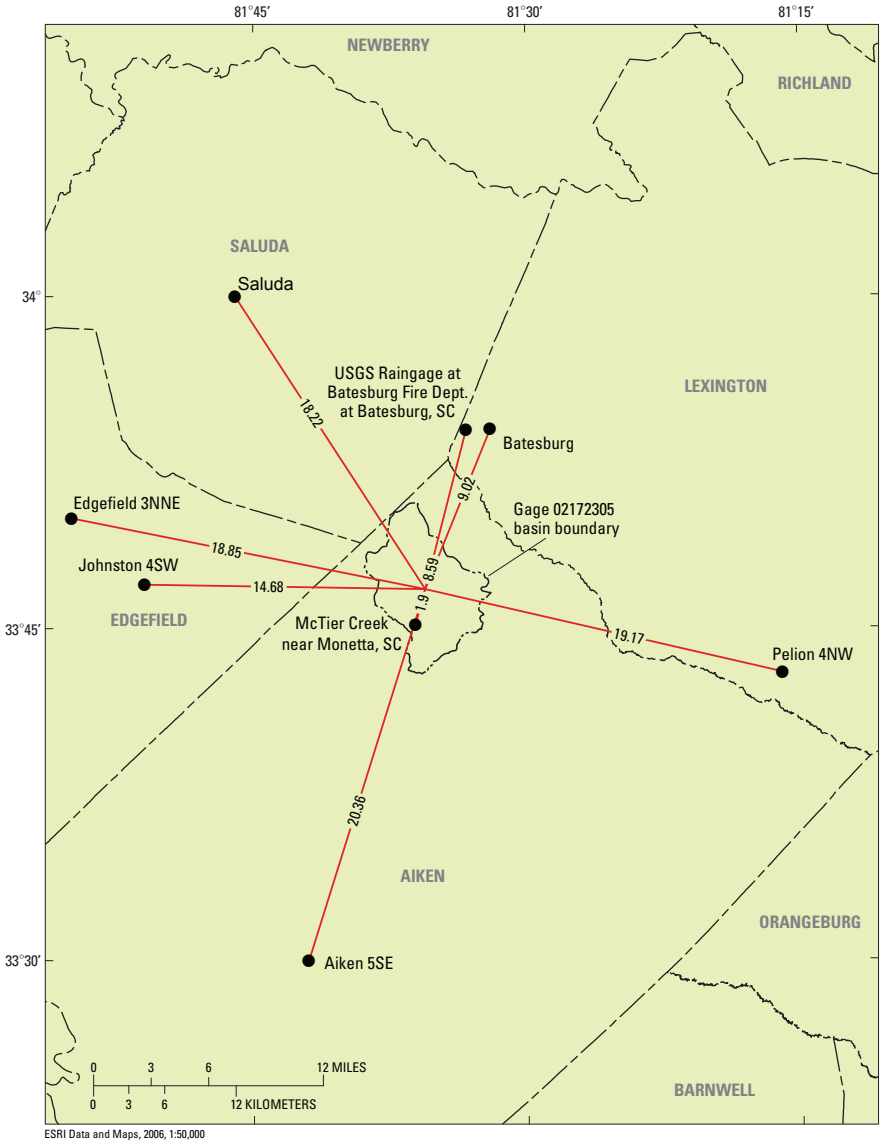

Figure 12. Meteorological stations in the vicinity of McTier Creek watershed, South Carolina, considered for use in this investigation. Distance units are in miles.

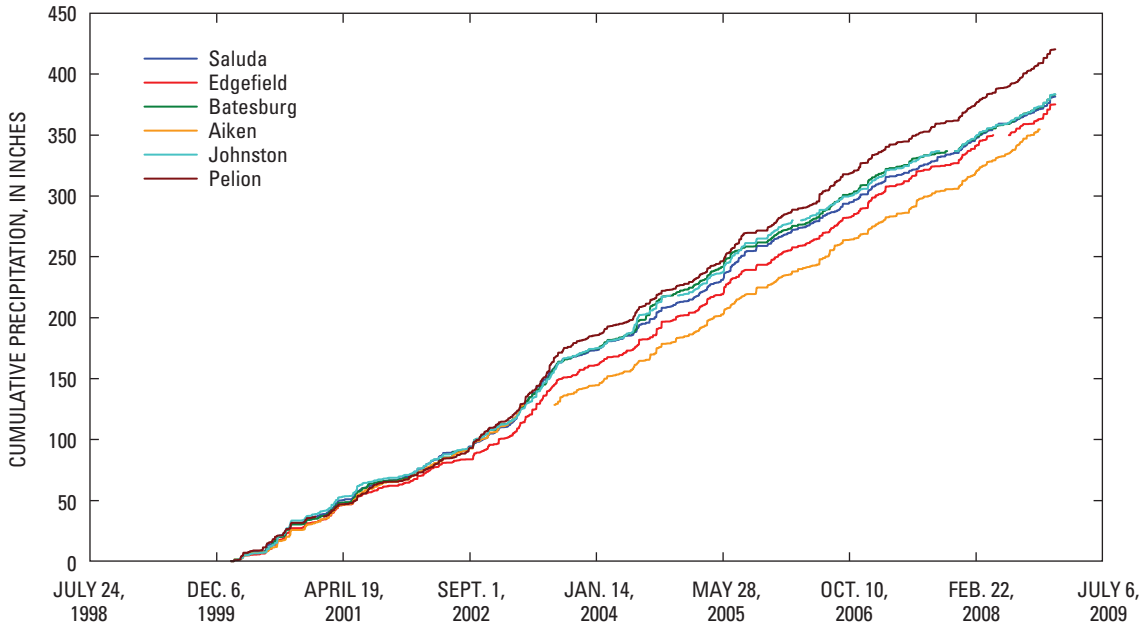

Figure 13. Single-mass curve reviews of the National Weather Service precipitation data.

the curve to deviate from curves at stations with no break in data collection. The slope would, however, still be useful for comparison with slopes for the other stations. In figure 13, this effect is illustrated with data missing from April 2003 through July 2003 for the Aiken 5SE station. Thus, the Aiken 5SE curve appears lower than the other curves beginning about August 2003, mainly due to the 4 months of missing record. The slope of the Aiken 5SE curve is still similar to those of the other stations.

The precipitation data were weighted using inverse distance weighting based on the distance from each NWS station to the centroid of the McTier Creek watershed (Shepard, 1968). Single-mass curves of the weighted data along with the single-mass curves for the individual stations also were reviewed. When plotted with the individual curves shown in figure 13, the weighted curve appears to be a reasonable representation (fig. 14).

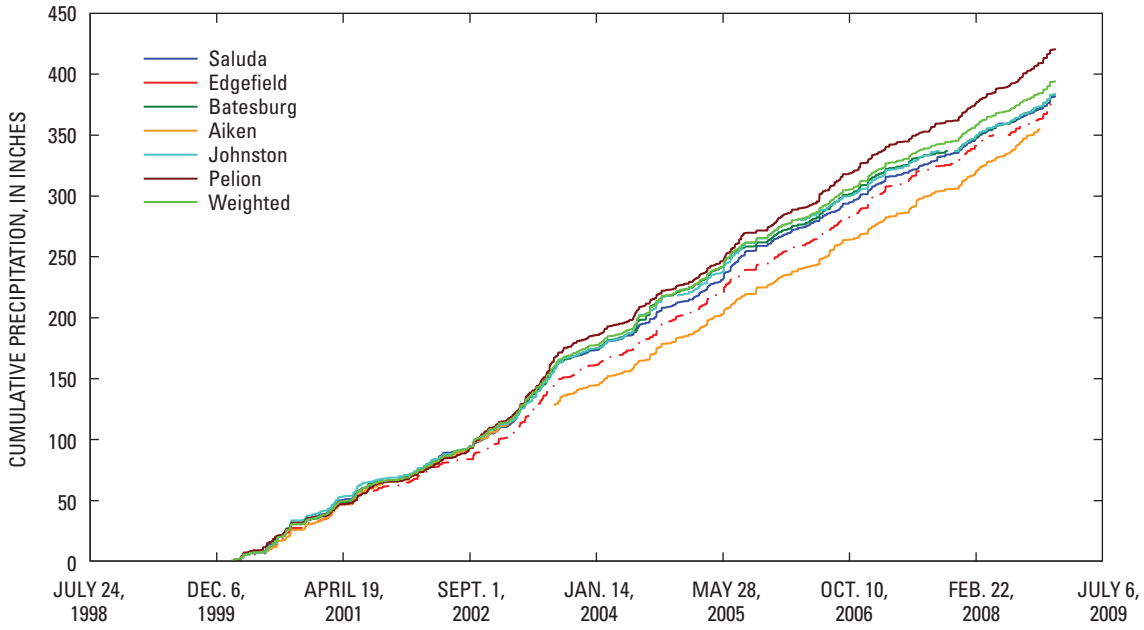

Figure 14. Single-mass curve reviews of the National Weather Service precipitation data along with a weighted curve computed using inverse distance weighting.

$$Z_k = \frac{\sum_{i=1}^{n} \frac{Z_i}{d_i^2}}{\sum_{i=1}^{n} \frac{1}{d_i^2}}, \quad (12)$$

where

Z_k is the meteorological value at the centroid of McTier Creek watershed,

Z_i is the meteorological value at the NWS station, and

d_i is the distance from the centroid of the watershed to the NWS station (in miles).

Similar analyses were made of the maximum and minimum air temperature data that were available at four of the six NWS stations listed in table 2. Average daily air temperatures were computed from that data and compared using single-mass curves. From those comparisons, it was noted that the minimum air temperatures for the Johnston 4SW gage tended to differ from those for the other three stations (fig. 15). To further check the quality of the Johnston 4SW minimum data, the inverse weighted minimum temperature was computed with and without the data from the Johnston 4SW gage. As can be seen in figure 16, when the Johnston 4SW gage was not included in the weighting, the inverse weighted minimum temperatures were higher, as indicated by a larger number of the data points plotting above the one-to-one line. Because of the uncertainty in these values, the Johnston 4SW station was not included in the final weighting of the average temperatures. For the final weighted average temperature, the average temperature for the three remaining stations was computed from the minimum and maximum air temperature and then weighted using inverse distance weighting to get a final set of average temperature data that was used in TOPMODEL and GBMM.

Watershed Characteristics

Along with the precipitation and air temperature data, other TOPMODEL and GBMM inputs included watershed characteristics describing the topographic features, soils characteristics, and watershed latitude. A 1:24,000-scale digital raster graphics coverage was used to delineate the watershed boundaries. Water-body features were determined using a 1:24,000-scale National Hydrography Dataset (NHD) and 2006 digital orthophoto quarter quadrangles. Impervious surface was determined from a 30-m impervious grid from the 2001 NLCD.

Soils characteristics were determined from the Soil Survey Geographic (SSURGO) Database (Natural Resources Conservation Service, 2008). After pre-processing of the SSURGO data (Michael E. Wieczorek, U.S. Geological Survey, written commun., December 2008), the watershed model soil parameters were computed in ArcGIS® using the zonal statistics tool. Both vertical and horizontal data were weighted to determine average watershed values. The names, units of measure, and data sources for the measured watershed characteristics used in TOPMODEL are listed in table 3, and those used as inputs to GBMM are listed in table 4.

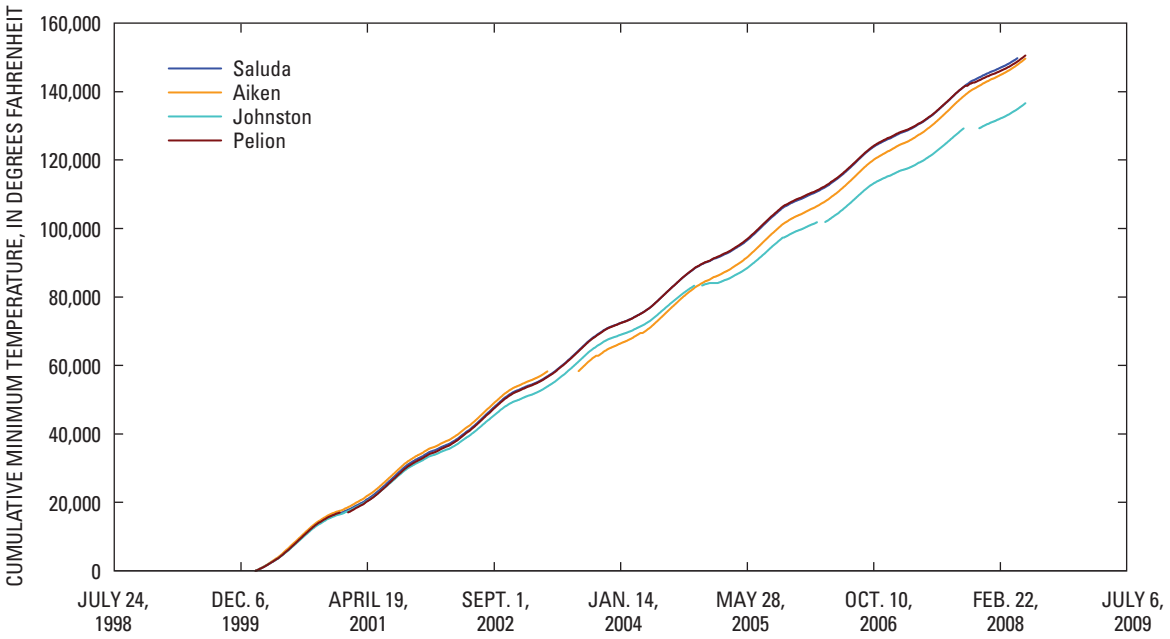

Figure 15. Single-mass curve reviews of the National Weather Service minimum air temperature data.

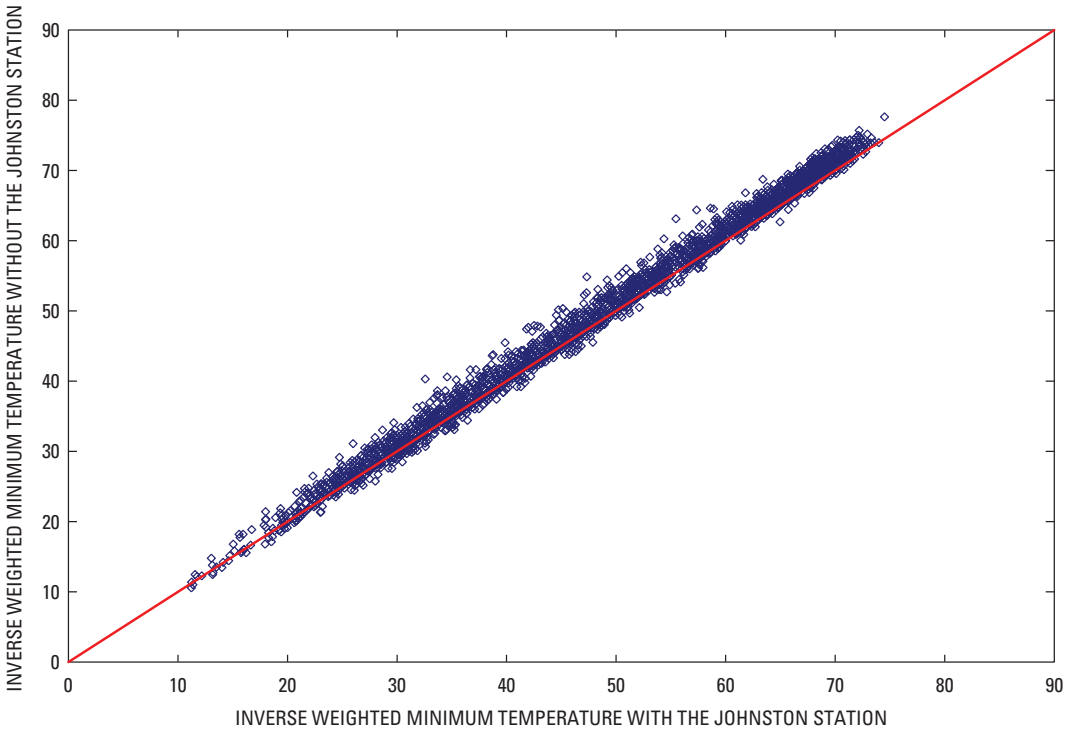

Figure 16. Comparison of inverse weighted minimum temperatures with and without the Johnston 4SW station data.

Table 3. Watershed characteristics for use with the topography based hydrological model.

[SSURGO, Soil Survey Geographic Database]

Watershed characteristic	Unit	Data source
total area	square kilometer	1:24,000 digital raster graphics (*http://topomaps.usgs.gov/drg/*)
lake area	square kilometer	1:24,000-scale National Hydrography Dataset (*http://nhd.usgs.gov/*)
stream area	square kilometer	1:24,000-scale National Hydrography Dataset
saturated conductivity	inches per hour	SSURGO (*http://www.soils.usda.gov/survey/geography/ssurgo/*)
soil depth	inches	SSURGO (calibration)
field capacity	unitless	SSURGO
water holding capacity	unitless	SSURGO
porosity	unitless	SSURGO
percent impervious	percent	National Land-Cover Dataset 2001 (*http://www.mrlc.gov/nlcd.php*)
percent road impervious	percent	National Land-Cover Dataset 2001 and National Map transportation layer (*http://nationalmap.gov/*)
latitude	decimal degrees	1:24,000 digital raster graphics
uplake area	square kilometer	1:24,000 digital raster graphics, 1:24,000-scale National Hydrography Dataset, and 2006 digital orthophoto quadrangles (*http://eros.usgs.gov/products/aerial/doq.php*)
effective impervious	decimal percent	Calibration
percent macropore	decimal percent	Calibration
scaling parameter (*m*)	inches	Calibration
depth of root zone	meter	Calibration
impervious runoff constant	unitless	Kennen and others (2008)
TR-55 curve number	unitless	Kennen and others (2008)
lake delay	unitless	Calibration

Table 4. Watershed and grid cell characteristics for use with the grid based mercury model.

[m, meter; cm, centimeter; SSURGO, Soil Survey Geographic Database; cm/m, centimeter per meter; g/cm^3, gram per cubic centimeter; K_{sat}, saturated conductivity; µm/s, micrometer per second]

Watershed characteristic	Unit	Data source
stream properties and connections	unitless	National Hydrography Datset (*ftp://nhdftp.usgs.gov/FOD_Data/*)
land-cover type (per grid cell)	unitless	National Land-Cover Dataset 2001 (30-meter resolution) (*http://www.mrlc.gov/nlcd.php*)
elevation	m	National Elevation Dataset (*http://seamless.usgs.gov/*)
hydrologic soil group (per grid cell)	unitless	SSURGO (*http://www.soils.usda.gov/survey/geography/ssurgo/*)
curve numbers (per grid cell)	unitless	Calibration
break points for curve number modifications	cm	Calibration
crop management factor (per grid cell)	unitless	SSURGO
land-use practice factor (per grid cell)	unitless	SSURGO
vegetation evapotranspiration coefficient (growing season; per grid cell)	unitless	SSURGO
vegetation evapotranspiration coefficient (non-growing season; per grid cell)	unitless	SSURGO
available water capacity (per grid cell)	cm/m	SSURGO
bulk density (per grid cell)	g/cm^3	SSURGO
K_{sat} (permeability; per grid cell)	µm/s	SSURGO
depth to bedrock	m	Estimated from SSURGO
percent clay (per grid cell)	percent	SSURGO
unsaturated soil depth	m	Calibration
initial shallow groundwater	cm/m	Calibration
groundwater seepage coefficient	per day	Calibration
groundwater recession coefficient	per day	Calibration
channel width and depth	m	Calculated within model from Rosgen (1996) for Eastern United States
Manning's roughness coefficient for channel	unitless	Bedient and Huber (1992)

Streamflow

Streamflow data included in this investigation were collected at the Monetta, New Holland, and South Fork Edisto stations (table 1). The South Fork Edisto data were not used in the model calibration but were used to assess the McTier Creek streamflow data in the context of a longer flow period. As previously discussed, the Monetta station has a historical record from October 1995 to September 1997. Streamflow data at Monetta used in this analysis were collected from February 2001 to September 2009. New Holland was established specifically for this study with streamflow data collection beginning in June 2007 and continuing through September 2009. Streamflow data at these stations were continuously collected at 15-minute intervals using techniques described by Rantz and others (1982). The process involves measuring water level (or stage) on a continuous basis. A series of streamflow measurements throughout a range of stages are measured and then used to develop a stage-streamflow relation also known as a rating curve. The rating curve is then used to determine streamflow from measured stage. Once the stage-streamflow rating is developed, periodic measurements are made on a regular basis to verify the stage-streamflow relation, and as necessary, adjustments (or shifts) to the stage record are applied to account for deviations from the stage-streamflow relation.

Topographic Wetness Index

TOPMODEL is based on the idea that the topography of a watershed exerts a dominant control on flow moving through upland basins (Beven and Kirkby, 1979). The topographic wetness index (TWI) combines local upslope contributing area and slope, and quantifies the topographical control on hydrological processes. For this investigation, the TWI was computed using ArcGIS in conjunction with a 10-m-resolution digital elevation model (DEM) and a 1:24,000-scale National Hydrography Dataset of stream features or flowlines.

The NHD streams were first converted to a grid by overlaying 10-m by 10-m grid cells on the NHD flowlines and designating as stream cells any grid cell containing a portion of an NHD flowline. Stream cells were then assigned a value of 0, and all other cells were assigned a value of 1 to distinguish water features from land features. To ensure that known streams were accurately represented in the DEM, the stream grid described above was used to "burn" the streams into the DEM by forcing the stream cells onto the DEM, thereby ensuring downstream flow once the cells' elevations are taken into account.

Any sinks in the DEM were then "filled" to ensure all land-surface cells sloped toward the streams. Sinks are non-stream grid cells (or groups of cells) with a lower elevation than the eight surrounding cells and are usually the result of erroneous data. The elevations of sinks were artificially raised using the Map Algebra tool in ArcGIS, which utilizes elevations of surrounding cells to determine the correct outfall or pour point within a group of cells.

The flow-direction grid, which indicates the direction of flow from each grid cell into adjacent cells, was then created from the "filled" DEM and used to derive the flow-accumulation grid, whose cell values indicate the number of upstream cells flowing into, or contributing to, downstream cells. Using a predetermined threshold value with the flow-accumulation grid, wetted grid cells, assumed to be headwaters in the more upslope areas of the watershed, were established.

The slope grid, which identifies the steepest downhill slope for a location on a surface, was created from the original DEM. All zero values in the slope grid were set to 0.01 because the TWI computation includes the slope in the denominator and, therefore, cannot have a value of zero.

Finally, the TWI was calculated by using the Map Algebra tool in ArcGIS to determine the natural log of the local upslope contributing area (flow-accumulation grid) divided by the local slope (tangent of the slope grid).

GBMM Curve-Number Estimates

GBMM implements numerous steps to prepare raster grids for estimating curve number runoff from each grid cell within the McTier Creek watershed. This is an automated process in the GBMM pre-processing module, which includes (1) burning the streams into the 10-m DEM, (2) filling sinks within the DEM, (3) creating a flow-direction grid, (4) developing a flow-accumulation grid, and (5) overlaying a 2001 NLCD raster grid with a raster grid of hydrologic soil group data from the SSURGO database. Steps 1–4 are similar to those implemented for TOPMODEL (see Topographic Wetness Index section). The final raster grid from step 5 includes unique land-cover/hydrologic soil group combinations for each grid cell. This raster is then linked to a table containing curve number values for each unique land-cover/hydrologic soil group combination. Based on each cell's curve number, runoff is routed daily using the flow accumulation grid developed in step 4 and equation 8. The equations for base curve-number modifications during wet periods, dry periods, the growing season, and non-growing season for each grid cell are in appendix 2.

Calibration of TOPMODEL and GBMM

Calibrations of TOPMODEL and GBMM were conducted independently using the same precipitation data, temperature data, and period of record. In the McTier Creek watershed, two USGS streamflow gages were available for comparison of observed daily mean flows with simulated daily mean flows: (1) Monetta and (2) New Holland (table 1). Initial calibration of model parameters for TOPMODEL and GBMM was done for Monetta using measured or estimated watershed characteristics as defined in tables 3 and 4. The continuous period of record from 2001 to 2009 at Monetta covers a full range of hydrologic conditions, including (1) a significant dry period in 2001–2002, which appears to be the driest period in about 70 years, based on comparisons with the long-term record at South Fork Edisto, and (2) a significantly wet period that occurred in 2003 (National Oceanic and Atmospheric Administration, 2008). The short period of record from October 1995 to September 1997 at Monetta is more representative of normal flow conditions and is similar to the 2004–2005 period. Consequently, only the February 2001 to September 2009 period was included in the model calibrations. To simplify references to the periods of record used in the calibration process, those periods will be referred to by the reference names listed in table 5.

For TOPMODEL, the parameter estimation program PEST was used to assist in calibrating the model parameters for which measured values were not available (Doherty, 2005). PEST is a nonlinear parameter estimator that adjusts model parameters until the fit between model estimates and field observations are optimized using a weighted least squares

Table 5. Station number and name, period of record used in the model calibration and confirmation simulations, and model simulation period reference name for the McTier Creek watershed, South Carolina.

Station number	Station name	Period of record used in model simulation	Model simulation period reference name
02172300	McTier Creek near Monetta, SC	Feb. 7, 2001–Sept. 30, 2009	Calibration period
02172300	McTier Creek near Monetta, SC	June 13, 2007–Sept. 30, 2009	Concurrent period
02172305	McTier Creek near New Holland, SC	June 13, 2007–Sept. 30, 2009	Confirmation period

scheme. For the McTier Creek TOPMODEL, the differences in estimated and observed daily mean flows were optimized.

Parameter adjustments for GBMM model calibration were conducted using an automated parameter optimization method (OSTRICH; Matott, 2005) with a global dynamically dimensioned search (DDS) algorithm (Tolson and Shoemaker, 2007) and a weighted sum of squared errors objective function. Subsequent trial-and-error parameter-fitting and calibration exercises were conducted to cross-check and complete this exercise due to the length of calibration model runs. The trial-and-error fitting also included minor modifications to the curve number table input for each unique land cover–soils combination, which could not be adjusted during the auto-calibration exercise.

The goodness-of-fit statistics used to assess subsequent trial-and-error parameter fitting and to explore different aspects of simulation errors for the two models were (1) the Nash-Sutcliffe coefficient of model-fit efficiency index (Nash and Sutcliffe, 1970), (2) Pearson's correlation coefficient (r), (3) the root mean square error (RMSE), (4) the bias, and (5) the mean absolute error (MAE). The Nash-Sutcliffe coefficient of model-fit efficiency, E, is calculated as

$$E = \frac{\sum_{i=1}^{N}(Qo_i - Qo)^2 - \sum_{i=1}^{N}(Qo_i - Qs_i)^2}{\sum_{i=1}^{N}(Qo_i - Qo)^2}, \quad (13)$$

where

Qo_i is the observed flow for time step i,
Qo is the mean observed flow for the simulation period,
Qs_i is the simulated flow for time step i, and
N is the number of time steps in the simulation period.

Pearson's correlation coefficient, r, is calculated as

$$r = \frac{\sum_{i=1}^{N}(Qo_i - Qo)(Qs_i - Qs)}{\left[\sum_{i=1}^{N}(Qo_i - Qo)^2 \sum_{i=1}^{N}(Qs_i - Qs)^2\right]^{\frac{1}{2}}}. \quad (14)$$

where Qs is the mean simulated flow for the simulation period, and other variables are as previously defined.

The RMSE is calculated as

$$RMSE = \sqrt{\frac{\sum(Qs_i - Qo_i)^2}{N}}. \quad (15)$$

The bias is calculated as

$$bias = \frac{\sum_{i=1}^{N} Qs_i - Qo_i}{N}. \quad (16)$$

The MAE is calculated as

$$MAE = \frac{\sum_{i=1}^{N} |Qs_i - Qo_i|}{N}. \quad (17)$$

In addition to the goodness-of-fit statistics, plots of simulated and observed daily mean flows were prepared. Flow-duration curves of simulated and observed daily mean flows were plotted along with various residual plots. These graphs were reviewed to determine potential bias during specific time periods and (or) specific flow regimes.

Simulation of the Streamflow for TOPMODEL and GBMM

TOPMODEL and GBMM were calibrated based on comparison of observed daily mean flows at Monetta for the calibration period (table 5). The calibration parameters were then applied at New Holland to simulate daily mean flows for the confirmation period. In order to better assess the application of the calibrated parameters at Monetta to the model simulations at New Holland, additional statistical and graphical assessments were made at Monetta for the concurrent period.

Simulations for Monetta for the Calibration Period

The measured and calibrated input parameters for simulations for Monetta for the calibration period are listed in table 6 for TOPMODEL and in table 7 for GBMM. For GBMM, parameters requiring grid cell-specific values (such as those based on soil and (or) land-cover types) and those calculated within the model but listed in table 4 are not listed in table 7.

Plots of the observed and simulated daily mean flows at Monetta show that both models perform relatively well with respect to capturing the timing and variability of the flows (figs. 17, 18). Observed and simulated daily mean flow data for TOPMODEL and GBMM are shown in more detail in figure 19. While simulated flows in some years match the observed data well (for example, years 2006–2009), other years exhibit a slightly weaker relation (for example, years 2003–2004) in matching peaks and temporal patterns between simulated and observed flows. A noticeable characteristic of

Table 6. Parameter values used for the TOPMODEL calibration for McTier Creek near Monetta for the calibration period.

[*, indicates adjustment during calibration; calibration period is Feb. 7, 2001–Sept. 30, 2009]

Model parameter	Value
Total area (square kilometers)	40.46
Lake area (square kilometers)	0.63
Stream area (square kilometers)	0.47
Saturated conductivity (inches per hour)	6.57
Soil depth (inches)	74.0*
Field capacity (unitless)	0.18
Water holding capacity (unitless)	0.094
Porosity (unitless)	0.39
Percent impervious	1.5*
Percent road impervious	1.0*
Latitude	33.754
Effective impervious (decimal percent)	0.8*
Conductivity multiplier	2.9*
Percent macropore (decimal percent)	0.5*
Scaling parameter (*m*)	47.0*
Depth of root zone (meters)	1.9*
Impervious runoff constant	0.10
TR-55 curve number	98
Uplake area (square kilometers)	34.0
Lake delay (unitless)	1.2*

Table 7. Parameter values used for GBMM calibration for McTier Creek near Monetta for the calibration period.

[*, indicates adjustment during calibration; calibration period is Feb. 7, 2001–Sept. 30, 2009]

Model parameter	Value
Break point for curve number: dry, growing season (centimeters)	4.56
Break point for curve number: wet, growing season (centimeters)	15.00
Break point for curve number: dry, non-growing season (centimeters)	1.07
Break point for curve number: wet, non-growing season (centimeters)	12.17
Depth to bedrock (meters)	1.8
Unsaturated soil depth (meters)	0.095*
Initial shallow groundwater (centimeters per meter)	10.67*
Groundwater seepage coefficient (per day)	0.026*
Groundwater recession coefficient (per day)	0.017*
Manning's roughness coefficient for channel	0.045

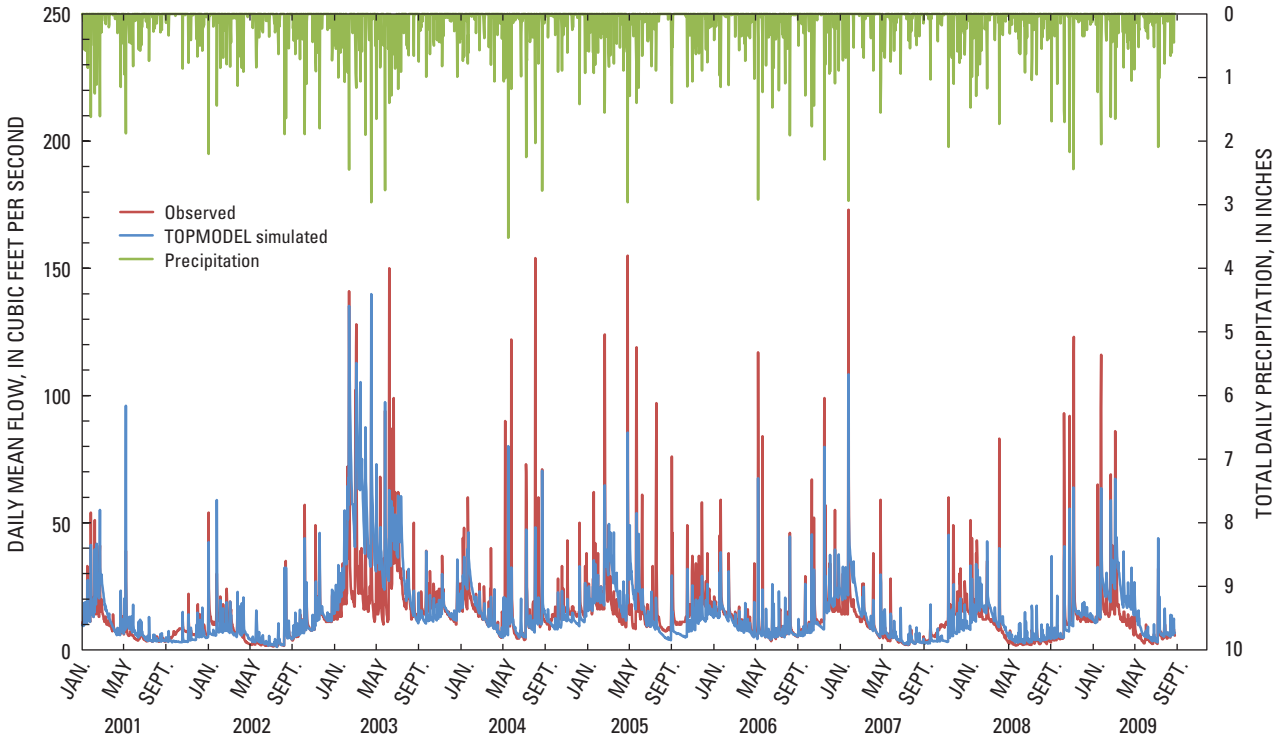

Figure 17. TOPMODEL simulated and observed daily mean flows at McTier Creek near Monetta for the calibration period (Feb. 7, 2001–Sept. 30, 2009), along with observed precipitation data.

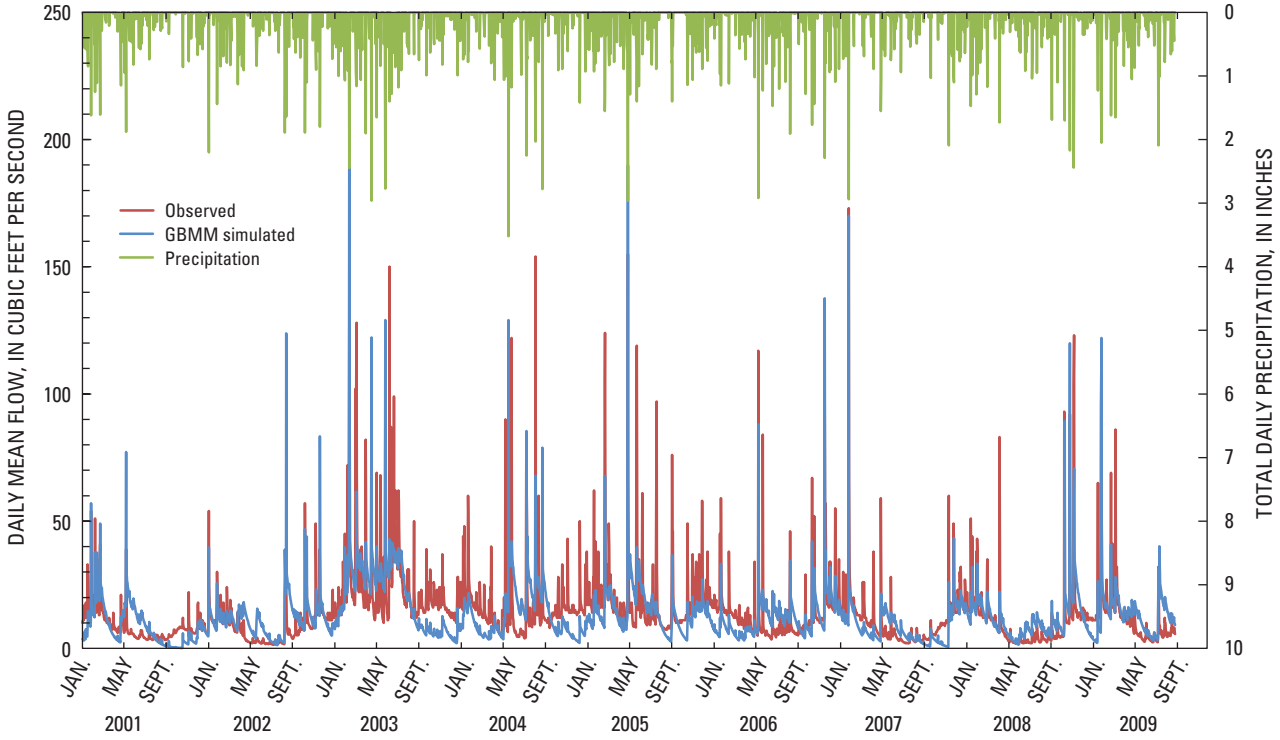

Figure 18. GBMM simulated and observed daily mean flows at McTier Creek near Monetta for the calibration period (Feb. 7, 2001–Sept. 30, 2009), along with observed precipitation data.

some of the GBMM-simulated hydrographs is the complexity of balancing groundwater recession and flow at the streamgage when flows peak and recede rapidly. This also is the case for certain periods for the TOPMODEL results. However, GBMM results suggest that groundwater recession, which affects the receding limb of the hydrograph, was more difficult to estimate with the spatially explicit curve-number approach (fig. 18). For example, for the 2003 spring and summer simulation, if the GBMM groundwater recession coefficient is increased above the calibrated value of 0.017, GBMM overpredicts peak flows. In TOPMODEL, hydrograph recession is related to soils, controlled by the assumption of exponential decay of hydraulic conductivity with soil depth. The calibration parameters associated with the groundwater recession in TOPMODEL seem appropriate for the majority of the flow conditions during the calibration period. To balance peak runoff and recession rates, however, excessively wet years such as 2003 seem to present a challenge for both a curve-number based model and a variable-source-area based model such as TOPMODEL. Conversely, both GBMM and TOPMODEL tend to perform well during periods when flow is more evenly distributed during most of the year.

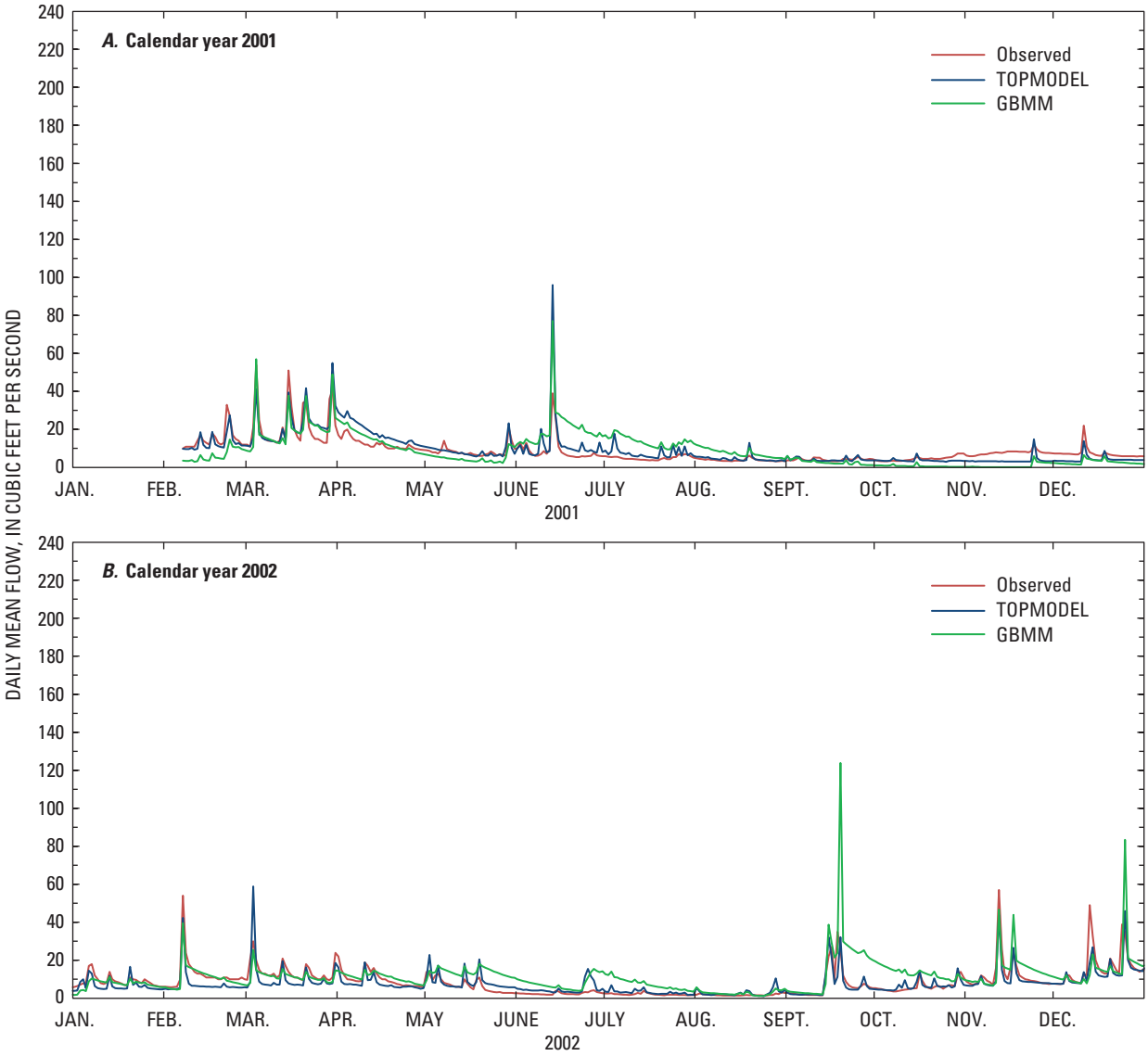

Figure 19. Simulated and observed daily mean flows at McTier Creek near Monetta for the calibration period (Feb. 7, 2001–Sept. 30, 2009), shown by calendar year.

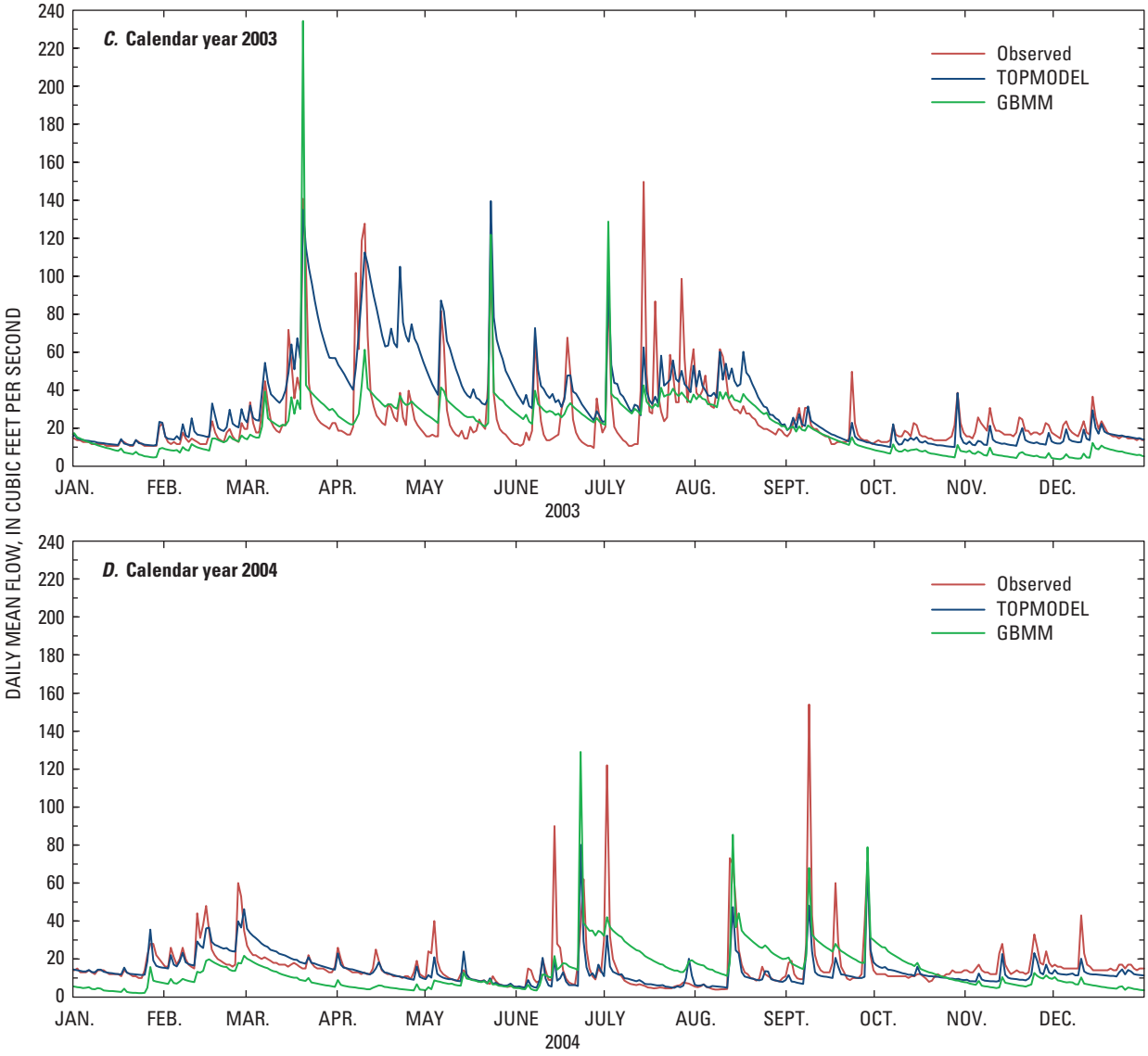

Figure 19. Simulated and observed daily mean flows at McTier Creek near Monetta for the calibration period (Feb. 7, 2001–Sept. 30, 2009), shown by calendar year.—Continued

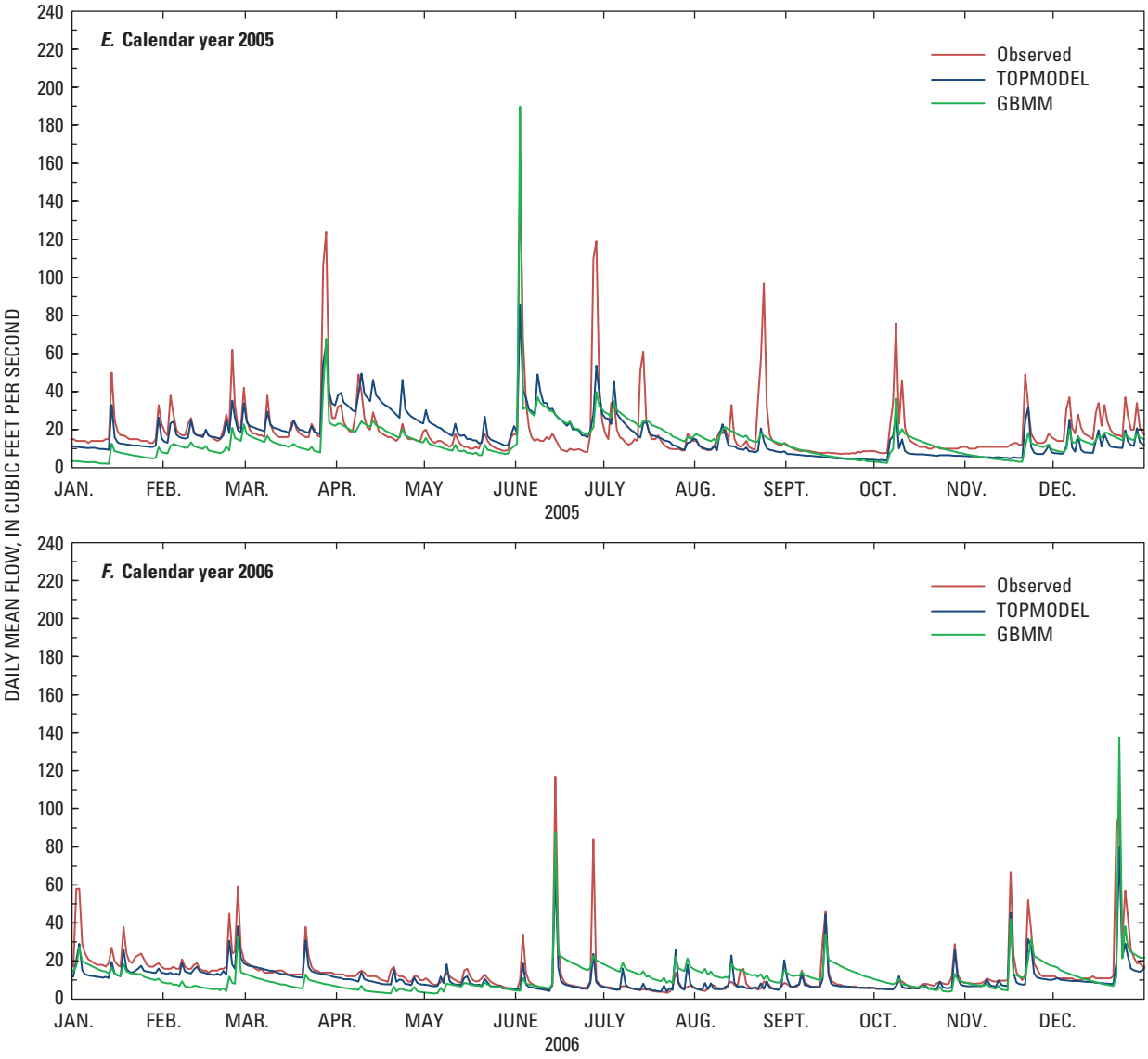

Figure 19. Simulated and observed daily mean flows at McTier Creek near Monetta for the calibration period (Feb. 7, 2001–Sept. 30, 2009), shown by calendar year.—Continued

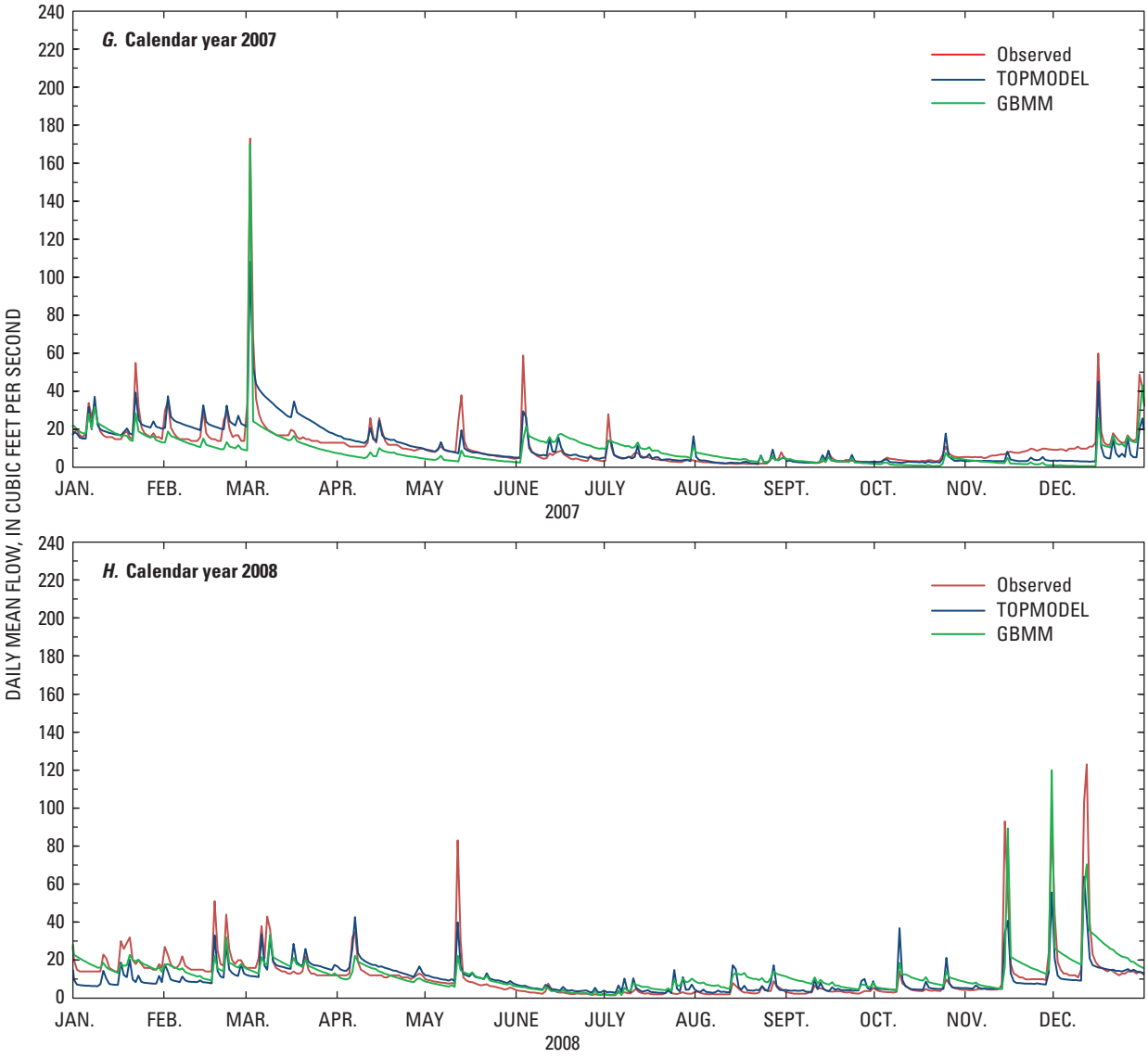

Figure 19. Simulated and observed daily mean flows at McTier Creek near Monetta for the calibration period (Feb. 7, 2001–Sept. 30, 2009), shown by calendar year.—Continued

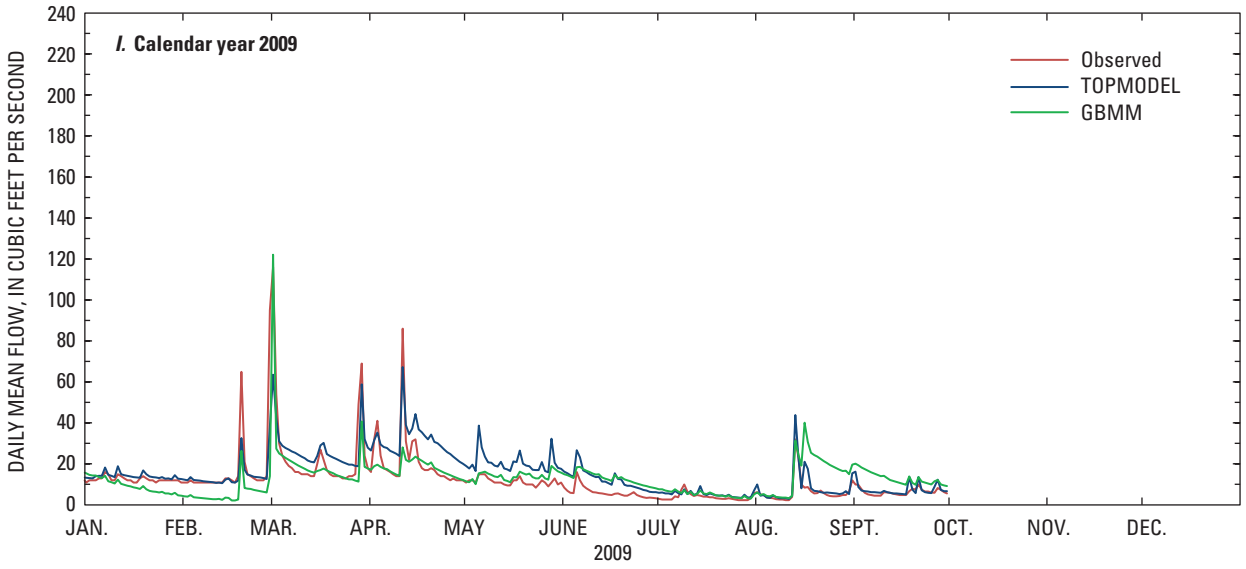

Figure 19. Simulated and observed daily mean flows at McTier Creek near Monetta for the calibration period (Feb. 7, 2001–Sept. 30, 2009), shown by calendar year.—Continued

Simulations at New Holland for the Confirmation Period

The New Holland streamgage is located at the downstream reach of the study area and represents an approximate doubling of the watershed area as compared to Monetta. As shown in table 5, the period of record available for model simulations was June 13, 2007, to September 30, 2009 (confirmation period). For both TOPMODEL and GBMM, the initial calibrated input parameters were set at the same levels as those determined during calibration at Monetta. For TOPMODEL, to get an improved fit at New Holland, the *m* value and percent macropore were slightly modified (47 to 46 and 0.5 to 0.4, respectively; table 8). These minor adjustments seem reasonable given the increase in watershed area between Monetta and New Holland. The TOPMODEL soils parameters for the New Holland watershed are almost the same as those for Monetta (tables 6, 8). Those parameters are average values for the entire watershed. Because the parameters remained fairly constant with those obtained at Monetta, even though the watershed area increased by almost 100 percent, commonality in the soils characteristics in the upper and lower watersheds of McTier Creek is indicated.

A plot of the observed and simulated daily mean flows at New Holland shows that both models perform reasonably well with respect to capturing the timing and variability of the flows (fig. 20). However, periods of underestimation and overestimation of flows are notable for both models. Also, issues relating to hydrograph recession that were discussed previously for the Monetta simulations are present.

Table 8. Parameter values used for the TOPMODEL calibration for McTier Creek near New Holland, South Carolina.

[*, indicates adjustment during calibration]

Model parameter	Value
Total area (square kilometers)	79.41
Lake area (square kilometers)	1.22
Stream area (square kilometers)	0.91
Saturated conductivity (inches per hour)	7.17
Soil depth (inches)	74.2*
Field capacity (unitless)	0.18
Water holding capacity (unitless)	0.09
Porosity (unitless)	0.39
Percent impervious	1.3*
Percent road impervious	0.9*
Latitude	33.718
Effective impervious (decimal percent)	0.8*
Conductivity multiplier	2.9*
Percent macropore (decimal percent)	0.5*
Scaling parameter (*m*)	45.0*
Depth of root zone (meters)	1.9*
Impervious runoff constant	0.10
TR-55 curve number	98
Uplake area (square kilometers)	59.0
Lake delay (unitless)	1.2*

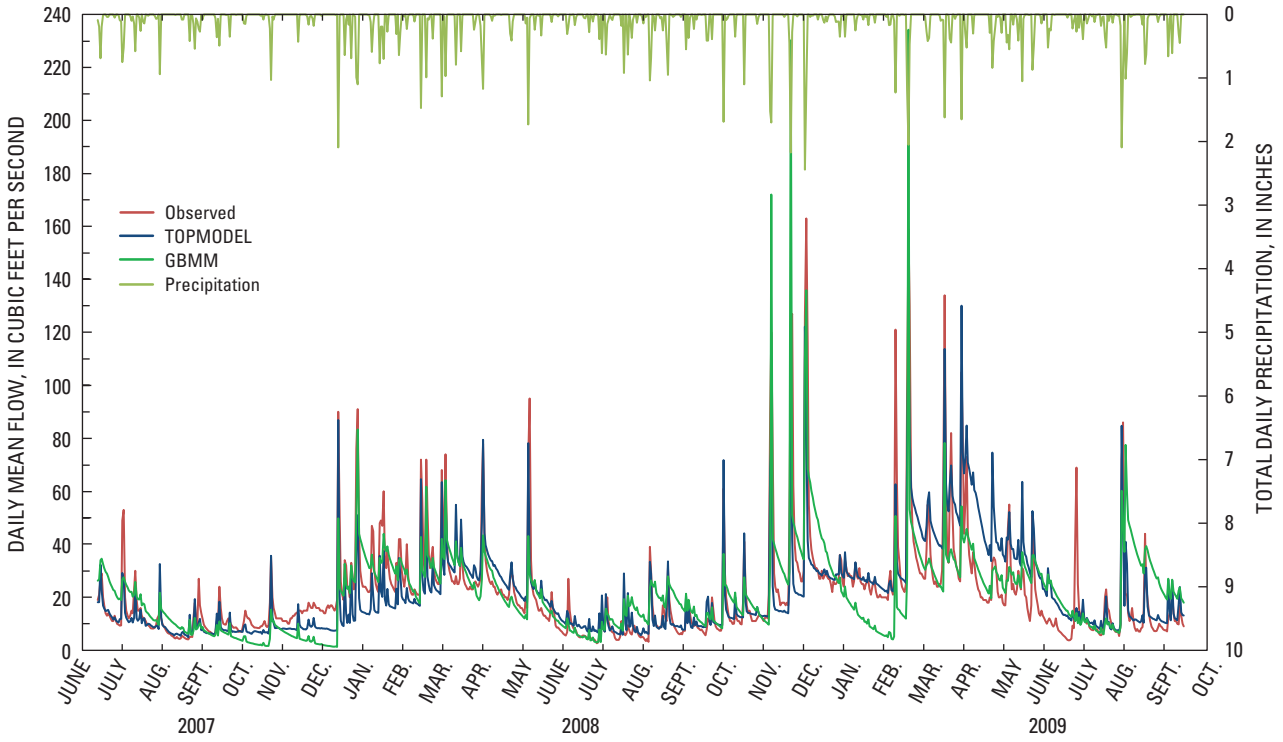

Figure 20. Simulated and observed daily mean flows at McTier Creek near New Holland for the confirmation period (June 13, 2007–Sept. 30, 2009).

Goodness-of-Fit Statistics for TOPMODEL and GBMM

As previously stated, the goodness-of-fit statistics used to assess the TOPMODEL and GBMM simulations with respect to how well they match the observed daily mean flows were (1) the Nash-Sutcliffe coefficient of model-fit efficiency index (E) (Nash and Sutcliffe, 1970), (2) Pearson's correlation coefficient (r), (3) the RMSE, (4) the bias, and (5) the MAE. The following sections provide details on these statistics for the two models relative to the simulation periods discussed earlier for the simulations at Monetta and New Holland.

Goodness-of-Fit Statistics at Monetta for the Calibration Period Simulations

The goodness-of-fit statistics between the simulated and observed daily mean flows at Monetta for the calibration period are listed in table 9. For TOPMODEL and GBMM, the mean and median simulated flows at Monetta are similar to the observed values suggesting that overall the models do a good job of matching the observed flows, with TOPMODEL doing a slightly better job with respect to the mean. The correlation coefficients also are relatively high, which further confirms a good fit between the simulated and observed flows. However, comparisons of the maximum and minimum flows indicate that TOPMODEL tended to perform somewhat better at the extremes. The standard deviation of the observed flows, which is a measure of the average spread of the data, is similar to that of the simulated flows; this also indicates that the models are capturing the variability of the daily mean flows, with TOPMODEL being slightly closer to the observed data than GBMM.

The bias is the mean of the residuals between the observed and simulated data. The bias indicates whether the model is, on average, over- or underpredicting the value being assessed. The bias for TOPMODEL was 0.23 cubic foot per second (ft^3/s), which indicates that on average, the model was slightly overpredicting the daily mean flows. For GBMM, the negative bias of –1.13 ft^3/s suggests a greater tendency to underpredict daily mean flows. The negative bias is potentially related to the application of the curve-number runoff approach in GBMM. The bias may be further explained by minor offsets in and interactions between calibrated parameters that could influence low-flow simulations, such as low seepage rates to the groundwater, rapid groundwater recession coefficients, and a deeper than average unsaturated soil zone. However, because (1) model input parameters fall within a realistic range of values for the watershed and (2) GBMM requires a lumped watershed value for these particular input parameters, the

Table 9. Goodness-of-fit statistics at McTier Creek near Monetta for the calibration period.

[ft³/s, cubic foot per second; RMSE, root mean square error; MAE, mean absolute error; r, Pearson's correlation coefficient; E, Nash-Sutcliffe coefficient of model-fit efficiency calibration period is Feb. 7, 2001–Sept. 30, 2009]

	Observed	Simulated (TOPMODEL)	Simulated (GBMM)
Maximum (ft³/s)	173	140	235
Mean (ft³/s)	14.0	14.2	12.9
Median (ft³/s)	11.0	10.5	10.6
Minimum (ft³/s)	1.40	1.11	0.11
Standard deviation (ft³/s)	14.3	13.6	12.1
Bias (ft³/s)		0.23	–1.13
RMSE (ft³/s)		10.4	9.04
MAE (ft³/s)		5.34	6.87
r		0.72	0.67
E		0.47	0.38

influence each parameter might exert on model bias potentially reflects the spatial variability of these watershed characteristics rather than poor calibration or measurements.

While the bias is a useful statistic, it does not provide any indication of the absolute differences between the observed and simulated data. That is, a bias of zero only indicates that the model is equally over- and underpredicting but provides no information on the magnitude of the over- or underpredictions. One approach to assessing such differences is by computing the variance, which is the average square of the residuals (Norman and Streiner, 1997). However, because the variance is not in the units of the original data, it is difficult to interpret. Consequently, the square root of the variance is taken and provides the RMSE, which is in the units of the original data. The RMSE represents the mean of the absolute distance between the observed and simulated values. A lower RMSE indicates a better fit between the observed and simulated data. For the calibration period at Monetta, the TOPMODEL and GBMM RMSE were 10.4 ft³/s and 9.04 ft³/s, respectively. Although lower RMSE indicates a better fit between the observed and simulated data, the difference between GBMM and TOPMODEL simulations was considered to be minimal.

Janssen and Heuberger (1993) noted that one weakness of the RMSE is that it is sensitive to outliers because the differences between observed and simulated data are squared. The MAE is less sensitive to outliers. The MAE is similar to the bias except that it is the mean of the absolute value of the residuals as opposed to the mean of the actual residuals. Thus, the MAE provides the average of the magnitude of the residuals. In general, the RMSE can be expected to be greater than or equal to MAE for the range of most values. The degree to which the RMSE exceeds the MAE provides an indication of the extent to which outliers exist in the data (Legates and McCabe, 1999). For the calibration period, the MAEs for TOPMODEL and GBMM were 5.34 and 6.87 ft³/s, respectively. For TOPMODEL and GBMM, the differences between the RMSE and MAE were 5.06 and 2.17 ft³/s, respectively. Thus, although the standard deviation and range of values are larger in the GBMM model runs, GBMM simulations appear to have fewer outliers than TOPMODEL simulations.

The Nash-Sutcliffe efficiencies (E) for the calibration period for TOPMODEL and GBMM were 0.47 and 0.38, respectively. An E value of 1.0 would indicate a perfect fit between the modeled and simulated data, and a value of zero or less would indicate that using the mean of the observed data would be a better predictor than the model (Krause and others, 2005). Because the E value is computed using the squared differences of the observed and simulated data, under- or overpredictions of the higher flow values tend to carry more weight. As a result, the wet period in 2003 would be assumed to have a substantial effect on the E value, which would be true of the RMSE as well. Krause and others (2005) noted that one disadvantage of the E value is that the differences between the simulated and observed data are squared. Therefore, substantial over- or underpredictions of high-flow values can have a considerable effect on the E value, whereas differences in the lower values have less influence. Consequently, the overall E value for the wet period in 2003 could be lower due to the large difference between simulated and observed flows. To reduce the problem of the square differences and, thus, the sensitivity to the extreme values, the E value can be computed using the natural logarithms of the observed and simulated data. For example, the TOPMODEL E value for the calibration period when computed using natural logarithms resulted in an E value of 0.68, which is a 36 percent improvement over the E value computed with the wet period included.

Goodness-of-Fit Statistics at Monetta for the Concurrent Period Simulations

The New Holland streamgage is located at the outlet of the study area. As discussed earlier, the streamgage was installed at that location to collect flow data during the mercury investigation and, thus, data are only available for the period from June 13, 2007, to September 30, 2009 (concurrent period). Therefore, in order to compare the New Holland model simulations with the Monetta simulations, the following goodness-of-fit statistics are provided for the Monetta simulation period that is concurrent with the New Holland simulation period. Plots of the simulated and observed data were previously shown in figure 19*G–I*, and a plot of the simulation at Monetta for the concurrent period also is shown in figure 21.

The goodness-of-fit statistics for the TOPMODEL show that for the concurrent period at Monetta, the mean, median, and minimum simulated daily mean flows are similar to those computed from the observed data (table 10). The standard deviation of the simulated data is slightly lower than that of the observed data but still indicates that the model reasonably captures the dynamics and variability of the daily mean flows.

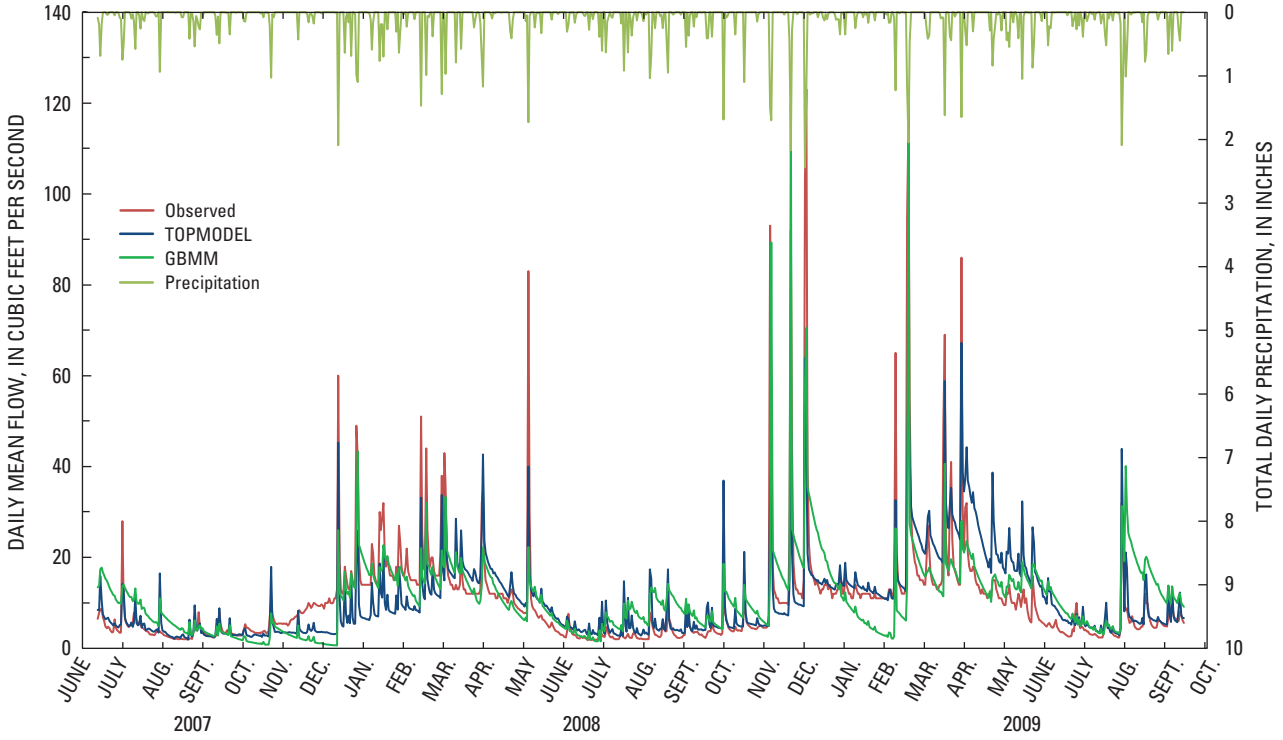

Figure 21. Simulated and observed daily mean flows for McTier Creek near Monetta for the concurrent period (June 13, 2007–Sept. 30, 2009).

Table 10. Goodness-of-fit statistics for McTier Creek near Monetta for the concurrent period (June 13, 2007–Sept. 30, 2009).

[ft³/s, cubic foot per second; RMSE, root mean square error; MAE, mean absolute error; r, Pearson's correlation coefficient; E, Nash-Sutcliffe coefficient of model-fit efficiency]

	Observed	Simulated (TOPMODEL)	Simulated (GBMM)
Maximum (ft³/s)	123	67	122
Mean (ft³/s)	10.4	10.7	11.1
Median (ft³/s)	7.5	7.3	10.0
Minimum (ft³/s)	1.8	2.0	0.62
Standard deviation (ft³/s)	12.0	9.0	9.5
Bias (ft³/s)		0.27	0.75
RMSE (ft³/s)		7.6	8.4
MAE (ft³/s)		4.2	5.0
r		0.78	0.72
E		0.61	0.51

Pearson's correlation coefficient, r, also indicates a good correlation between the observed and simulated daily mean flows. The E coefficient is improved with the longer period model from 2001 to 2009 as are the RMSE and MAE. For this period, the difference between the RMSE and MAE was the same for both models (3.4 ft³/s).

As was the case for TOPMODEL, the r and E statistics for GBMM are higher for this shorter period (2007–2009), suggesting a good fit with the streamgage data. This is expected because (1) the 2007–2009 period was less hydrologically variable than the previous simulation period, which included the diverse precipitation years of 2001–2003, and (2) the sample size (N) is lower for the shorter period. Though the observed and GBMM-simulated maximum and mean daily flows are similar, the minimum daily flows simulated by GBMM are lower than the observed data, which further supports previous discussions of GBMM's tendency toward underestimating flows in this watershed during low-flow periods. Overall, the goodness-of-fitness statistics indicate that both models generally provide a good representation of the streamflow in McTier Creek for the concurrent period.

Goodness-of-Fit Statistics at New Holland for Confirmation Period Simulations

The efficiency and correlation coefficients (E and r, respectively) for the confirmation period simulations at New Holland (table 11) are similar to those for the concurrent period at Monetta (table 10). In addition, the mean of the simulations for both models is almost equal to that of the measured data. As at Monetta, GBMM undersimulated the minimum flow. For the maximum flow at Monetta, the GBMM estimate was close to the observed maximum flow, but at New Holland, the GBMM maximum flow was well above the observed maximum flow. For TOPMODEL, the minimum flow at New Holland is about twice the observed minimum flow; at Monetta, the minimum simulated flow from TOPMODEL and the observed minimum flow at the streamgage were almost equal. Although the bias at New Holland is smaller than that at Monetta for both models, the MAE is larger, suggesting an overall average larger deviation from the observed data than was the case at Monetta. As was true for the concurrent period at Monetta, the differences between the RMSE and the MAE for TOPMODEL and GBMM were about equal (4.5 and 4.8 ft^3/s, respectively). The standard deviation for both models again suggests that the variability of the simulated flows is similar to the observed flow.

Table 11. TOPMODEL and GBMM calibration statistics at McTier Creek near New Holland for the confirmation period (June 13, 2007–Sept. 30, 2009).

[ft^3/s, cubic foot per second; RMSE, root mean square error; MAE, mean absolute error; r, Pearson's correlation coefficient; E, Nash-Sutcliffe coefficient of model-fit efficiency]

	Observed	Simulated (TOPMODEL)	Simulated (GBMM)
Maximum (ft^3/s)	163	130	234
Mean (ft^3/s)	21.8	21.6	21.6
Median (ft^3/s)	17.0	14.9	19.5
Minimum (ft^3/s)	2.6	5.0	1.2
Standard deviation (ft^3/s)	19.9	17.1	18.2
Bias (ft^3/s)		0.15	0.22
RMSE (ft^3/s)		11.7	13.8
MAE (ft^3/s)		7.2	9.0
r		0.80	0.73
E		0.64	0.49

Flow-Duration Curves, Single-Mass Curves, and Residuals

Along with temporal plots of simulated and observed daily mean flows for the TOPMODEL and GBMM models, several other graphical tools were used to assess how well the models capture the characteristics of the observed data at the Monetta and New Holland gages. Those graphical tools include flow-duration and single-mass curves along with various plots of model residuals, which are the differences between the observed and simulated values. These graphical tools are discussed in this section, and plots are presented for the various simulation periods previously discussed.

Flow-Duration Curves

The flow-duration curve is a cumulative frequency curve that shows the percentage of time during which specified flows were equaled or exceeded for the given period of analysis (Searcy, 1959). The flow-duration curves at Monetta for the calibration period are shown in figure 22*A*. In general, the flow-duration characteristics of the simulated flows from TOPMODEL and GBMM match those of the observed flows reasonably well. However, GBMM tends to underestimate flows that are equaled or exceeded approximately 2–5 percent of the time (high flows) and 95–100 percent of the time (lower flows). Underestimating simulated flows may reflect the overall capacity of the curve-number runoff method to capture saturation excess overland flow response, which could be a significant contributor during peak runoff periods (Schneiderman and others, 2007). The curve-number method is biased toward infiltration-excess overland flow because the infiltration capacity of soils is one of the two main factors determining curve-number runoff (Garen and Moore, 2005; Walter and Shaw, 2005). Saturation-excess overland flow is particularly important in the McTier Creek watershed, which has abundant riparian wetland areas that are more likely to respond rapidly to a soil saturation surplus.

The flow-duration curves for TOPMODEL and GBMM at the Monetta gage for the concurrent period tend to match the observed curve reasonably well with TOPMODEL, providing an overall slightly better fit (fig. 22*B*). As with the longer period shown in figure 22*A*, GBMM deviates from the observed curve for the lowest flows (those exceeded 95 to 100 percent of the time). This again likely reflects the complex calibration balance between seasonal curve number thresholds and groundwater recession rates. GBMM flow rates are lower than observed base-flow rates for the fall of 2007 and winter of 2009, which were both relatively dry precipitation periods in the watershed (fig. 21).

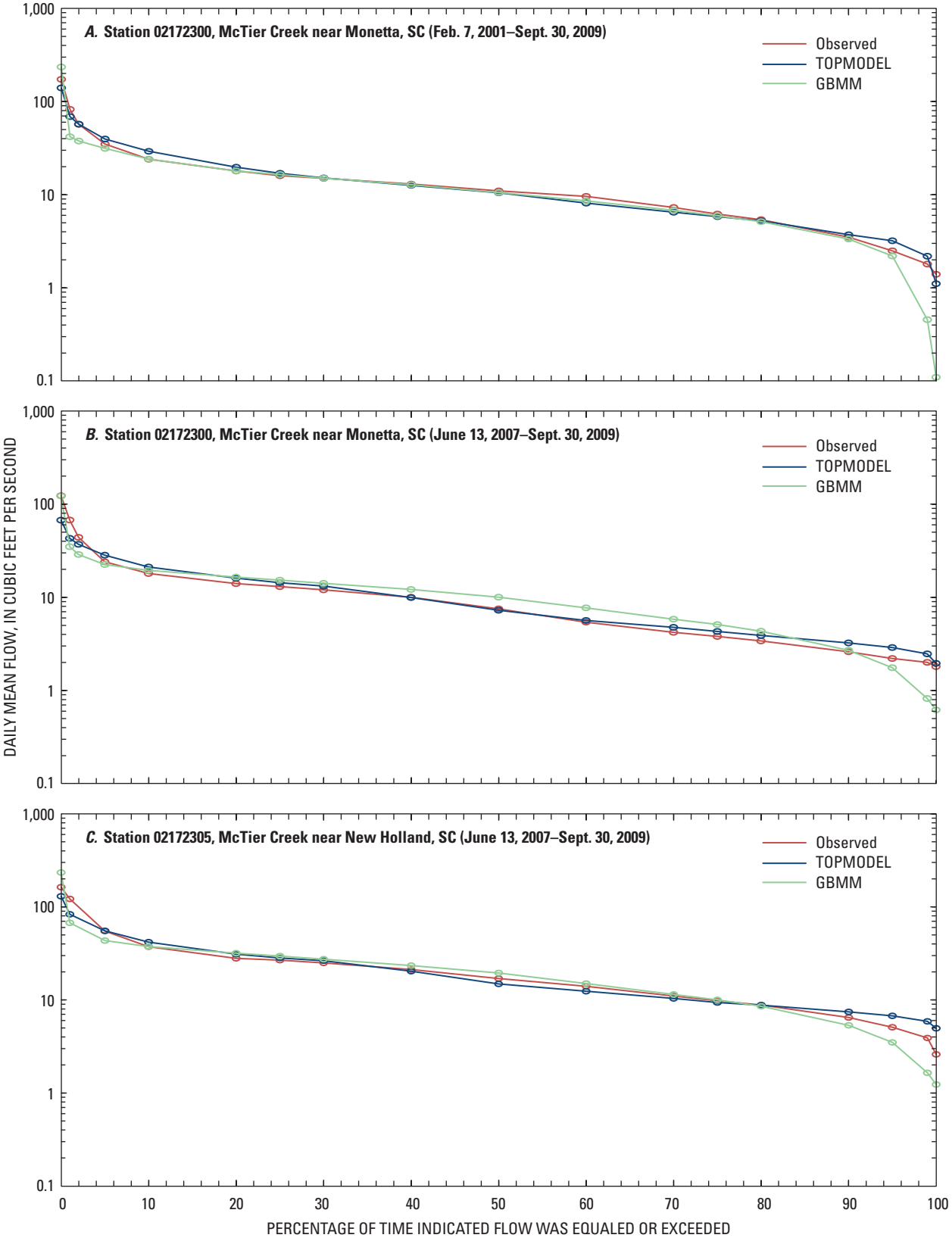

Figure 22. Flow-duration curves of simulated and observed daily mean flow at (*A*) Monetta for the calibration period, (*B*) Monetta for the concurrent period, and (*C*) New Holland for the confirmation period.

The flow-duration curves for TOPMODEL and GBMM at the New Holland gage for the confirmation period show that the flow-duration curve characteristics of simulated flows are similar to those of the observed daily mean flows (fig. 22*C*). For the flows that are equaled or exceeded about 90 or more percent of the time (the lowest flows), the duration curves for the simulated flows for both models continue to have shapes similar to those for the observed flows but diverge with TOPMODEL duration values being higher than observed values and GBMM duration values being lower than observed values. This is consistent with the flow-duration curves at Monetta (fig. 22*B*).

Single-Mass Curves

Figure 23*A* shows a single-mass curve that presents the cumulative daily mean flows and represents the cumulative volume of daily mean flow for the calibration period. Both TOPMODEL and GBMM show a good fit with the observed curve through the winter of 2003. However, after 2003, GBMM begins to underpredict the cumulative volume, and TOPMODEL begins to overpredict the cumulative volume. The significant change in the slopes of the single-mass curves indicates changes in the hydrologic regime. From figure 19*C*, it can be seen that the abrupt change in the slope of the mass curve for the measured data was due to the significantly wet period that occurred in the spring of 2003. In addition, the difference in the magnitude of the cumulative volume from TOPMODEL and the cumulative volume of the observed flows is likely related to the slower rates of hydrograph recession for the TOPMODEL simulations during the wet period as compared to those of the observed hydrographs and of the GBMM simulations. For the total period analyzed, however, the difference between the simulated and measured total volume for TOPMODEL was about 5 percent (fig. 23*A*) and was slightly less than 10 percent for GBMM. It is worth noting that the USGS considers the accuracy of a streamflow record to be "good" if about 95 percent of the daily flows are within 10 percent of the true flow (Novak, 1985). As a point of comparison, Donigian and others (1984) present general guidelines for characterizing calibrations for the Hydrologic Simulation Program–Fortran (HSPF) watershed model. For annual and monthly volumes, HSPF model calibration is considered very good when the error is less than 10 percent, good when the error is 10 to 15 percent, and fair when the error is 15 to 25 percent (Ockerman, 2005).

For the concurrent period at Monetta, the single-mass curves for TOPMODEL and GBMM have shapes similar to that of the observed data, and GBMM volumes tend to more closely track those of the observed data than the TOPMODEL values do throughout the simulation period (fig. 23*B*). The deviation of the TOPMODEL curve is likely due to its underestimation of several large peak-flow events that occurred during the concurrent period (fig. 21). Nonetheless, for the total simulation period, the differences in the total volume of the TOPMODEL and GBMM simulations with respect to the total observed volume only were about 3 percent and 7 percent, respectively.

The single-mass curves for the confirmation period at New Holland are shown in figure 23*C*. The curves are consistent with those for the concurrent period at Monetta. The shapes of the single-mass curves for TOPMODEL and GBMM cumulative flows are similar to that for the observed data, and the GBMM data more closely follow the observed data than do the TOPMODEL data throughout much of the simulation period. However, the total volumes for the simulation period for both models are within about 1 percent of the total volume of the observed daily mean flow at New Holland.

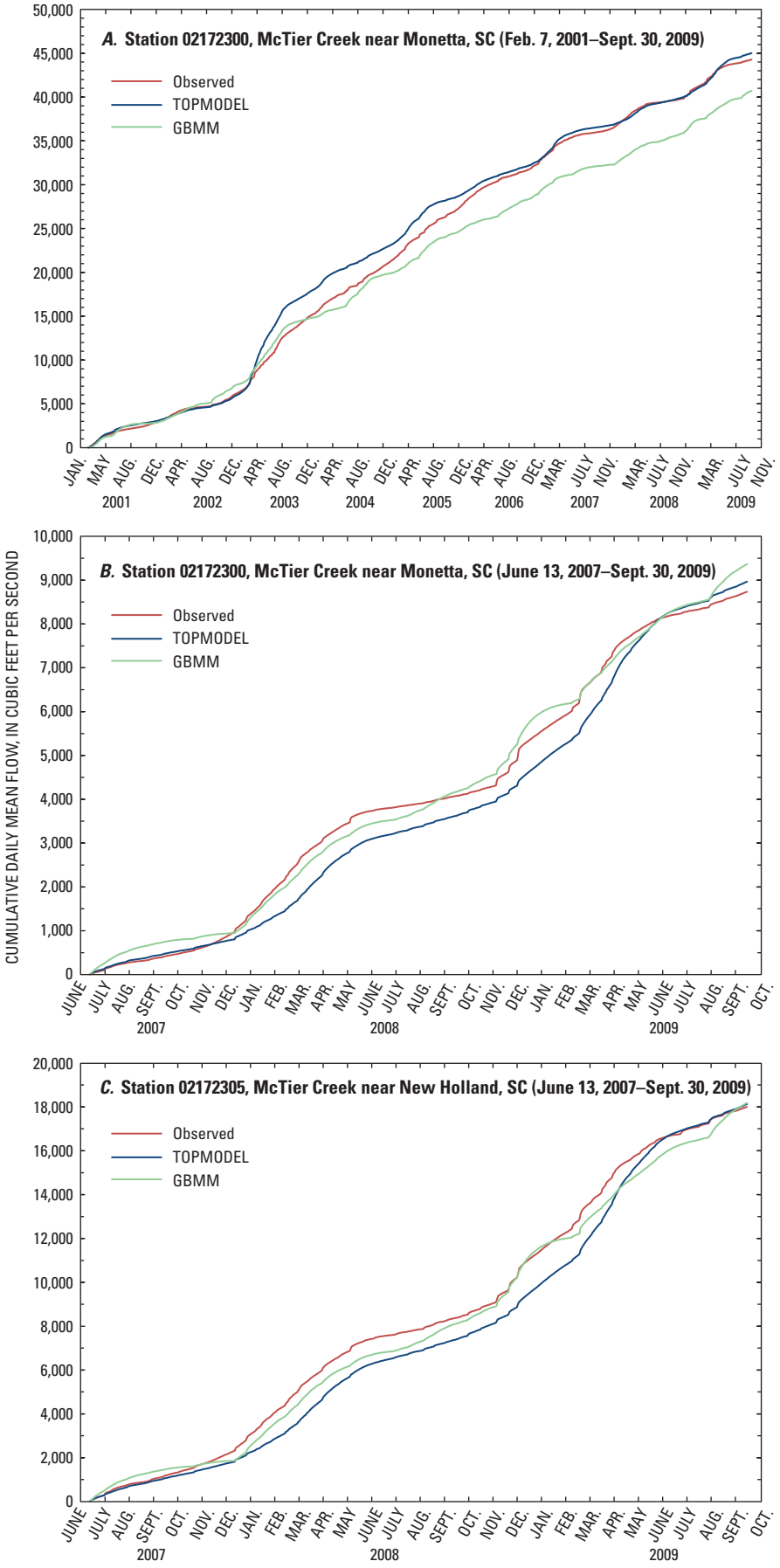

Figure 23. Single-mass curves of simulated and observed daily mean flow at (*A*) Monetta for the calibration period, (*B*) Monetta for the concurrent period, and (*C*) New Holland for the confirmation period.

Residuals

For the Monetta site, scatter plots of simulated and observed daily mean flows for the calibration period for TOPMODEL and GBMM are shown in figures 24*A* and 25*A*, respectively. For the TOPMODEL simulated flows, no significant bias exists as shown by the values being evenly spread about the one-to-one line (line of agreement); however, some bias exists at the extremes. For GBMM simulated flows, the flows also are evenly distributed about the one-to-one line with some bias at the extremes. As discussed earlier, the residuals also reflect the issue of the GBMM recession rates.

The scatter plots of TOPMODEL and GBMM simulations at Monetta for the concurrent period show that the

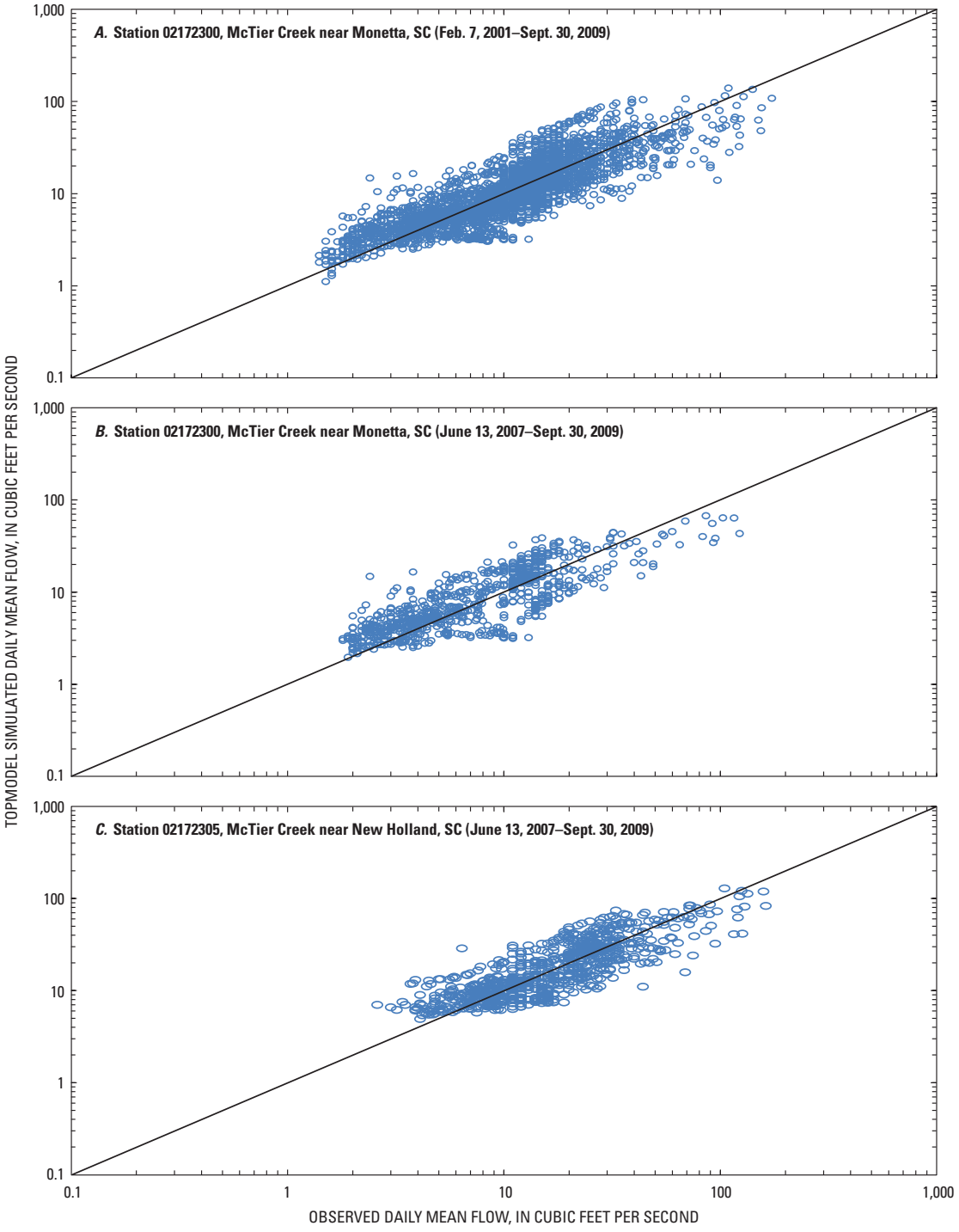

Figure 24. Scatter plots of observed and TOPMODEL simulated daily mean flow at (*A*) McTier Creek near Monetta for the calibration period, (*B*) McTier Creek near Monetta for the concurrent period, and (*C*) McTier Creek near New Holland for the confirmation period.

majority of modeled flow values are scattered about the one-to-one line, indicating no consistent bias (figs. 24*B*, 25*B*). Some bias at the flow extremes, however, does exist.

The scatter plots for the New Holland simulations for the confirmation period are presented in figures 24*C* and 25*C*, respectively. Overall, the results are similar to those for Monetta with the majority of flow values being well spread about the one-to-one line with some bias at the extremes. In addition, the GBMM issue relating to recession rates for the lower flows is evident.

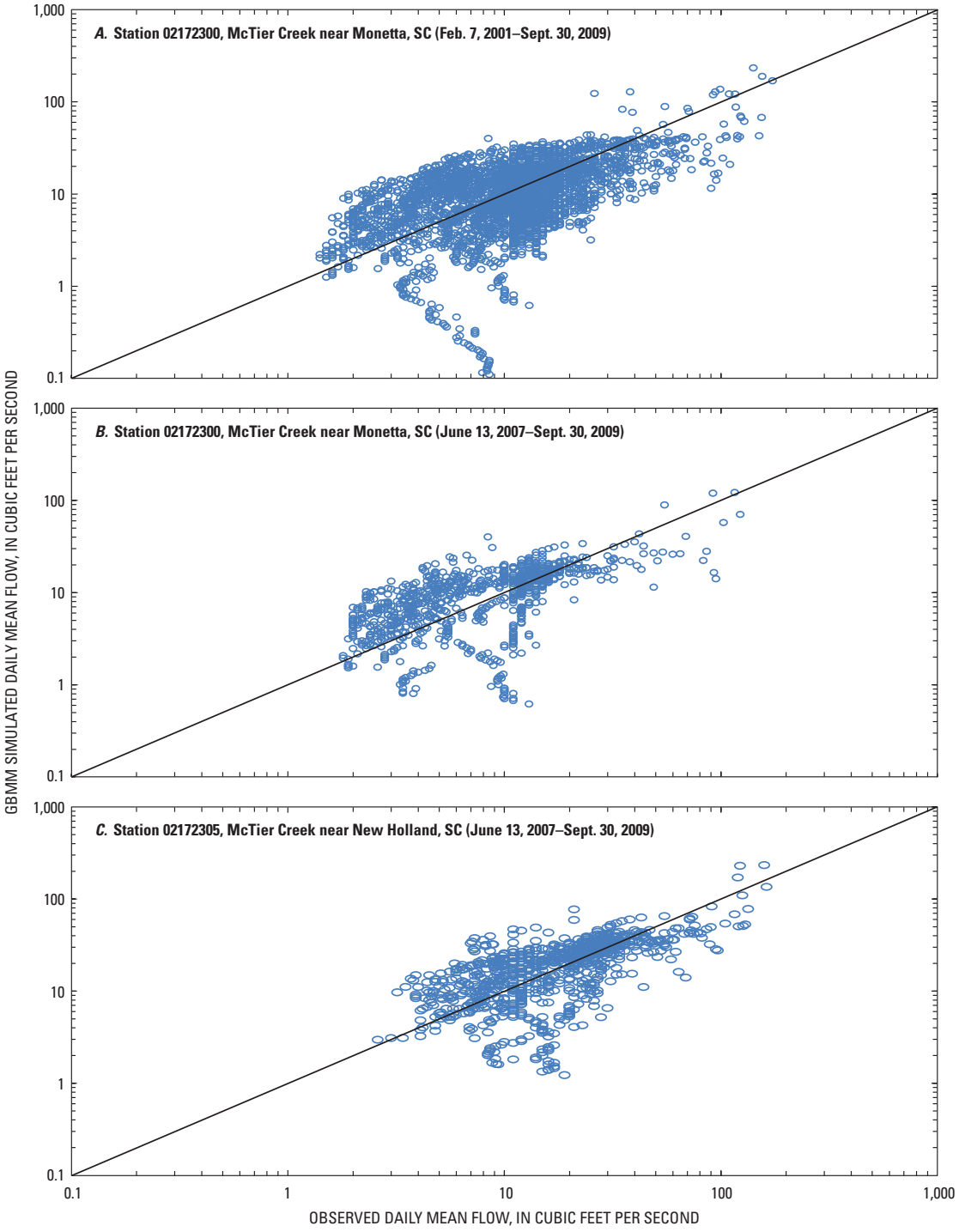

Figure 25. Scatter plots of observed and GBMM simulated daily mean flow at (*A*) McTier Creek near Monetta for the calibration period, (*B*) McTier Creek near Monetta for the concurrent period, and (*C*) McTier Creek near New Holland for the confirmation period.

Residuals and Simulated Flow

For the calibration period, the TOPMODEL residuals are in good agreement for the majority of the data points. TOPMODEL residuals begin to develop a heteroscedastic relation as the flows increase, which indicates a non-constant variance (Helsel and Hirsch, 1995; fig. 26*A*). About 80 percent of the simulated flows are about 20 ft^3/s or less (fig. 22*A*). Consequently, much of the heteroscedasticity is probably related to the high residuals from the wet period in 2003 and peak flows for which TOPMODEL tended to underpredict. Although not quite as pronounced, a similar pattern is evident for the concurrent and confirmation periods at both Monetta and New Holland, respectively (fig. 26*B*, *C*). For GBMM, a

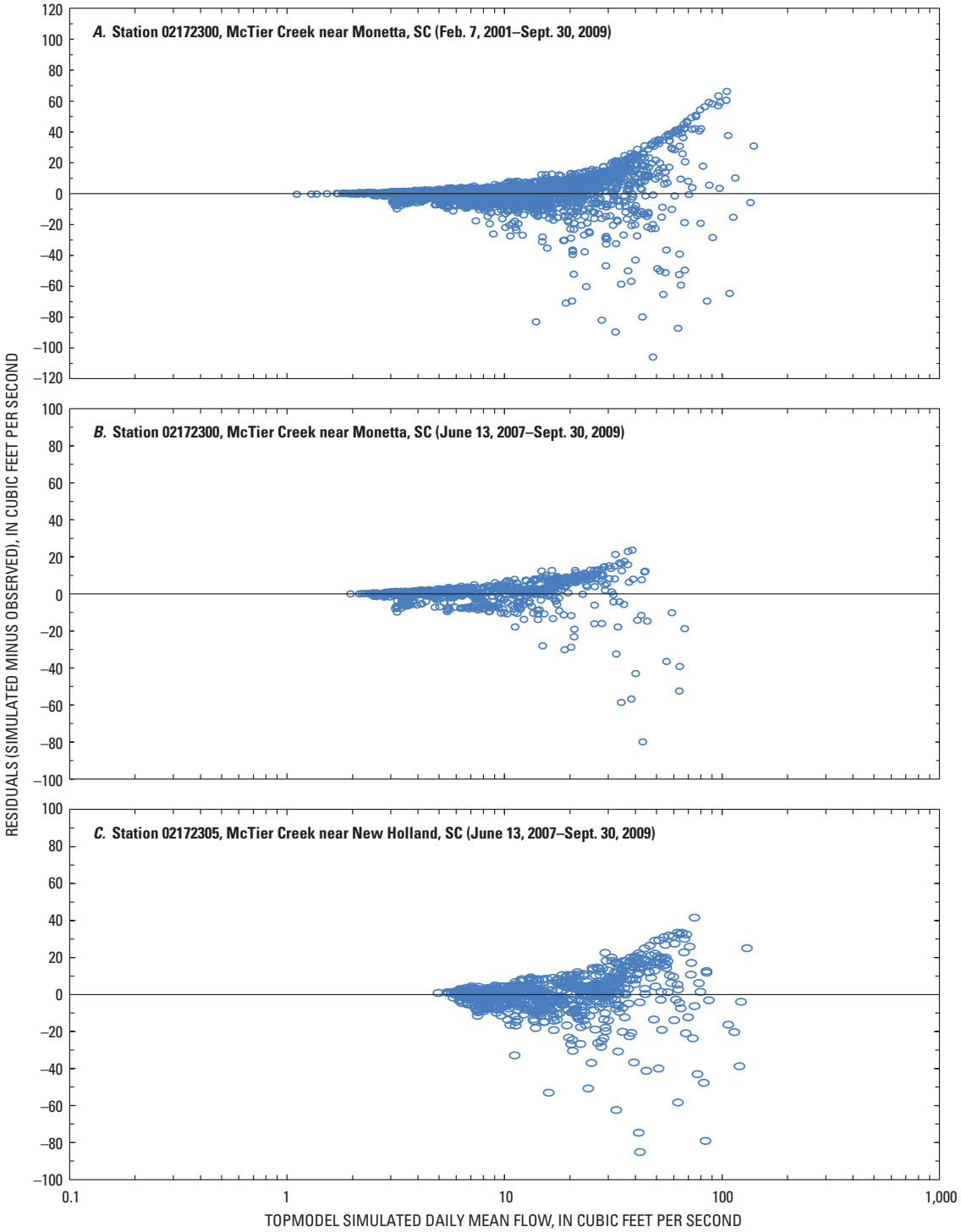

Figure 26. Residuals and TOPMODEL simulated daily mean flow at (*A*) McTier Creek near Monetta for the calibration period, (*B*) McTier Creek near Monetta for the concurrent period, and (*C*) McTier Creek near New Holland for the confirmation period.

relatively consistent pattern in the residuals is evident up to a mean daily flow of approximately 10 ft³/s, with the exception of the systematic underprediction below about 1 ft³/s (fig. 27*A*). Above 10 ft³/s, the mean daily flows become more variable as indicated by the heteroscedastic shape as was noted for TOPMODEL. Similar to the TOPMODEL results, approximately 80 percent of the simulated mean daily flows from the 2001 to 2009 period are below approximately 20 ft³/s. Thus, the wet 2003 period likely exerts an influence on GBMM results as well. The GBMM residuals for the concurrent and confirmation periods at Monetta and New Holland, respectively, show similar patterns, with the New Holland residuals showing more variability (fig. 27*B*, *C*).

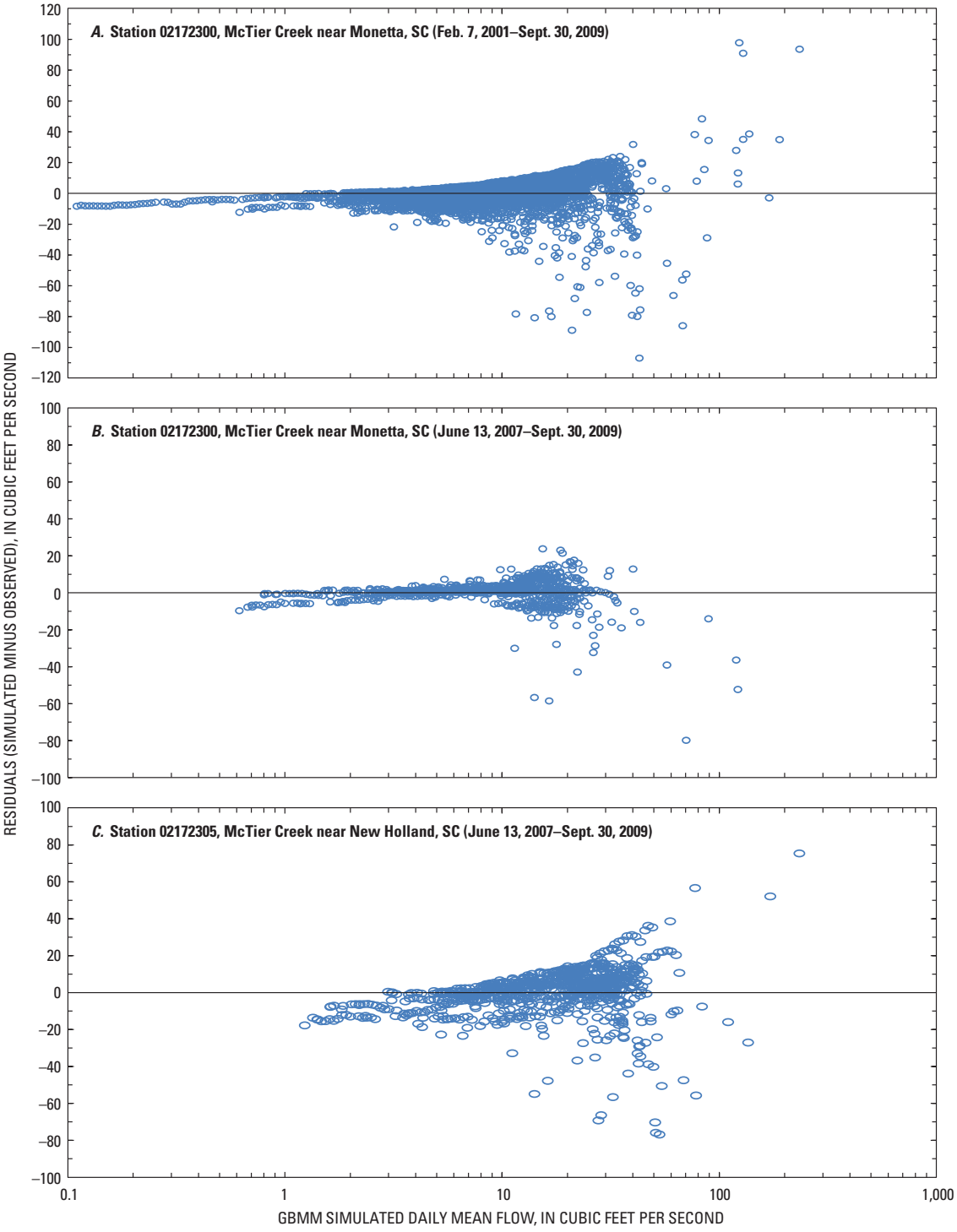

Figure 27. Residuals and GBMM simulated daily mean flow at (*A*) McTier Creek near Monetta for the calibration period, (*B*) McTier Creek near Monetta for the concurrent period, and (*C*) McTier Creek near New Holland for the confirmation period.

Residuals (Temporal)

Finally, temporal plots of residuals are shown in figures 28 and 29 for TOPMODEL and GBMM, respectively. Although there appears to be some seasonal pattern to the TOPMODEL residuals, such as residual values being negative in the fall, those patterns are not always consistent (no significant cluster of negative residuals in the fall of 2002, 2006, or 2008). The plot of simulated and observed flows by year (fig. 20) shows that during low flows, which typically occur in the fall, the model accuracy is low. As previously discussed, the TOPMODEL assumption that the water table parallels the

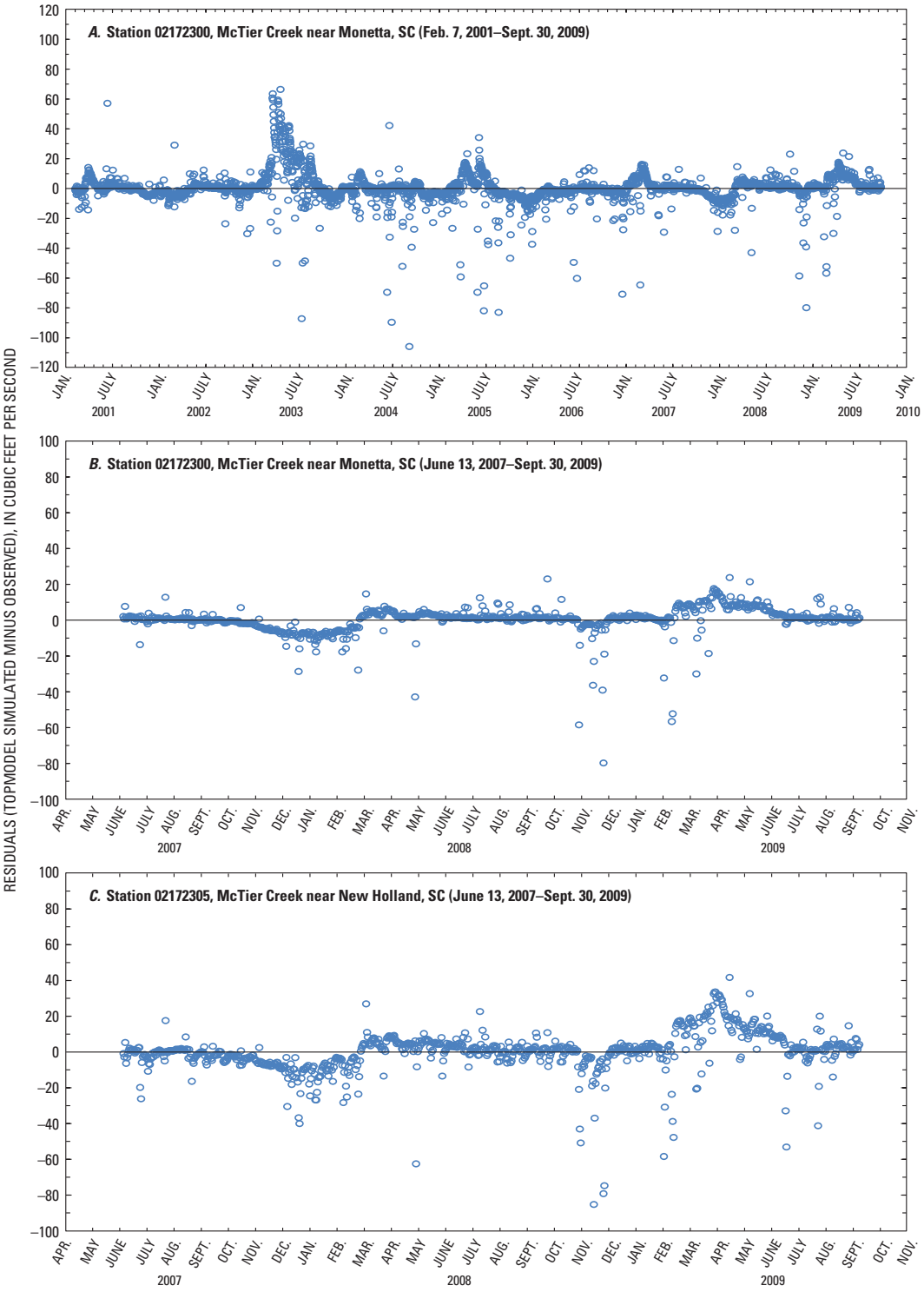

Figure 28. Residuals of simulated (TOPMODEL) and observed daily mean flow at (*A*) McTier Creek near Monetta for the calibration period, (*B*) McTier Creek near Monetta for the concurrent period, and (*C*) McTier Creek near New Holland for the confirmation period.

topography is questionable during the lowest flow periods. The cluster of positive residuals in the spring of 2003 indicates an extended period of overprediction by TOPMODEL for the calibration period. For the concurrent and confirmation periods, respectively, the temporal plots of TOPMODEL residuals have similar patterns at Monetta and New Holland with the majority of the residuals being relatively close to zero and with the model underpredicting in the fall of 2007 and overpredicting in the spring of 2009 (fig. 28*B*, *C*). Again, it is worth noting that fall tends to be the time of the year when the lowest streamflow occurs, and spring tends to be when the highest streamflow occurs. This pattern suggests that the extremes present the most challenge for TOPMODEL, even though the model did well throughout the entire year for 2008.

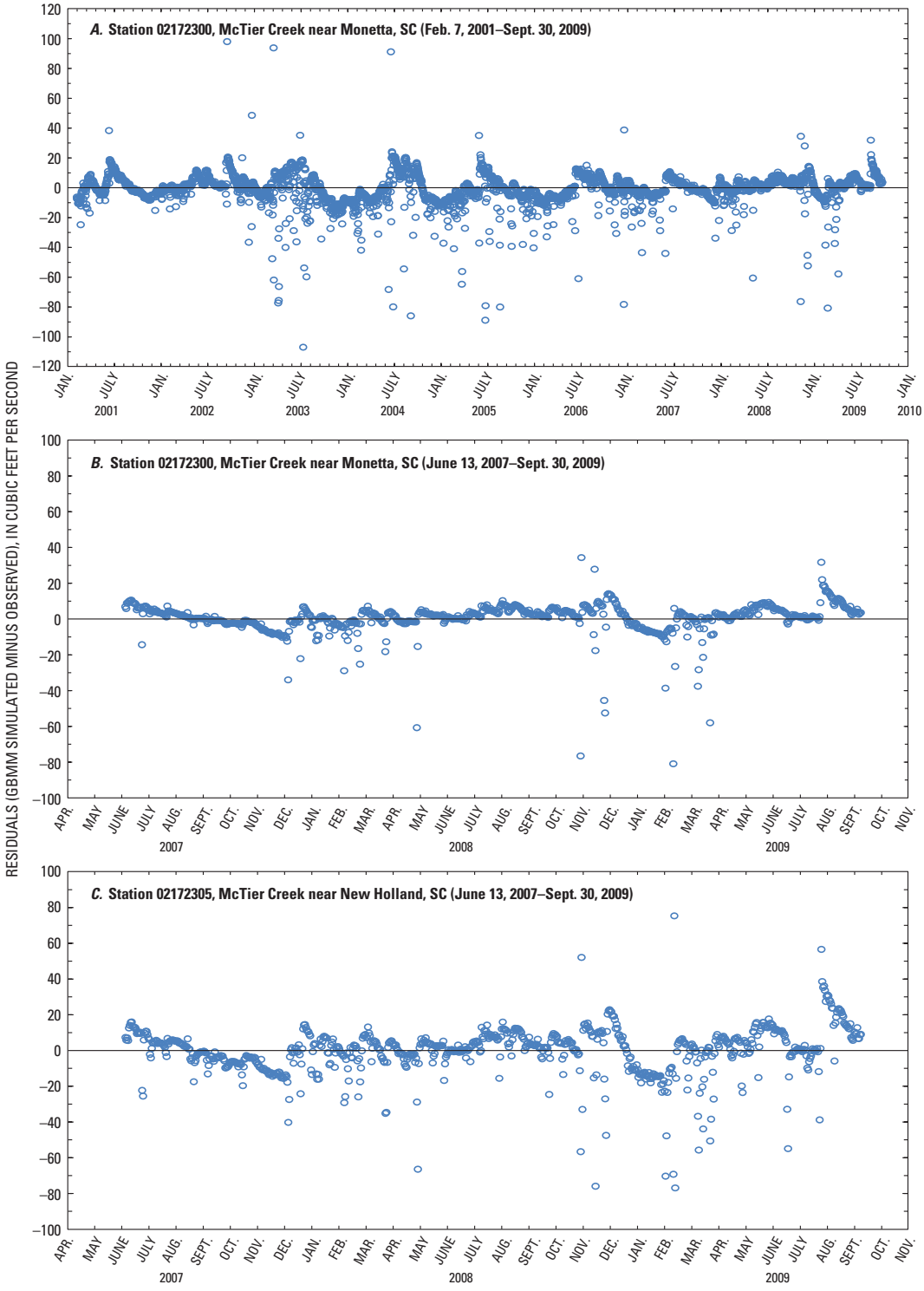

Figure 29. Residuals of simulated (GBMM) and observed daily mean flow at (*A*) McTier Creek near Monetta for the calibration period, (*B*) McTier Creek near Monetta for the concurrent period, and (*C*) McTier Creek near New Holland for the confirmation period.

A temporal plot of the GBMM residuals at Monetta also suggests some seasonal patterns in model errors (fig. 29*A*). For example, for most years during the calibration period, GBMM overpredicts slightly during the summer but underpredicts in the winter, though the pattern in the over- and underpredictions tends to vary. During the summer months, rainfall often occurs in sporadic events. Because the duration of these events is brief, the uplands may remain hydrologically disconnected from the stream. Thus, even though event-based antecedent precipitation rates produce rapid runoff using GBMM's curve-number methodology, observed watershed runoff may not respond as quickly as the curve-number approach suggests, and slight overpredictions occur for summer. Additionally, a cluster of positive residuals reflects GBMM's overprediction during the wet spring and early summer of 2003, similar to TOPMODEL results (fig. 29*A*).

For the concurrent and confirmation periods at Monetta and New Holland, respectively, the GBMM residuals indicate some seasonality, but no strong, consistent pattern occurs, which is similar to the TOPMODEL residuals (fig. 29*B*, *C*). Underpredictions in the fall of 2007 and the winter of 2009 are most evident, with the most noticeable overpredictions occurring in the fall of 2008 and late summer of 2009. As with TOPMODEL, slightly more variability is noticeable at New Holland, which has a drainage area that is about twice the size of the drainage area at Monetta.

Watershed Model Uncertainties and Limitations

All watershed models employ mathematical descriptions based on simplifying assumptions about the processes that underlie complex natural systems (Beven, 2002). The extent to which these simplifications deviate from the hydrologic reality is a fundamental source of uncertainty in such models (Ockerman, 2005). The mathematical structures of TOPMODEL and GBMM differ substantially, each capturing the actual hydrologic character of the McTier Creek watershed to varying degrees. Runoff simulations in TOPMODEL involve a semi-distributed approach using the variable-source-area concept where saturation excess overland flow and subsurface flow are the dominant runoff generating mechanisms. Further, runoff response is based on the general assumption that the water table mirrors the watershed's topography and that hydraulic conductivity decreases exponentially with depth. In comparison, GBMM's runoff methodology involves a spatially explicit modified curve-number approach based on soil infiltration capacity and land cover, which assumes that infiltration excess overland flow is the dominant runoff-generating process in the watershed. While output from both models fit the daily hydrograph relatively well, neither model captures the full complexity of hydrologic processes in the watershed. In addition to such systematic errors, limitations in the input data needed for the model are another source of error.

TOPMODEL and GBMM simulations are driven by time series of precipitation and air temperature. As a result, model accuracy is dependent on the accuracy of these data. The precipitation and air temperature data for this investigation were obtained from the NWS meteorological data network at stations located in the vicinity of the McTier Creek watershed. To improve the areal coverage of the data, inverse-distance weighting techniques were used to generate a better representation of the "average" meteorological conditions in the watershed. Variations in average daily temperatures at the various NWS stations around McTier Creek tend to be relatively minor. However, rainfall can vary greatly over small distances; thus, the assumption of spatially uniform rainfall is unrealistic, especially during summer months when convective storms can produce spatially variable amounts of rainfall. For the McTier Creek watershed specifically, these events could produce large precipitation amounts that may not even be captured in the TOPMODEL input data. During an investigation in Mecklenburg County, NC, from July 1995 through June 1997, precipitation data were collected at 46 sites (Robinson and others, 1998). The results of that investigation showed that the distribution of annual rainfall in parts of Mecklenburg County ranged from 35 to 50 inches. With respect to particular events, the distribution of recurrence intervals for a 24-hour rainfall duration in the city of Charlotte for the storm of August 26–27, 1995, based on 24 rainfall-gaging stations, ranged from less than 2 years to more than 100 years (Hershfield, 1961; Hazell and Bales, 1997). Consequently, there will always be some level of uncertainty in rainfall-runoff models that assume uniform rainfall over the watershed.

In addition to the meteorological data, TOPMODEL and GBMM inputs include soils parameters and other watershed characteristics. The McTier Creek watershed tends to have similar soils characteristics; therefore, average values probably represent most parts of the watershed well. Nonetheless, some amount of uncertainty is introduced into the model simulations from both the uncertainty in the soil measurements used to develop the SSURGO coverages and the process of using a single, average value to represent the entire watershed being modeled. In addition, watershed characteristics, such as watershed area, stream area, and imperviousness, are computed from available GIS coverages. Certainly the use of GIS techniques has increased the accuracy of these watershed characteristics, but some level of uncertainty in those measurements still remains and will be part of the uncertainty in the model simulations.

Another area of uncertainty is related to the accuracy of the observed streamflow data. For USGS streamflow records, accuracy depends primarily on the stability of the stage-streamflow relation, and the frequency and reliability of stage and streamflow measurements (Novak, 1985). Four accuracy classifications are used to rate station records. A rating of "excellent" indicates that about 95 percent of the daily mean flows are within 5 percent of the true flow; "good" ratings are within 10 percent; "fair" are within 15 percent; and "poor" means that daily flows have less than "fair" accuracy.

For the most recent period of record collected at Monetta, the records for water years 2001, 2002, 2003, 2005, 2006, and 2008 were rated as fair (Cooney and others, 2002; Cooney and others, 2003; U.S. Geological Survey, 2004, 2006, 2009). For water years 2004 and 2007, the records were rated as good (U.S. Geological Survey, 2005, 2008).

Watershed Model Uses

The purpose of using the watershed models previously described is to provide a framework for a better understanding of the spatial and temporal variability of the relation between hydrology and mercury in the McTier Creek watershed. A few examples of potential ways in which the models can be used are provided below.

Mapping Saturated Areas

One of the outputs from TOPMODEL is the percentage of the watershed predicted to be saturated for each modeled time step. This information along with the topographic wetness indices can be used to map the saturated areas throughout the watershed, providing a depiction of the hydrologic conditions that may trigger connections between the riparian wetlands and the channel and where these connections are occurring. Information on the timing and magnitude of these connections may provide insight into potential mobilization of mercury from the wetlands to the receiving streams.

The relation between the simulated daily mean flow and fraction of saturated area at New Holland during the confirmation period is shown in figure 30. From that period, the total saturated areas for a low-flow condition (7.0 ft^3/s on Aug. 8, 2007) and high-flow condition (130 ft^3/s on Apr. 11, 2009) are shown in figure 31. Although the percentage of the watershed shown to be saturated at any one time during this simulation period was relatively small, the increase in amount of area saturated from the low-flow to high-flow condition was approximately 350 percent. With respect to delivery of constituents that can affect the water quality of the stream, such an increase may be substantial. Thus, the use of the saturated area and other flow components from TOPMODEL can provide additional insight to the relation between the hydrology and the water quality in the watershed.

Modeling Hydrology in Subwatersheds

TOPMODEL can be used for modeling the hydrology of ungaged watersheds. Such an application on a larger-scale basis than the McTier Creek watershed was recently documented by Williamson and others (2009) for a project in which

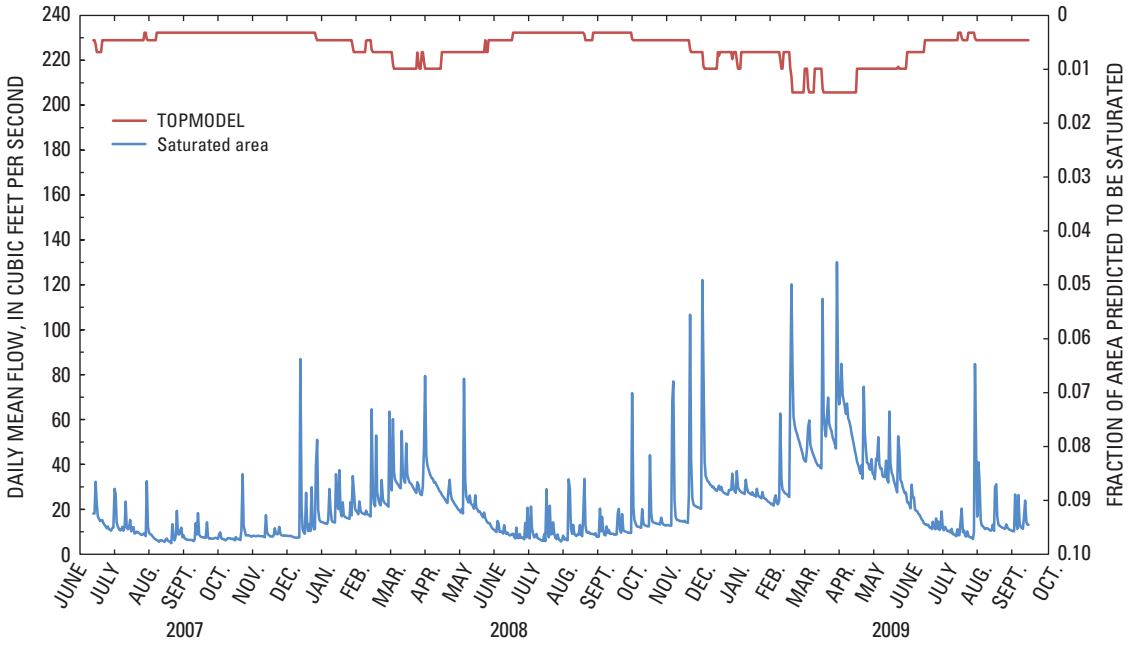

Figure 30. Simulated (TOPMODEL) daily mean flow and saturated area at McTier Creek near New Holland for the confirmation period.

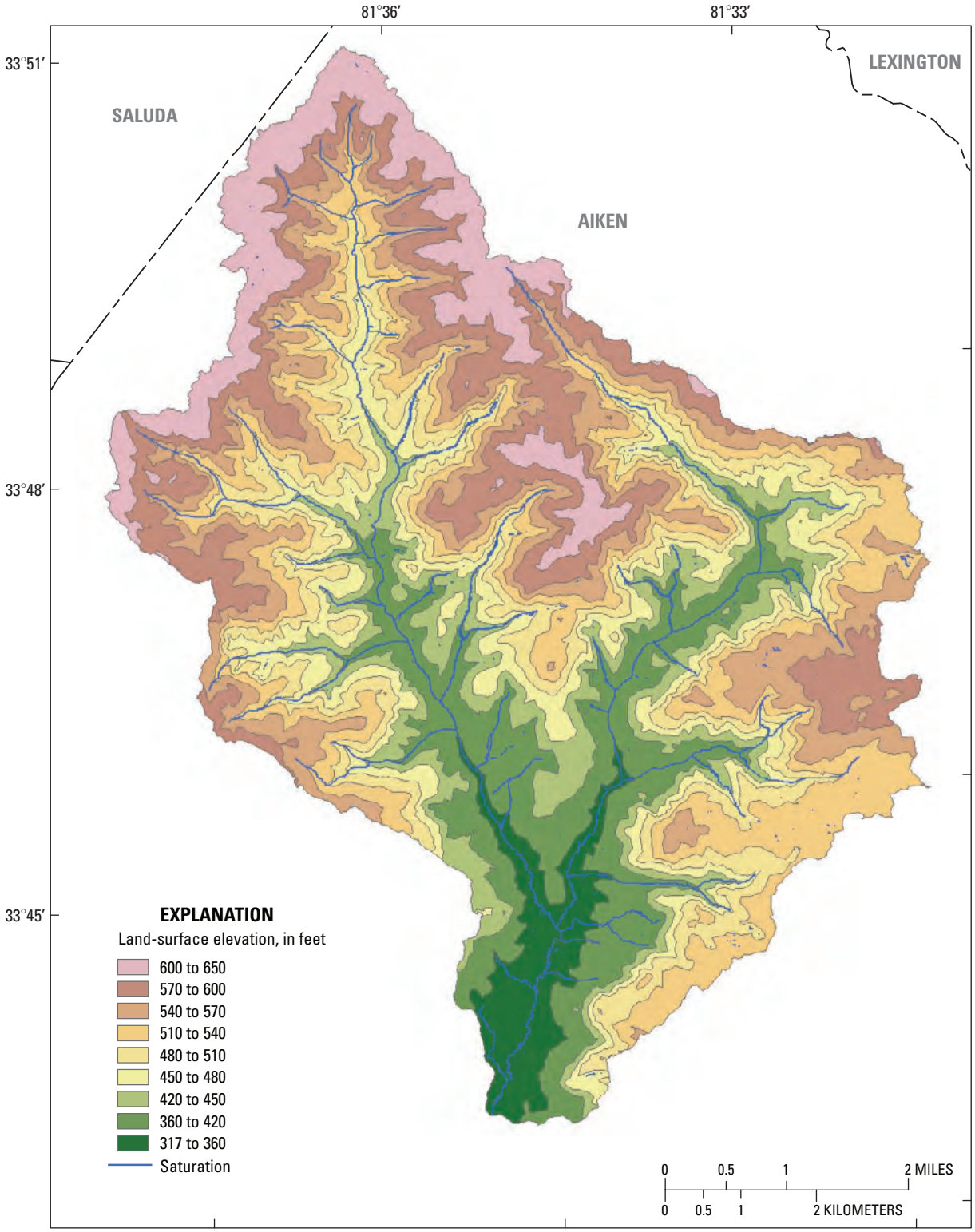

Figure 31*A*. Saturated areas from TOPMODEL simulations in the McTier Creek watershed under low-flow conditions on August 8, 2007.

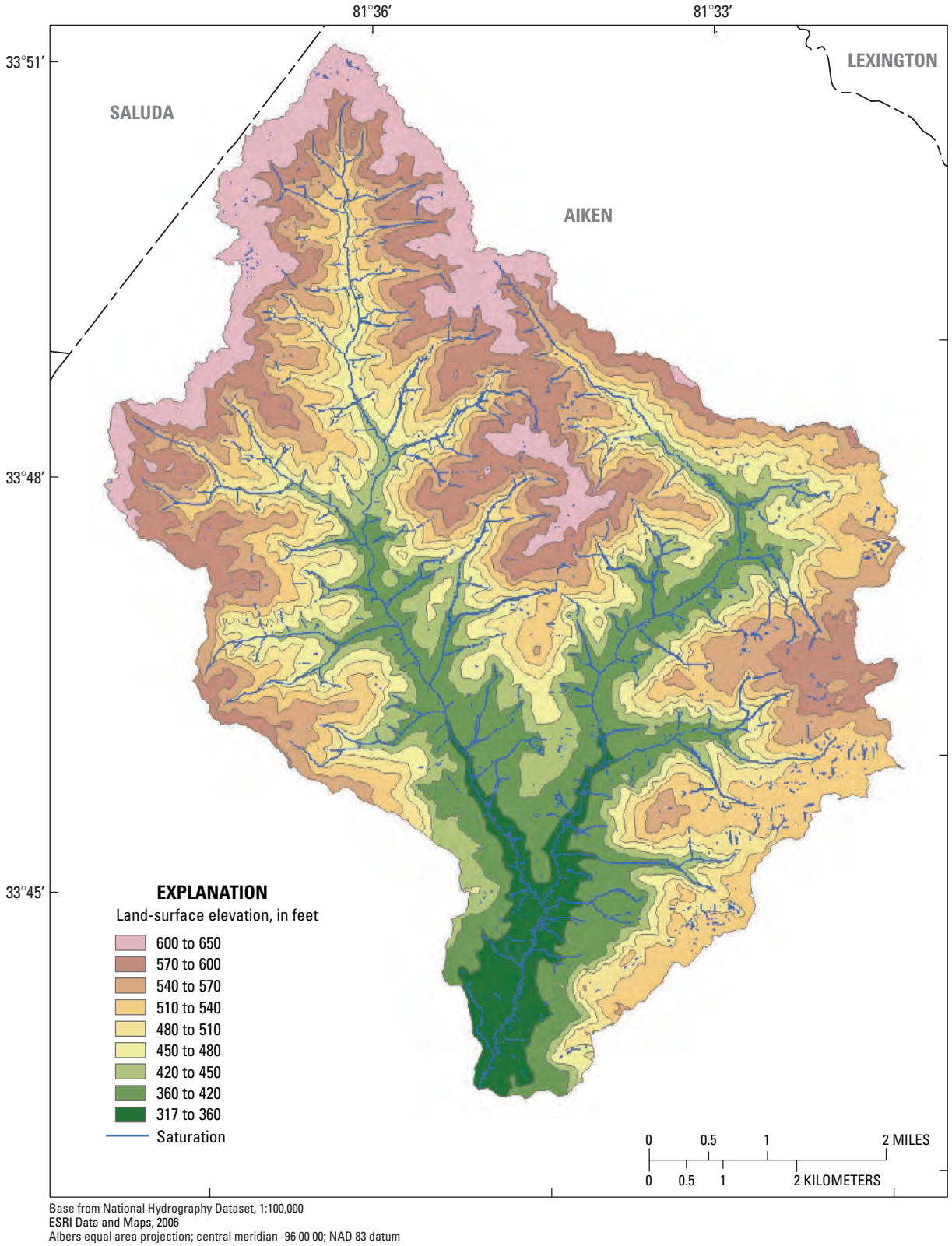

Figure 31*B*. Saturated areas from TOPMODEL simulations in the McTier Creek watershed under high-flow conditions on April 11, 2009.

TOPMODEL is being used in Kentucky to assist with managing the State's water-supply resources. Calibration of the model was done at a limited number of gaged locations, and then the calibrated parameters were used along with measured soils and watershed characteristics to model the hydrology in ungaged watersheds with similar characteristics.

For McTier Creek, a similar approach was applied. The McTier Creek watershed was subdivided into 12 subwatersheds (fig. 32). The calibrated parameters from Monetta and New Holland were then used along with the measured soils and watershed characteristics from the subwatersheds to simulate flows for the concurrent and confirmation periods, respectively. Consequently, the subwatersheds' models are separate, individual TOPMODEL applications. The topographic wetness indices were computed for each subwatershed. The same temperature and precipitation data used

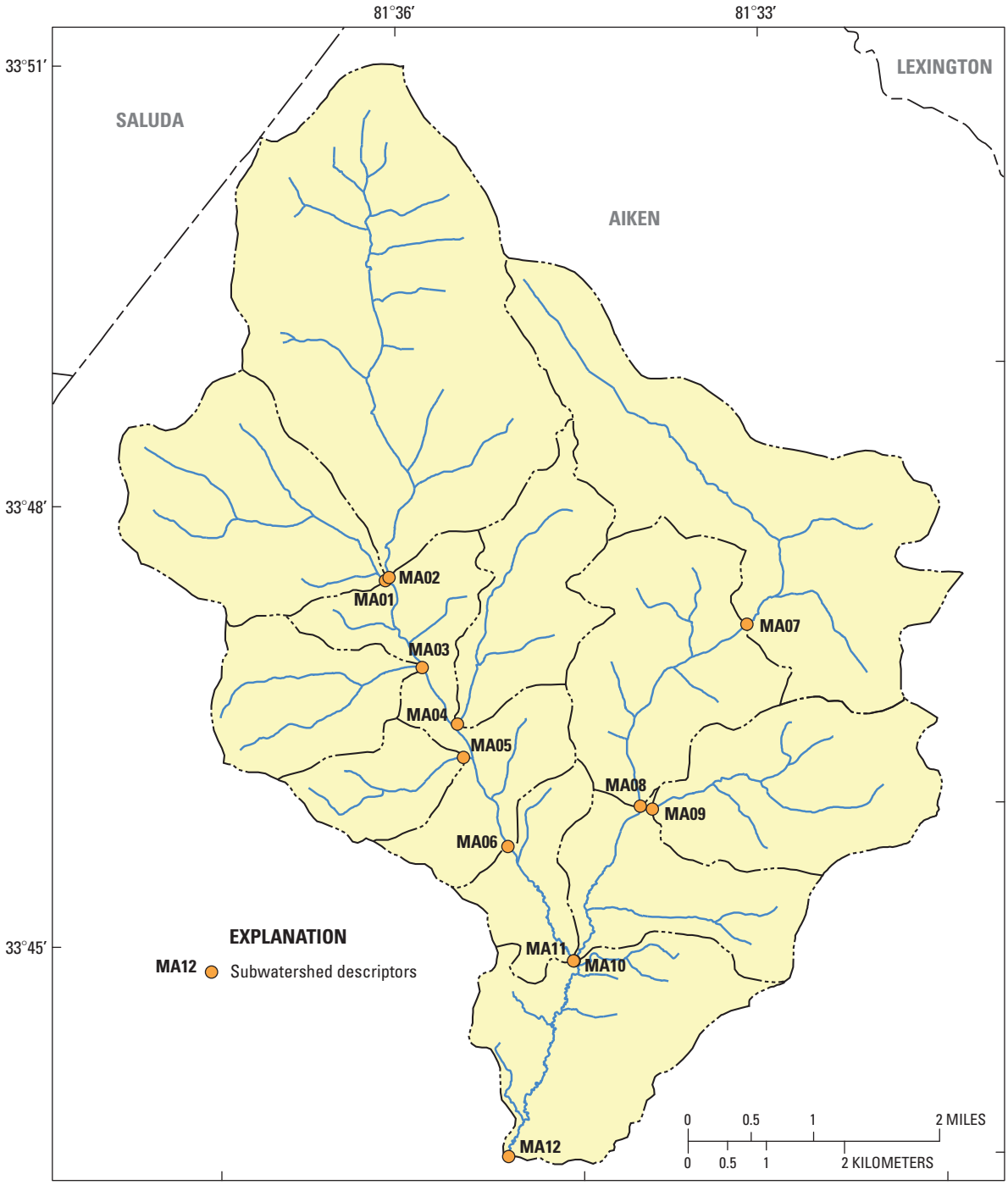

Figure 32. McTier Creek subwatersheds, Aiken County, South Carolina.

for the models at Monetta and New Holland were used for the subwatershed models. The simulated streamflow values for subwatersheds MA01 to MA06 were summed and compared to the streamflow values at Monetta, and the streamflow values for subwatersheds MA01 to MA12 were summed and compared to the simulated streamflow values at New Holland (figs. 33, 34, respectively). Figure 35 shows the simulated flows for the Monetta and New Holland gages plotted with the summation of the simulated subwatershed flows along the line of agreement. The sum of the simulated daily mean flow values from the subwatersheds matches the simulated flow values for the gages very well. The total volume of the subwatersheds as compared to the total volume at Monetta and New Holland was within about 1 and 3 percent, respectively. Modeling of the subwatersheds allows for assessment of mercury in various parts of the McTier Creek watershed. In addition, the subwatershed flows can be used as hydrology inputs for other models such as the U.S. Environmental Protection Agency Water-Quality Analysis Simulation Program (WASP) model, which can be used for a more comprehensive modeling of the mercury mechanisms in the watershed.

Loadings from TOPMODEL Flow Components

Another benefit of TOPMODEL simulations is the assessment of constituent loadings from various flow paths in the McTier Creek watershed. As discussed in appendix 1,

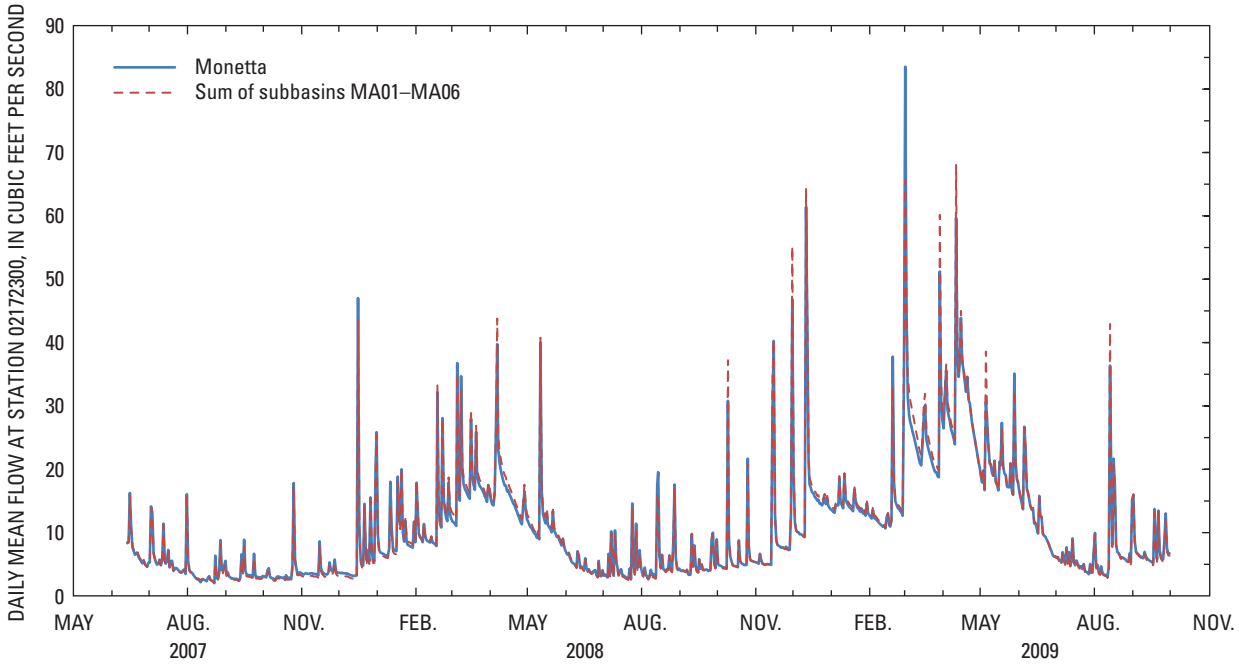

Figure 33. Simulated daily mean flow for the concurrent period at McTier Creek near Monetta and the sum of the simulated daily mean flow for subwatersheds MA01 to MA06.

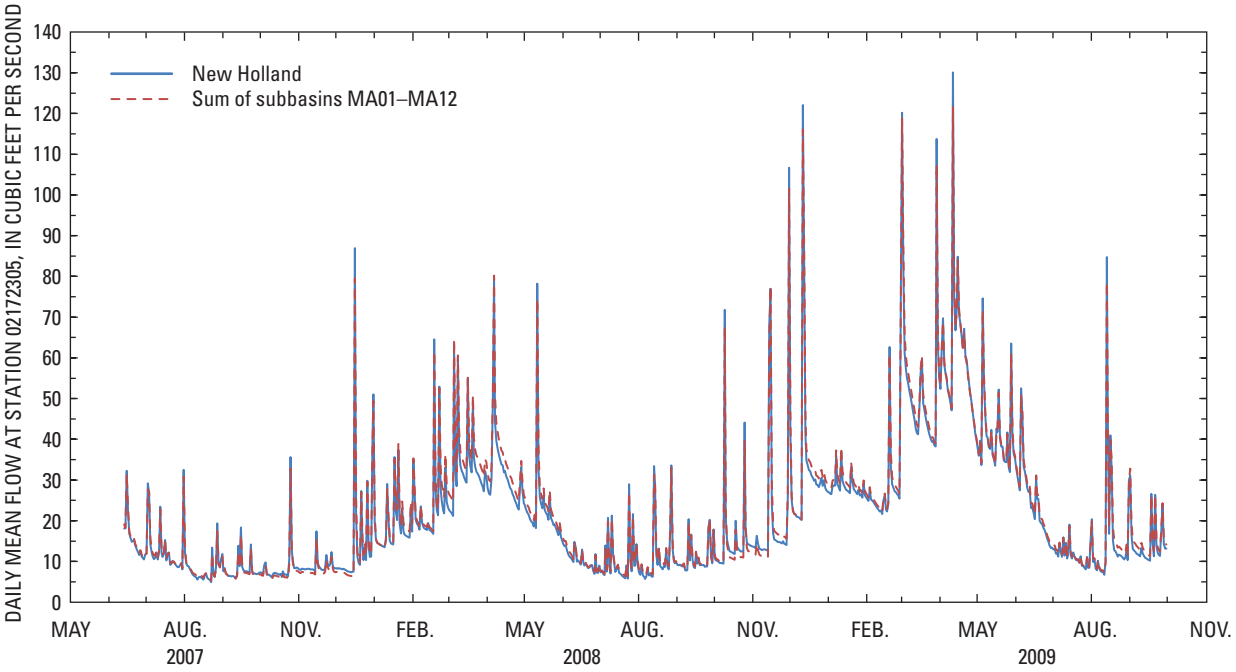

Figure 34. Simulated daily mean flow for the confirmation period at McTier Creek near New Holland and the sum of the simulated daily mean flow for subwatersheds MA01 to MA12.

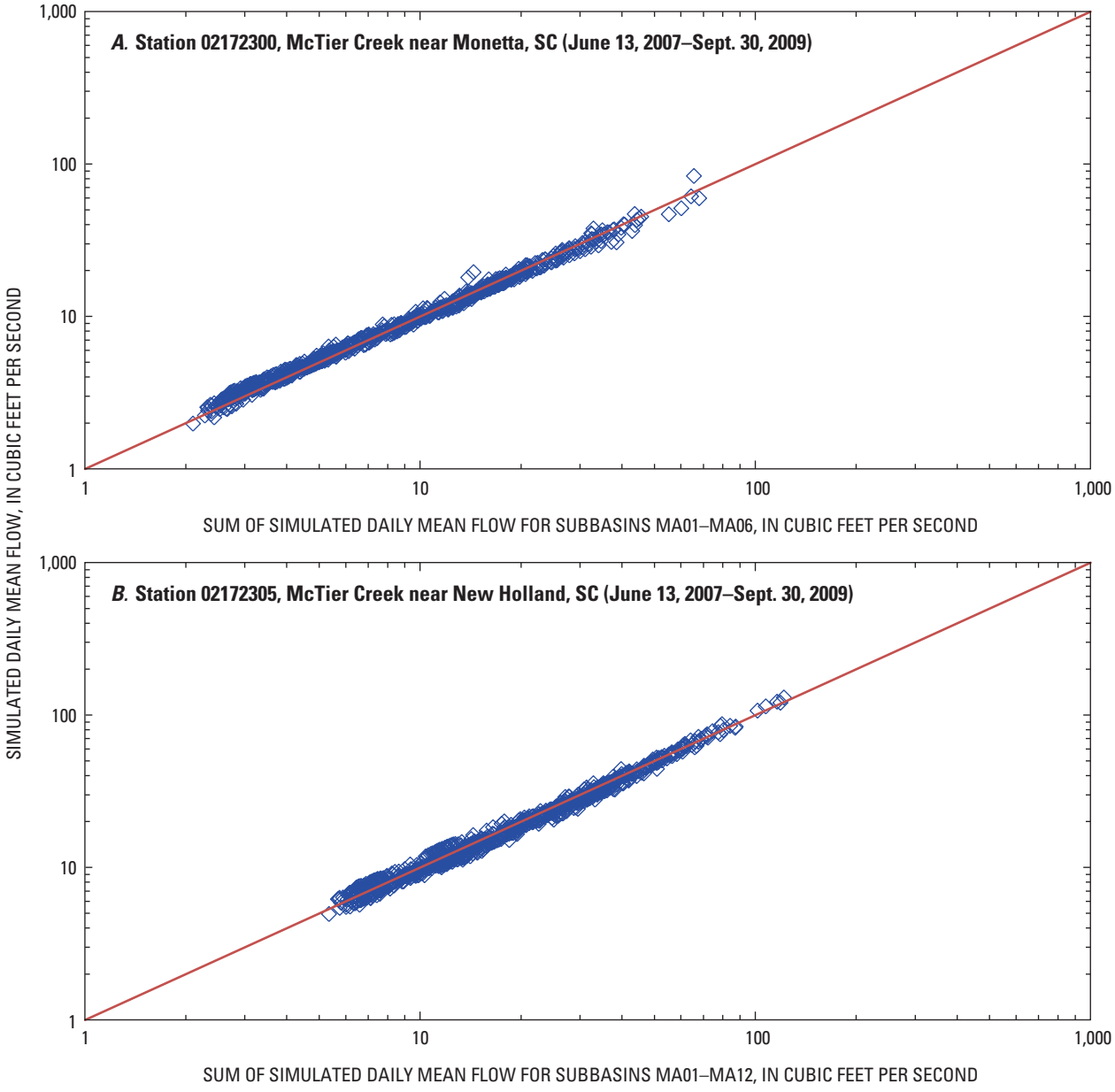

Figure 35. Simulated daily mean flow for (*A*) the concurrent period at McTier Creek near Monetta and the sum of the simulated daily mean flow for subwatersheds MA01 to MA06, and (*B*) the confirmation period at McTier Creek near New Holland and the sum of simulated daily mean flow for subwatersheds MA01 to MA12.

TOPMODEL output provides flow estimates from various surface and subsurface pathways (fig. 11). Those pathways include total in-stream flow, return flow, subsurface flow, overland saturation flow, infiltration-excess overland flow, impervious flow, and flow from water bodies (such as lakes and ponds). An example of the TOPMODEL estimates of these flow components is shown in the time-series plot in figure 36. Those assorted flows and constituent concentrations measured at various locations in the watershed can be used to assess constituent loadings as measured in the channel to help provide insight into how those total loads are being delivered to the stream. Initial assessments can be made using relatively conservative constituents and evaluated from a simple conservative mixing approach or other mixing approaches (Hornberger and others, 1994; Boyer and others, 1996).

Estimating Water, Sediment, and Mercury Balances with GBMM

GBMM is one of the first models designed to simulate spatially explicit watershed mercury processing and fluxes from watersheds to surface-water systems. Therefore, aside from its ability to predict streamflow at assessment points along a stream network, an important feature of GBMM is its capacity to estimate daily mass balances for water, sediment, and mercury within each ArcGIS grid cell in a study watershed. This mass balance simulation feature was recently applied to assess GBMM's long-term water balance response to inputs of diverse spatially explicit precipitation datasets when the model was previously calibrated using rain-gage data (Golden and others, 2010).

Identifying Spatially Explicit Mercury Source Areas in Watersheds

Another feature of GBMM is its capacity to calculate the amount of mercury derived from each land-cover type in a watershed. Such spatially explicit characterization of mercury source areas is particularly useful in studies assessing the effects of land cover or climate change on water, sediment, and mercury fluxes. A current research application of GBMM focuses on estimating the response of mercury and nitrogen fluxes to land-cover changes in a Piedmont watershed in North Carolina. Initial model estimates from the basic case scenario (for example, current land cover) fall within the range of measured mercury concentrations at the stream gage, and land-cover change scenarios yield distinct changes in mercury fluxes (H.E. Golden, U.S. Environmental Protection Agency, oral commun., April 27, 2010). For example, when pasture land is converted to a suburbanized landscape, mercury loading to the watershed outlet increases due to increased flows and particulate transport from new impervious surfaces.

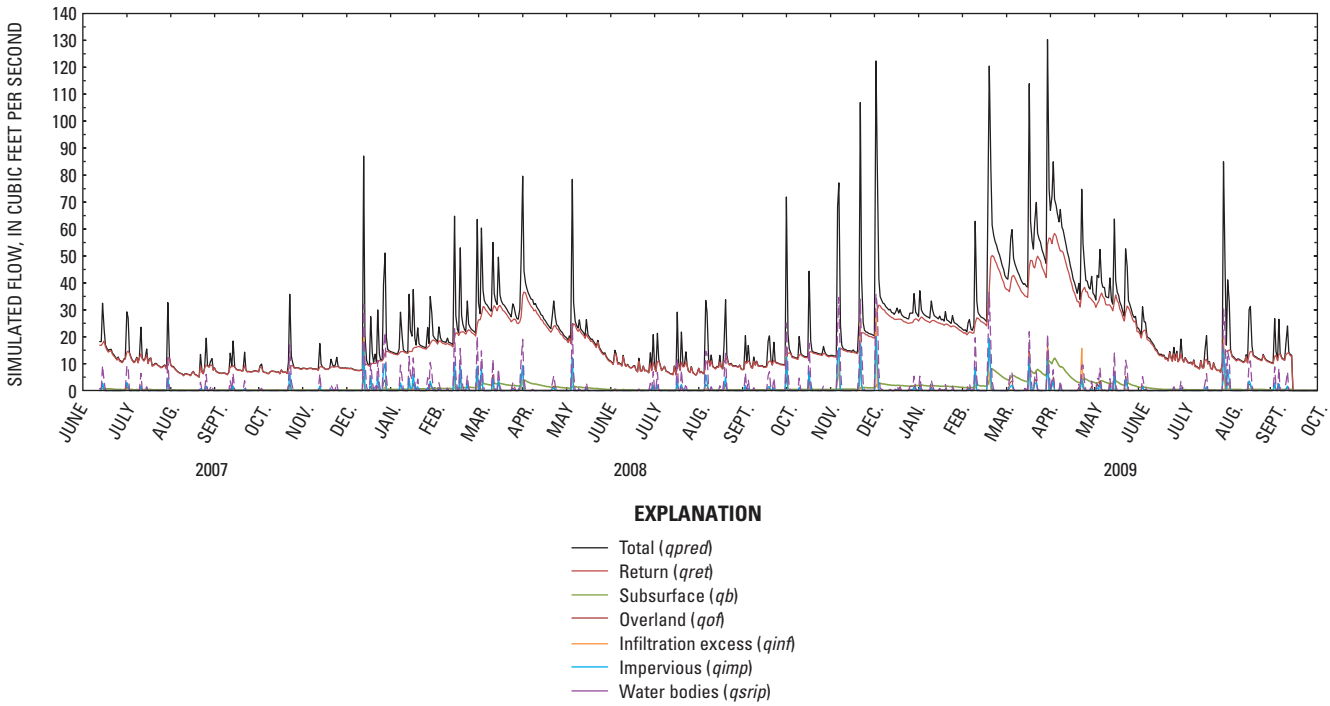

Figure 36. TOPMODEL flow components from simulation at McTier Creek near New Holland for the confirmation period.

Summary

As part of a larger scientific investigation to expand the understanding of linkages between hydrologic, geochemical, and ecological processes that drive fish-tissue mercury concentrations within the Edisto River Basin, two watershed hydrology models—the topography-based hydrological model (TOPMODEL) and the grid-based mercury model (GBMM)—were calibrated and applied to the McTier Creek watershed. McTier Creek is a small headwater stream located in the Edisto River Basin and is a tributary to the South Fork Edisto River. The models were a collaborative effort between the U.S. Geological Survey (USGS) and the U.S. Environmental Protection Agency, National Exposure Research Laboratory.

TOPMODEL and GBMM were calibrated independently but used the same meteorological data and the same period of record of observed data. Although the two models used the same datasets for calibration, no attempt was made to use the same calibration techniques that would be required if hydrologic model comparison was the goal of this study. Two USGS streamflow-gaging stations were available for comparison of observed daily mean flow with simulated daily mean flow: (1) 02172300, McTier Creek near Monetta, SC, and (2) 02172305, McTier Creek near New Holland, SC. The Monetta gage has historic record covering the period from February 2001 to September 2009. The New Holland gage, which is located at the outlet of the study reach, was established specifically for this investigation and has streamflow record available from June 2007 to September 2009.

To assess the streamflow record at Monetta in the context of a longer flow period, comparisons of average monthly mean flows at Monetta were made with a long-term streamflow-gaging station on the South Fork Edisto River. The data indicated that the yield of the average monthly mean flow for Monetta is similar to that of the South Fork Edisto River. Minimum monthly mean flows at South Fork Edisto for the complete period of record (about 70 years) were compared with those for the period of record that is concurrent with Monetta (2001 to 2009). The results showed that the 8-year period of record at Monetta captures the lowest flow period in about 70 years. In addition, the spring of 2003 tended to be a significantly wet period for the period of record at Monetta. Along with several years of more normal flows, the period of record available for model calibration at Monetta should provide for model calibrations that are rather robust with respect to encompassing a wide range of flow conditions.

A number of quantitative assessments (goodness-of-fit statistics) providing insight into how well the model simulations matched the observed daily mean flows were used in this investigation. The assessments included the Nash-Sutcliffe coefficient of model-fit efficiency index, Pearson's correlation coefficient, the root mean square error, the bias, and the mean absolute error. Simulation periods for Monetta included February 2001 to September 2009 (calibration period) and a period that was concurrent with New Holland, which was June 2007 to September 2009 (concurrent period). The period simulated at New Holland (June 2007 to September 2009) was referred to in the text as the confirmation period. For the calibration period, TOPMODEL and GBMM tended to capture the variability and timing of the observed flows quite well. Although not very different, the goodness-of-fit statistics indicate that TOPMODEL tended to perform slightly better with a bias of 0.23 cubic foot per second (ft^3/s), a root mean square error of 10.4 ft^3/s, a mean absolute error of 5.34 ft^3/s, a correlation coefficient of 0.72, and a Nash-Sutcliffe efficiency coefficient of 0.47 as compared to the corresponding values for GBMM of –1.13 ft^3/s, 9.04 ft^3/s, 6.87 ft^3/s, 0.67, and 0.38, respectively. Both models tended to perform best under normal flow conditions and tended to perform worse during extreme conditions and with situations involving the complexity of balancing groundwater recession and streamflow when flows peak and recede rapidly. Simulated and observed flow data indicated that GBMM tended to underpredict flows during periods of sustained low flows. This is likely due to the issue of having to calibrate with a single groundwater recession coefficient that is applied to flows throughout a wide range of hydrologic conditions.

References Cited

Bedient, P.B., and Huber, W.C., 1992, Hydrology and floodplain analysis (2d ed.): New York, Addison-Wesley Publishing Co., 692 p.

Bennett, D.G., and Patton, J.C., 2008, eds., A geography of the Carolinas: Boone, NC, Parkway Publishers, 266 p.

Benoit, J.M., Gilmour, C.C., Heyes, A., Mason, R.P., and Miller, C.L., 2003, Geochemical and biological controls over methylmercury production and degradation in aquatic ecosystems, *in* Cai, Y., and Braids, O.C., eds., Biogeochemistry of environmentally important trace elements: Washington, DC, American Chemical Society, p. 262–297.

Beven, K.J., 1978, The hydrological response of headwater and sideslope areas: Hydrological Sciences Bulletin, v. 23, p. 419–437.

Beven, K.J., 1984, Infiltration into a class of vertically nonuniform soils: Hydrological Sciences Journal, v. 29, p. 425–434.

Beven, K.J., 1997, Distributed hydrological modeling—Applications of the TOPMODEL concept: Chichester, England, John Wiley and Sons Ltd.

Beven, K.J., 2001, Rainfall-runoff modeling—The primer: Chichester, England, John Wiley and Sons Ltd.

Beven, K.J., 2002, Towards a coherent philosophy for modeling the environment—Proceedings of the Royal Society: Mathematical, Physical and Engineering Sciences, v. 458, no. 2026, p. 2465–2484.

Beven, K.J., and Kirkby, M.J., 1979, A physically based, variable contributing area model of basin hydrology: Hydrological Sciences Bulletin, v. 24, p. 43–69.

Beven, K.J., Lamb, R., Quinn, P.F., Romanowicz, R., and Freer, J., 1995, TOPMODEL, *in* Singh, V.P., ed., Computer models of watershed hydrology: Highlands Ranch, CO, Water Resources Publications, p. 627–668.

Beven, K.J., and Wood, E.F., 1983, Catchment geomorphology and the dynamics of runoff contributing areas: Journal of Hydrology, v. 65, p. 139–158.

Bloom, N.S., 1992, On the chemical form of mercury in edible fish and marine invertebrate tissue: Canadian Journal of Fisheries and Aquatic Science, v. 49, p. 1010–1017.

Bloxham, W.M., 1976, Low-flow characteristics of streams in the Inner Coastal Plain of South Carolina: South Carolina Water Resources Commission Report No. 5, 41 p.

Boyer, E.W., Hornberger, G.M., Bencala, K.E., and McKnight, D., 1996, Overview of a simple model describing variation of dissolved organic carbon in an upland catchment: Ecological Modeling, v. 85, p. 183–188.

Bradley, P.M., Chapelle, F.H., and Journey, C.A., 2009, Comparison of methylmercury production and accumulation in sediments of the Congaree and Edisto River Basins, South Carolina, 2004–06: U.S. Geological Survey Scientific Investigations Report 2009–5021, 9 p.

Brigham, M.E., Wentz, D.A., Aiken, G.R., and Krabbenhoft, D.P., 2009, Mercury cycling in stream ecosystems—1. Water column chemistry and transport: Environmental Science & Technology, v. 43, p. 2720–2725.

Brumbaugh, W.G., Krabbenhoft, D.P., Helsel, D.R., Wiener, J.G., and Echols, K.R., 2001, A national pilot study of mercury contamination of aquatic ecosystems along multiple gradients—Bioaccumulation in fish: U.S. Geological Survey Biological Science Report 2001–0009, 25 p.

Burt, T.P., and Butcher, D.P., 1985, Topographic controls of soil moisture distributions: Journal of Soil Science, v. 36, p. 469–486.

Chasar, L.C., Scudder, B.C., Stewart, A.R., Bell, A.H., and Aiken, G.R., 2009, Mercury cycling in stream ecosystems—3. Trophic dynamics and methylmercury bioaccumulation: Environmental Science & Technology, v. 43, p. 2733–2739.

Clarkson, T., Magos, L., and Myers, G., 2003, The toxicology of mercury—Current exposures and clinical manifestations: New England Journal of Medicine, v. 349, p. 1731–1737.

Compeau, G.C., and Bartha, R., 1985, Sulfate-reducing bacteria—Principal methylators of mercury in anoxic estuarine sediment: Applied and Environmental Microbiology, v. 50, p. 498–502.

Cooke, C.W., 1936, Geology of the Coastal Plain of South Carolina: U.S. Geological Survey Bulletin 867, 196 p.

Cooney, T.W., Drewes, P.A., Ellisor, S.W., Lanier, T.H., and Melendez, F., 2002, U.S. Geological Survey Water-Data Report SC–01–1, 666 p.

Cooney, T.W., Drewes, P.A., Ellisor, S.W., Lanier, T.H., and Melendez, F., 2003, U.S. Geological Survey Water-Data Report SC–02–1, 683 p.

Crow, Peter, 2005, The influence of soils and species on tree root depth: Forestry Commission Information Note, United Kingdom, accessed March 5, 2009, at *http://www.forestry.gov.uk/pdf/FCIN078.pdf/$FILE/FCIN078.pdf*.

Dai, T., Ambrose, R.B., Alvi, K., Wool, T., Manguerra, H., Chokshi, M., Yang, H., and Kraemer, S., 2005, Characterizing spatial and temporal dynamics—Development of a grid-based watershed mercury loading model, *in* Moglen, G.E., ed., Managing watersheds for human and natural impacts—Engineering, ecological, and economic challenges: Williamsburg, VA, American Society of Civil Engineers, July 19–22, 2005 [variously paged].

Doherty, John, 2005, PEST—Model independent parameter estimation user manual (5th ed.): Watermark Numerical Computing, 336 p.

Donigian, A.S., Jr., Imhoff, J.C., Bicknell, B.R., and Kittle, J.L., Jr., 1984, Application guide for Hydrological Simulation Program—FORTRAN (HSPF): U.S. Environmental Protection Agency, Environmental Research Laboratory, EPA–600/3–84–065, 177 p.

Dunne, T., and Black, R.D., 1970, Partial area contributions to storm runoff in a small New England watershed: Water Resources Research, v. 6, p. 1296–1311.

Dunne, T., and Leopold, L.B., 1978, Water in environmental planning: New York, W.H. Freeman and Company, 818 p.

Dunne, T., Moore, T.R., and Taylor, C.H., 1975, Recognition and prediction of runoff-producing zones in humid regions: Hydrological Sciences Bulletin, v. 20, p. 305–327.

Eidson, J.P., Lacy, C.M., Nance, Luke, Hansen, W.F., Lowery, M.A., and Hurley, N.M., Jr., 2005, Development of a 10- and 12-digit hydrologic unit code numbering system for South Carolina, 2005: U.S. Department of Agriculture, Natural Resources Conservation Service, 38 p., 1 pl.

Elsenbeer, H., Cassel, K., and Castro, J., 1992, Spatial analysis of soil hydraulic conductivity in a tropical rain forest catchment: Water Resources Research, v. 28, p. 3201–3214.

Fleming, E.J., Mack, E.E., Green, P.G., and Nelson, D.C., 2006, Mercury methylation from unexpected sources—Molybdate-inhibited freshwater sediments and an iron-reducing bacterium: Applied and Environmental Microbiology, v. 72, p. 457–464.

Garen, D.C., and Moore, D.S., 2005, Curve number hydrology in water quality modeling—Uses, abuses, and future directions: Journal of the American Water Resources Association, v. 41, p. 377–388.

Golden, H.E., Knightes, C.D., Cooter, E.J., Dennis, R.L., Gilliam, R.C., and Foley, K.M., 2010, Linking air quality and watershed models for environmental assessments—Analysis of the effects of model-specific precipitation estimates on calculated water flux: Environmental Modelling & Software, v. 25, p. 1722–1737, doi: 10.1016/j.envsoft.2010.04.015.

Green, W.H., and Ampt, G.A., 1911, Studies on soil physics—I. The flow of air and water through soils: Journal of Agricultural Science, v. 4, p. 1–24.

Griffith, G.E., Omernik, J.M., Comstock, J.A., Schafale, M.P., McNab, W.H., Lenat, D.R., MacPherson, T.F., Glover, J.B., and Shelburne, V.B., 2002, Ecoregions of North Carolina and South Carolina: U.S. Geological Survey color poster with map, scale 1:1,500,000 (accessed November 9, 2010, at *http://www.epa.gov/naaujydh/pages/ecoregions/ncsc_eco.htm*.

Grigal, D.F., 2002, Inputs and outputs of mercury from terrestrial watersheds—A review: Environmental Review, v. 10, p. 1–39.

Haith, D.A., Mandel, R., and Wu, R.S., 1992, GWLF—Generalized watershed loading functions, version 2.0, user's manual: Ithaca, NY, Department of Agricultural and Biological Engineering.

Hall, B.D., Aiken, G.R., Krabbenhoft, D.P., Marvin-DiPasquale, M., and Swarzenski, C.M., 2008, Wetlands as principal zones of methylmercury production in southern Louisiana and the Gulf of Mexico region: Environmental Pollution, v. 154, p. 124–134.

Hall, B.D., Bodaly, R.A., Fudge, R.J.P., Rudd, J.W.M., and Rosenberg, D.M., 1997, Food as the dominant pathway of methylmercury uptake by fish: Water, Air, and Soil Pollution, v. 100, p. 13–24.

Hamon, W.R., 1961, Estimating potential evapotranspiration: Journal of the Hydraulics Division, Proceedings of the American Society of Civil Engineers, v. 87, p. 107–120.

Hay, L.E., 1998, Stochastic calibration of an orographic precipitation model: Hydrological Processes, v. 12, p. 613–634.

Hazell, W.F., and Bales, J.D., 1997, Real-time rainfall measurement in the city of Charlotte and Mecklenburg County, North Carolina: U.S. Geological Survey Fact Sheet FS–052–97, 4 p.

Helsel, R.M., and Hirsch, D.R., 1995, Studies in environmental science 49—Statistical methods in water resources: Amsterdam, Elsevier Science, 529 p.

Hershfield, D.M., 1961, Rainfall frequency atlas of the United States: Washington, DC, Department of Commerce, Weather Bureau, Technical Paper No. 40, 114 p.

Hewlett, J.D., and Hibbert, A.R., 1967, Factors affecting the response of small watersheds to precipitation in humid areas, *in* Sopper, W.E., and Lull, H.W., eds., Forest hydrology: New York, Pergamon Press.

Homer, C., Huang, C., Yang, L., Wylie, B., and Coan, M., 2004, Development of a 2001 National Land-Cover Database for the United States: Photogrammetric Engineering and Remote Sensing, v. 70, no. 7, p. 829–840.

Hornberger, G.M., Bencala, K.E., and McKnight, D.M., 1994, Hydrological controls on dissolved organic carbon during snowmelt in the Snake River near Montezuma, Colorado: Biogeochemistry, v. 25, p. 147–165.

Hornberger, G.M., Beven, K.J., Cosby, B.J., and Sappington, D.E., 1985, Shenandoah watershed study—Calibration of a topography-based, variable contributing area hydrological model to a small forested catchment: Water Resources Research, v. 21, p. 1841–1850.

Hornberger, G.M., Raffensperger, J.P., Wiberg, P.L., and Eshleman, K.N., 1998, Elements of physical hydrology: Baltimore, MD, The John Hopkins University Press.

Horton, J.W., Jr., and Dicken, C.L., 2001, Preliminary digital geologic map of the Appalachian Piedmont and Blue Ridge, South Carolina segment: U.S. Geological Survey Open-File Report 01–298, 21 p.

Horton, R.E., 1933, The role of infiltration in the hydrologic cycle: EOS, Transactions, American Geophysical Union, v. 14, p. 446–460.

Inamdar, Shreeram, 2009, Course notes from Bioresources Engineering 622, University of Delaware, accessed September 24, 2009, at *http://udel.edu/~inamdar/BREG622/TOPIndex.pdf*.

Janssen, P.H.M., and Heuberger, P.S.S., 1993, Calibration of process-oriented models: Ecological Modelling, v. 83, p. 55–66.

Keith, F., and Kreider, J.F., 1978, Principles of solar engineering: Washington, DC, Hemisphere Publishing Corporation.

Kennen, J.G., Kauffman, L.J., Ayers, M.A., Wolock, D.M., and Colarullo, S.J., 2008, Use of an integrated flow model to estimate ecologically relevant hydrologic characteristics at stream biomonitoring sites: Ecological Modelling, v. 211, p. 57–76.

Kim, N.W., and Lee, J., 2008, Temporally weighted average curve number method for daily runoff simulation: Hydrological Processes, v. 22, p. 4936–4948.

Kirkby, M.J., and Chorley, R.J., 1967, Throughflow, overland flow and erosion: Bulletin of the International Association of Scientific Hydrology, v. 12, p. 5–21.

Krause, P., Boyle, D.P., and Base, F., 2005, Comparison of different efficiency criteria for hydrological model assessment: Advances in Geosciences, v. 5, p. 89–97.

Legates, D.R., and McCabe, G.J., Jr., 1999, Evaluating the use of "goodness-of-fit" measures in hydrologic and hydroclimatic model validation: Water Resources Research, v. 35, no. 1, p. 233–241.

Lins, H.F., Hirsch, R.M., and Kiang J., 2010, Water—The Nation's fundamental climate issue—A white paper on the U.S. Geological Survey role and capabilities: U.S. Geological Survey Circular 1347, 9 p.

Marshall, W.D., ed., 1993, Assessing change in the Edisto River Basin—An ecological characterization: South Carolina Water Resources Commission Report No. 177, 149 p.

Matott, L.S., 2005, OSTRICH—An optimization software tool, documentation and user's guide, version 1.6: Buffalo, NY, University at Buffalo, accessed May 13, 2009, at *http://www.groundwater.buffalo.edu/*.

Mergler, D., Anderson, H.A., Chan, L.H.M., Mahaffey, K.R., Murray, M., Sakamoto, M., and Stern, A.H., 2007, Methylmercury exposure and health effects in humans—A worldwide concern: Ambio, v. 36, p. 3–11.

Nash, J.E., and Sutcliffe, J.E., 1970, River flow forecasting through conceptual models—Part I. A discussion of principles: Journal of Hydrology, v. 10, p. 282–290.

National Oceanic and Atmospheric Administration, 2008, U.S. Climate Division Dataset Mapping Page: U.S. Department of Commerce, National Oceanic and Atmospheric Administration, Earth System Research Laboratory, accessed October 16, 2008, at *http://www.cdc.noaa.gov/USclimate/USclimdivs.html*.

Natural Resources Conservation Service, 1986, Urban hydrology for small watersheds: U.S. Department of Agriculture Technical Release 55.

Natural Resources Conservation Service, 2008, Soil survey geographic (SSURGO) database, accessed June 8, 2008, at *http://www.soils.usda.gov/survey/geography/ssurgo/*.

Neitsch, S.L., Arnold, J.G., Kiniry, J.R., and Williams, J.R., 2005, Soil and water assessment tool—Theoretical documentation, version 2005: Temple, TX, Grassland, Soil and Water Research Center, Agricultural Research Service and Blackland Research Center, Texas Agricultural Experiment Station.

Norman, G.R., and Streiner, D.L., 1997, PDQ statistics: St. Louis, MO, Mosby-Year Book, Inc.

Novak, C.E., 1985, WRD data reports preparation guide: U.S. Geological Survey Open-File Report 85–480, 199 p., 2 apps.

Nystrom, P.G., Willoughby, R.H., and Kite, L.E., 1986, Cretacious-Tertiary stratigraphy of the upper edge of the Coastal Plain between North Augusta and Lexington, South Carolina: Carolina Geological Society Field Trip Guidebook, October 11 and 12, 1986, South Carolina Geological Survey, Columbia, South Carolina.

Ockerman, D.J., 2005, Simulation of streamflow and estimation of recharge to the Edwards aquifer in the Hondo Creek, Verde Creek, and San Geronimo Creek watersheds, South-Central Texas, 1951–2003: U.S. Geological Survey Scientific Investigations Report 2005–5252, 37 p.

Peterson, S.A., Van Sickle, John, Herlihy, A.T., and Hughes, R.M., 2007, Mercury concentration in fish from streams and rivers throughout the western United States: Environmental Science & Technology, v. 41, no. 1, p. 58–65.

Rantz, S.E., and others, 1982, Measurement and computation of streamflow: U.S. Geological Survey Water-Supply Paper 2175, v. 2, 631 p.

Robinson, J.B., Hazell, W.F., and Garrett, R.G., 1998, Precipitation, streamflow, and water-quality data from selected sites in the city of Charlotte and Mecklenburg County, North Carolina, 1995–97: U.S. Geological Survey Open-File Report 98–67, 220 p.

Rosgen, D.L., 1996, Applied river morphology: Pagosa Springs, CO, Wildland Hydrology.

Rypel, A.L., Arrington, D.A., and Findaly, R.H., 2008, Mercury in southeastern U.S. riverine fish populations linked to water body type: Environmental Science & Technology, v. 42, p. 5118–5124.

Searcy, J.K., 1959, Flow-duration curves, manual of hydrology—Part 2. Low-flow techniques: U.S. Geological Survey Water-Supply Paper 1542–A, 33 p.

Schneiderman, E.M., Steenhuis, T.S., Thongs, D.J., Easton, Z.M., Zion, M.S., Neal, A.L., Mendoza, G.F., and Walter, M.T., 2007, Incorporating variable source area hydrology into a curve-number-based watershed model: Hydrological Processes, v. 21, p. 3420–3430.

Shepard, Donald, 1968, A two-dimensional interpolation function for irregularly-spaced data: Proceedings of the 1968 Association for Computing Machinery (ACM) National Conference, p. 517–524.

Singh, V.P., 1995, Computer models of watershed hydrology: Highlands Ranch, CO, Water Resources Publications.

South Carolina Department of Health and Environmental Control, 2006, South Carolina fish consumption advisories for 2006: South Carolina Department of Health and Environmental Control, Division of Water, accessed February 2007 at *http://www.scdhec.gov/environment/water/fish/docs/advtb.pdf*.

South Carolina Department of Natural Resources, 2009, South Carolina State Climatology Office, Aiken County, accessed August 6, 2009, at *http://www.dnr.sc.gov/climate/sco/ClimateData/countyData/county_aiken.php*.

St. Louis, V.L., Rudd, J.W.M., Kelly, C.A., Beaty, K.G., Bloom, N.S., and Flett, R.J., 1994, Importance of wetlands as sources of methyl mercury to boreal forest ecosystems: Canadian Journal of Fisheries and Aquatic Sciences, v. 51, p. 1065–1076.

Swain, E.B., Jakus, P.M., Rice, G., Lupi, F., Maxson, P.A., Pacyna, J.M., Penn, A., Spiegel, S.J., and Veiga, M.M., 2007, Socioeconomic consequences of mercury use and pollution: Ambio, v. 36, p. 45–61.

Tetra Tech, 2006, Development of second-generation of mercury watershed simulation technology—Grid-based mercury model version 2.0, user's manual: Fairfax, VA.

Tolson, B.A., and Shoemaker, C.A., 2007, Dynamically dimensioned search algorithm for computationally efficient watershed model calibration: Water Resources Research, v. 43, doi:10.1029/2005WR004723.

U.S. Department of Agriculture, Natural Resources Conservation Service, 1986, Urban hydrology for small watersheds: Technical Release 55, Washington, DC.

U.S. Department of Agriculture, Natural Resources Conservation Service, National Soil Survey Center, 1995, Soil survey geographic (SSURGO) data base, data use information: Miscellaneous Publication Number 1527, 110 p.

U.S. Environmental Protection Agency, 2008, Fish advisories, accessed January 11, 2009, at *http://www.epa.gov/fishadvisories/*.

U.S. Environmental Protection Agency, 2009, The BASINS 4 documentation, accessed April 1, 2009, at *http://www.epa.gov/waterscience/basins/bsnsdocs.html*.

U.S. Geological Survey, 2004, Water-resources data, South Carolina, water year 2003: U.S. Geological Survey Water-Data Report WDR–SC–04–1, accessed December 2, 2009, at *http://pubs.usgs.gov/wdr/*.

U.S. Geological Survey, 2005, Water-resources data, South Carolina, water year 2004: U.S. Geological Survey Water-Data Report WDR–SC–05–1, accessed December 2, 2009, at *http://pubs.usgs.gov/wdr/*.

U.S. Geological Survey, 2006, Water-resources data, South Carolina, water year 2005: U.S. Geological Survey Water-Data Report WDR–SC–05–1, accessed December 2, 2009, at *http://pubs.usgs.gov/wdr/*.

U.S. Geological Survey, 2007a, Facing tomorrow's challenges—U.S. Geological Survey science in the decade 2007–2017: U.S. Geological Survey Circular 1309, available at *http:// pubs.er.usgs.gov/usgspubs/cir/cir1309*.

U.S. Geological Survey, 2007b, Water-resources data for the United States, water year 2006: U.S. Geological Survey Water-Data Report WDR–US–2006, accessed December 2, 2009, at *http://wdr.water.usgs.gov/*.

U.S. Geological Survey, 2008, Water-resources data for the United States, water year 2007: U.S. Geological Survey Water-Data Report WDR–US–2007, accessed December 2, 2009, at *http://wdr.water.usgs.gov/*.

U.S. Geological Survey, 2009, Water-resources data for the United States, water year 2008: U.S. Geological Survey Water-Data Report WDR–US–2008, accessed December 2, 2009, at *http://wdr.water.usgs.gov/*.

Walter, M.T., and Shaw, S.B., 2005, DISCUSSION—Curve number hydrology in water quality modeling—Uses, abuses, and future directions: Journal of the American Water Resources Association, v. 41, p. 1491–1492.

Whipkey, R.Z., 1965, Subsurface stormflow from forested slopes: Hydrological Sciences Bulletin, v. 10, p. 74–85.

Williamson, T.N., Odom, K.R., Newson, J.K., Downs, A.C., Nelson H.L., Jr., Cinotto, P.J., and Ayers, M.A., 2009, The water availability tool for environmental resources (WATER)—A water-budget modeling approach for managing water-supply resources in Kentucky—Phase I—Data processing, model development, and application to non-karst areas: U.S. Geological Survey Scientific Investigations Report 2009–5248, 34 p.

Wolock, D.M., 1993, Simulating the variable-source-area concept of streamflow generation with the watershed model TOPMODEL: U.S. Geological Survey Water-Resources Investigations Report 93–4124, 33 p.

Wolock, D.M., and Hornberger, G.M., 1991, Hydrological effects of changes in levels of atmospheric carbon dioxide: Journal of Forecasting, v. 10, p. 105–116.

Yeardley, R.B., Jr., Lazorchak, J.M., and Paulsen, S.G., 1998, Elemental fish tissue contamination in northeastern U.S. lakes—Evaluation of an approach to regional assessment: Environmental Toxicology and Chemistry, v. 17, no. 9, p. 1875–1884.

Appendix 1

Model Components in TOPMODEL

The version of TOPMODEL used in this investigation was documented by Kennen and others (2008), and much of the information included in this appendix comes from that paper. For a more detailed discussion of the mathematical underpinnings of TOPMODEL, see Beven and Kirkby (1979), Beven (1997), Hornberger and others (1998), Wolock (1993), or Beven (2001).

TOPMODEL is a process-oriented watershed hydrology model that systematically accounts for water from the time that it enters the watershed as precipitation until it leaves the watershed through evapotranspiration, by direct withdrawal, or as streamflow. TOPMODEL simulates snow accumulation and melt, evapotranspiration, streamflow derived from water that moves overland into the stream and water that moves through the subsurface into the stream, and routing of flow from delivery to the stream to the watershed outlet. Because of the characteristics of the McTier Creek watershed, the snow related and routing algorithms were not utilized in this study.

In the water balance, rain on a given day is used first to satisfy the potential evapotranspiration for the day. The remainder moves overland to a stream if the rain falls on impervious surface that is connected to a stream (*qimp*), soil that is already saturated (*qof*), or soil through which the water cannot infiltrate rapidly enough (*qinf*) (fig. 11). Precipitation that falls on a surface-water body is added to the streamflow (*qsrip*). The remaining water infiltrates the upper soil zone. Any water stored in the saturated subsurface zone is assumed to move downslope toward the stream channel and enters the stream as return flow (*qret*) in saturated areas and (or) subsurface flow (*qb*) at the streambanks. The portion of the subsurface water that drains into the stream depends on the volume in storage and the values of the TOPMODEL parameters. The major paths that water follows in the version of TOPMODEL used in this investigation are shown in figure 11 along with the abbreviation names, shown in the parentheses, as provided in the program's output file.

Precipitation

Precipitation is the main forcing function in TOPMODEL. For this study, spatial estimates of precipitation and temperature for the McTier Creek watershed were determined by inverse-distance weighting using data obtained from nearby National Weather Service stations (table 2; fig. 12). More robust methods are available, which take into account such factors as elevation (Hay, 1998). However, given the size of the McTier Creek watershed and the Coastal Plain environment as opposed to a more mountainous setting, it was concluded that the inverse-distance weighting procedure was sufficient.

Evapotranspiration

Evapotranspiration is a function of the potential rate (the rate that would occur if unlimited water were available) and the actual amount of water that is available in the soil. Potential evapotranspiration is calculated using the Hamon formula (Hamon, 1961), the maximum possible clear-sky duration of sunshine, the mass density of water in air as a function of air temperature, and an empirical relation, which includes an empirical constant. Duration of sunshine is estimated from watershed latitude by calculating the solar declination and the sunset-hour angle (Keith and Kreider, 1978). Any precipitation not exceeding the potential evapotranspiration rate for a given day is assumed to be part of the actual evapotranspiration. If precipitation is insufficient to meet the potential evapotranspiration, then evapotranspiration depletes water from the root zone of the soil (as described by Beven and others, 1995) until it is exhausted. The maximum root-zone water storage is estimated as a function of the root-zone depth and the available water capacity of the soil. For the McTier Creek watershed, the root zone was assumed to be 1.9 meters (m) thick based on information from Crow (2005) and calibration parameterization assessments using PEST (Doherty, 2005).

Impervious-Area Runoff

Impervious-area runoff is calculated as a function (effective portion) of the total impervious surface cover (ISC) in a watershed using the TR-55 curve-number method (Natural Resources Conservation Service, 1986). The value of ISC is treated as a starting point for the calculation of impervious-area runoff because not all impervious areas of a watershed are effective in generating direct runoff. After evapotranspiration is removed from the daily rainfall, impervious-area runoff is computed for the effective ISC by assuming an initial runoff curve number for paved surfaces of 98. The runoff curve number is then adjusted (higher for wetter conditions, lower for drier conditions) on the basis of the 5-day antecedent rainfall. Wet antecedent conditions (5-day antecedent rainfall greater than 2.81 centimeters (cm) for the non-growing season or greater than 5.63 cm for the growing season) yield a curve number of 99.1, and dry conditions (5-day antecedent rainfall less than 1.28 cm for the non-growing season or less than 3.58 cm for the growing season) yield a curve number as low as 95.3. Runoff is computed and assumed to enter the stream channel directly. Any water remaining (precipitation minus evapotranspiration and runoff) is distributed uniformly to the water budget that governs the pervious-area runoff components of the watershed.

Pervious-Area Runoff

In TOPMODEL, the major processes considered are subsurface flow, saturation overland flow (also known as Dunne overland flow (Dunne and Black, 1970)), return flow,

infiltration excess overland flow (also known as Horton overland flow (Horton, 1933)), and precipitation/evapotranspiration over water. The starting point for deriving expressions to compute subsurface flow, saturation overland flow, and return flow is the continuity equation, applied at a location in the watershed, and Darcy's Law (Beven, 1984). If steady-state conditions with a spatially uniform recharge rate to the water table are assumed, continuity holds that the outflow from a location is equal to the inflow to that location minus the change in storage. Flow is a function of the surface area upslope from that location, the transmissivity of the saturated thickness, the hydraulic gradient, and the distance traversed by subsurface flow at the location.

As noted previously in equation 1, the transmissivity of the saturated thickness at a point is computed by assuming that saturated hydraulic conductivity decreases exponentially with depth (measured positively in the downward direction) as a function of a parameter, *f*, that controls the rate of decrease (Beven, 1984; Elsenbeer and others, 1992). A TOPMODEL convention is to use a scaling (or decay) parameter, *m*, to account for the vertical distribution of hydraulic conductivity over the soil column based on *f* and the drainable soil porosity. The value of *m* is given as

$$m = (\text{porosity} - \text{field capacity}) \div f. \qquad (1\text{–}1)$$

The parameter, *m*, in equation 1–1 is arguably the single most important variable in determining the fit of the generated hydrograph to a measured hydrograph. Beven (2001) states that a physical interpretation of the decay parameter *m* is that it controls the effective depth or active storage of the catchment soil profile. A larger value of *m* effectively increases the active storage of the soil profile, whereas a small value generates a shallow effective soil with pronounced transmissivity decay.

The topographic wetness index (TWI; eq. 2) is based on the concept that topography defines the three-dimensional configuration of the gravitational effects on soil-moisture drainage (Wolock, 1993). A geographic information system (GIS) is used to compute the TWI from the digital topography (digital elevation model). The TWI is defined as the natural log of the contributing area draining to a point divided by the local slope at that point. As infiltrated water moves downslope in the subsurface, it collects in the topographically flatter areas where hillslope drainage converges. The gradient of downslope areas combined with the transmissivity of the soil profile at a location (soil hydraulic conductivity times soil depth) determines the ability of subsurface water to move farther downslope. The mean of these soil properties and the distribution of the TWI are the basis for the distribution of soil moisture (Kirkby and Chorley, 1967; Dunne and others, 1975; Beven, 1978; Burt and Butcher, 1985) and the generation of runoff from pervious areas. Figure 1–1 shows a graphical representation of the TWI distributions for the McTier Creek watershed. The dark areas on the TWI figure have the largest values and, therefore, are the most likely to become saturated.

TOPMODEL equations are expressed in terms of the saturation deficit for the entire watershed (average saturation deficit). The saturation deficit is conceptually and mathematically equivalent to the depth to the water table multiplied by the readily drained soil porosity. The saturation deficit at any location is determined by the average saturation deficit and the difference between the mean TWI and the value of the TWI at the location. Large values of the index indicate the locations within a watershed most likely to be saturated and produce overland flow and return flow. These locations are topographically convergent and have gentle slopes and low transmissivity; that is, they drain a large portion of the upslope area of the watershed and have limited capacity to conduct water downslope from the drained area. The scaling parameter, *m*, affects the range of variability in the saturation deficit over the watershed given the distribution of the TWI. For McTier Creek, the watershed was divided into 30 classes of TWI for the purpose of determining the values of saturation overland flow and return flow (fig. 1–2). Each class represents a range of TWI values for a percentage of the watershed. The range of TWI values in each class is narrow enough that the watershed area represented is assumed to act similarly in terms of hydrological response. The TWI classes are determined by subtracting the lowest TWI value in the watershed from the highest TWI value and then evenly dividing into the number of desired classes. TWI values for the entire watershed are then placed into their respective class. The average for each class is simply the sum of all TWI values divided by the number of TWI values stored in that class. The saturation deficit is calculated for each class of TWI. Any location in the watershed where the saturation deficit is less than or equal to zero is saturated and has the potential to produce saturation overland flow; any location where the saturation deficit is less than zero produces return flow. For TWI classes with a saturation deficit that is less than zero, saturation overland flow is equal to the difference between precipitation and evapotranspiration multiplied by the area represented by the TWI class, and return flow is the absolute value of the saturation deficit multiplied by the area represented by the TWI class. For TWI classes with a positive saturation deficit, the values of saturation overland flow and return flow are zero. The values of saturation overland flow and return flow for the entire watershed are computed by summing the values for each of the TWI classes.

Saturation Overland Flow

Saturation overland flow is generated from precipitation falling directly on saturated soil areas that are common where the water table rises to the land surface. The rise in the water table that creates saturated areas occurs because of infiltration of precipitation into the soil and (or) soil-water movement and accumulation downslope. Saturated areas commonly develop near existing stream channels and expand as rainfall increases during a storm; they are predicted by the TWI. TOPMODEL

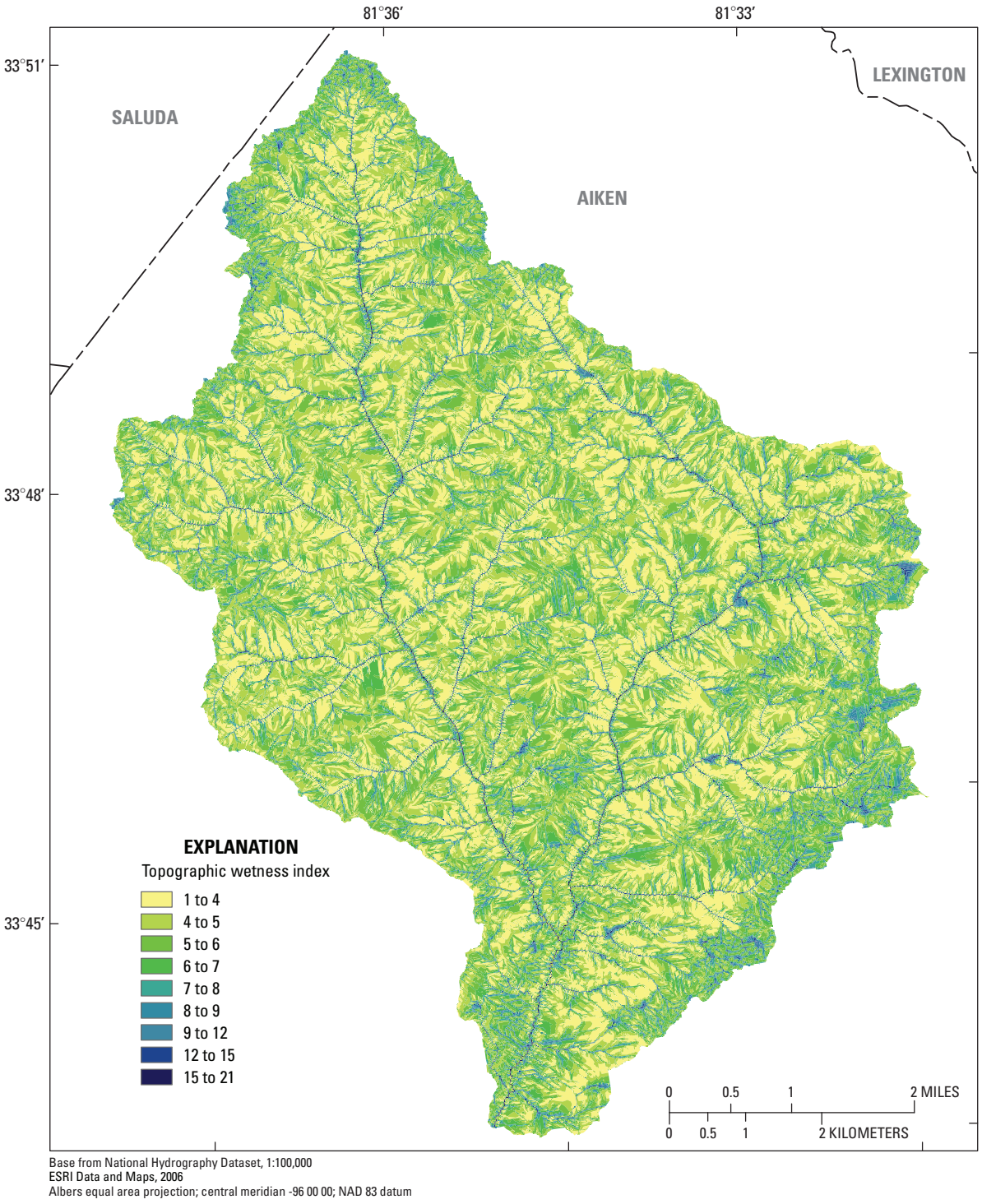

Figure 1–1. Topographic wetness indices for the McTier Creek watershed in South Carolina.

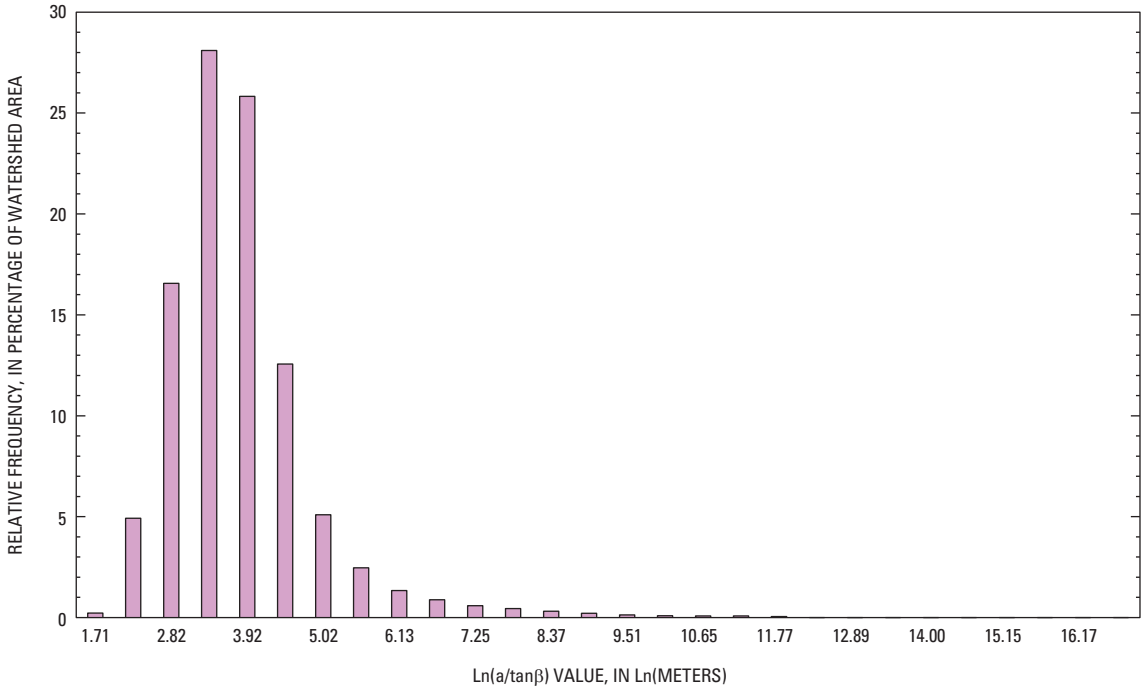

Figure 1–2. Relative frequency distribution of topographic wetness indices values for McTier Creek watershed in South Carolina.

computes the amount of saturation overland flow by multiplying the amount of precipitation adjusted for evapotranspiration by the area of the watershed that is represented by classes of the TWI that have a saturation deficit that is less than or equal to zero.

Subsurface Flow

Return flow (Dunne and Black, 1970), one type of subsurface flow, is generated from downslope drainage of subsurface water and its subsequent emergence in saturated areas. The water table rises by vertical drainage of water from above or lateral drainage of water from other parts of the watershed. Where the contributions of water are sufficiently large, the water table rises to the land surface, the area becomes saturated, and return flow is produced. TOPMODEL computes the volume of return flow for each TWI class that has a negative saturation deficit by multiplying the absolute value of the saturation deficit by the area represented by the TWI class. A negative saturation deficit represents water above the land surface.

Subsurface stormflow (Hewlett and Hibbert, 1967), another type of subsurface flow, is generated if the near-surface soil zone is very transmissive (large saturated hydraulic conductivity) and hillslopes are steep. Where these two factors are present, this rapid subsurface flow occurs when infiltration rates are greater than precipitation rates, such as in well-vegetated areas. Dunne and Leopold (1978) also noted that runoff is produced from subsurface stormflow when a rainstorm causes the water table to rise near the stream while remaining relatively stationary under the higher part of the hillside. This rise near the stream causes an increase in the slope of the water table in that area and, according to Darcy's Law, should result in an increase in the subsurface flow. In the computer code for the version of TOPMODEL used in this study, subsurface flow is the generic term used for the state variable *qb*. Some researches use the term base flow for low values of *qb*, while others use the term subsurface stormflow for high values of *qb* (D.M. Wolock, U.S. Geological Survey, written commun., June 2009). TOPMODEL does not conceptually split the subsurface stormflow and more traditional base flow (L.J. Kauffman, U.S. Geological Survey, written commun., March 2009). In addition, conceptually differentiating between return flow and subsurface stormflow also can be difficult; however, together, they are a major component of streamflow. In TOPMODEL, they are calculated by two separate but related algorithms.

Infiltration-Excess Overland Flow

Infiltration-excess overland flow is generated by overland flow that is produced when precipitation rates exceed infiltration rates. This type of overland flow typically occurs during periods of high rainfall intensity in areas of low soil permeability or in disturbed, compacted, or poorly vegetated areas. Infiltration-excess overland flow is computed using the Green-Ampt equation (Green and Ampt, 1911) as implemented by Beven (1984). Rather than use only the mean

soil permeability in the calculation of the infiltration excess, calculations are based on the mean soil permeability and an expected variance of the log of soil permeability.

Lake Storage

The McTier Creek watershed has a number of small lakes or ponds (fig. 1). Lake or pond storage can dampen and delay surface runoff in some watersheds. To account for the lake-storage effects or delays in runoff, the portion of watershed area upstream from any lakes was determined. A decay function was then applied to a fraction of the runoff equivalent to the lake-affected fraction of the watershed. The remaining runoff was treated as previously described. In the version of TOPMODEL being used in this investigation, lake storage is represented by the variable *dsrip*. A positive *dsrip* indicates water being stored in the lakes, and a negative *dsrip* indicates water being released from the lakes (L.J. Kauffman, U.S. Geological Survey, written commun., September 2, 2009).

Open-Water Bodies

In TOPMODEL, precipitation falling directly on open-water bodies, such as lakes, ponds, and the stream-channel water surface, also are considered in the water budget. For the open-water bodies, evapotranspiration is always satisfied, and any precipitation generates streamflow. With respect to the output from the version of TOPMODEL used in this investigation, the variable *qsrip* represents streamflow directly from open-water bodies (fig. 36; L.J. Kauffman, U.S. Geological Survey, written commun., September 2, 2009). When precipitation is greater than the potential evapotranspiration (PET), *qsrip* is positive and increases the total predicted streamflow. On days when PET is greater than the precipitation, *qsrip* is negative and represents evaporation directly from the open-water bodies. The evaporation represented by negative *qsrip* is accounted for by being proportionally taken from *qb* (subsurface flow) and *qret* (return flow).

Appendix 2

Model Components of GBMM: Hydrology Module

The main components of GBMM's hydrology module are similar to those of the TOPMODEL simulations and follow from the GBMM Streamflow Concepts section of the report. This appendix discusses the main model components in greater detail.

Precipitation

Precipitation is the primary forcing function for GBMM's hydrology module. The best possible estimates of rainfall and temperature, which influence evapotranspiration calculations, within the watershed are required. Precipitation inputs to GBMM are the same as those used for TOPMODEL, which follow an inverse-distance weighting scheme using data obtained from nearby NWS stations (see Data Collection section of the report).

Evapotranspiration

Potential evapotranspiration is estimated using the Hamon formula (Hamon, 1961). This calculation is used along with a vegetation cover factor for each land-cover type during growing and non-growing seasons to calculate actual evapotranspiration.

$$ET = \min\left(PET * VCF, S_w + P_{tot} - R_o - WP\right), \quad (2\text{–}1)$$

where

ET is the actual evapotranspiration (in centimeters),
PET is the Hamon-derived potential evapotranspiration (in centimeters),
VCF is the vegetation cover factor (derived from Soil and Water Assessment Tool (SWAT) land-cover coefficients for both the growing and non-growing seasons), and
WP is the soil water content at wilting point (in centimeters).

Wilting point is calculated using Neitsch and others, (2005):

$$WP = 0.4 * mc * BD * d_{unsat}, \quad (2\text{–}2)$$

where *mc* is the percentage of clay content in the soil layer, *BD* is the bulk density of the soil (in grams per cubic centimeters), and d_{unsat} is the unsaturated soil depth (in meters). If, however, the soil water content is in excess of the field capacity water content for each time step, percolation to groundwater (P_c, in centimeters per day) is estimated, using the formula

$$P_c = S_{w(excess)}, \quad (2\text{–}3)$$

where $S_{w(excess)}$ is drainage excess water in the unsaturated zone calculated by

$$S_{w(excess)} = S_w + P_{tot} - R_0 - ET - FC, \quad (2\text{–}4)$$

where *FC* is water content in the soil at field capacity (in centimeters), which is found with the following equation:

$$FC = WP + \left(AWC * d_{unsat} \right), \quad (2–5)$$

where AWC is the available water capacity in unsaturated soil (in centimeters per meter).

Impervious-Area Runoff

For impervious surfaces, modified curve-number algorithms are used, and ranges of impervious land cover for urban areas can be found in Neitsch and others (2005). Calculations for curve-number runoff are found in the Pervious-Area Runoff section of this appendix. Impervious urban land cover is categorized into two groups: (1) grid cells hydrologically connected to the watershed's surface and subsurface drainage area and (2) grid cells not hydrologically connected to the drainage area. Separate curve-number calculations are implemented on impervious land cover depending on this categorization. A curve number of 98 is used for all impervious surfaces directly connected to the drainage area; however, for disconnected portions of impervious grids, modified equations are used:

$$CN = \frac{CN_2 * \left[1 - imp_{tot} + \frac{imp_{dcon}}{2} \right] + 98 * \left[\frac{imp_{dcon}}{2} \right]}{\left[1 - imp_{con} \right]} \quad (2–6)$$

for $(imp_{tot} \le 0.30)$ or

$$CN = \frac{CN_2 * \left[1 - imp_{tot} \right] + 98 * imp_{dcon}}{\left[1 - imp_{con} \right]} \quad (2–7)$$

for $(imp_{tot} > 0.30)$,

where

CN is the composite curve number,
CN_2 is the pervious curve number,
imp_{tot} is the fraction of the grid area that is impervious (both directly connected and disconnected),
imp_{con} is the fraction of the grid area that is impervious and hydraulically connected to the drainage system, and
imp_{dcon} is the fraction of the grid area that is impervious but not hydraulically connected to the drainage system.

Pervious-Area Runoff

For pervious surfaces, surface runoff in GBMM is estimated using the modified SCS-CN method. A curve-number estimate is calculated for each 30-m grid cell using the formula:

$$D_S = \frac{2540}{CN} - 25.4, \quad (2–8)$$

where D_s is the detention storage (in centimeters), and CN is the curve number. Curve numbers for the standard average moisture conditions are estimated by way of select vegetation and soil combinations (Haith and others, 1992) but are modified based upon antecedent moisture condition. Vegetation characteristics are derived from the NLCD 2001 Land-Cover Data (Homer and others, 2004), and soil data include the hydrologic soil group from the Soil Survey Geographic (SSURGO) Data Base (Natural Resources Conservation Service, 2008).

Curve-number modifications for dry (CN_1) and wet (CN_3) conditions are

$$CN_1 = \frac{CN_2}{(2.334 - 0.01334 * CN_2)} \text{ and} \quad (2–9)$$

$$CN_3 = \frac{CN_2}{(0.4036 + 0.0059 * CN_2)}. \quad (2–10)$$

The curve number used for each day is a linear function of the 5-day antecedent moisture:

$$A_{5d} = \sum_{n=t-5}^{t-1} (P_{tot,n}), \quad (2–11)$$

where A_{5d} is the 5-day antecedent moisture (in centimeters), and P_{tot} is the total available input water at the surface (for example, rainfall + snowmelt, in centimeters). The value of A_{5d} determines the thresholds above and below which CN_3 or CN_1 will be implemented, respectively. These values vary depending on whether the simulation time step occurs during the growing season or the dormant season. Therefore, the four critical values of $A_{5d,}$ (growing and non-growing season and threshold values for CN_3 and CN_1) can be adjusted during the hydrologic calibration process. Runoff from the curve number is then routed as described in the GBMM Streamflow Concepts section of this report.

Lake Storage

Lake storage and water flux can be an important component to the hydrologic balance in many watersheds. The current version of GBMM maintains a place holder for lake, wetland, and pond water balances; however, these balances currently cannot be simulated in GBMM.

Manuscript approved on September 22, 2010

Prepared by:
USGS Enterprise Publishing Network
Raleigh Publishing Service Center
3916 Sunset Ridge Road
Raleigh, NC 27607

For additional information regarding this publication, contact:
USGS South Carolina Water Science Center
720 Gracern Road, Suite 129
Columbia, SC 29210–7651
phone: 803–750–6100
http://sc.water.usgs.gov/


EXPLANATION
Topographic wetness index
1 to 4
4 to 5
5 to 6
6 to 7
7 to 8
8 to 9
9 to 27
48'